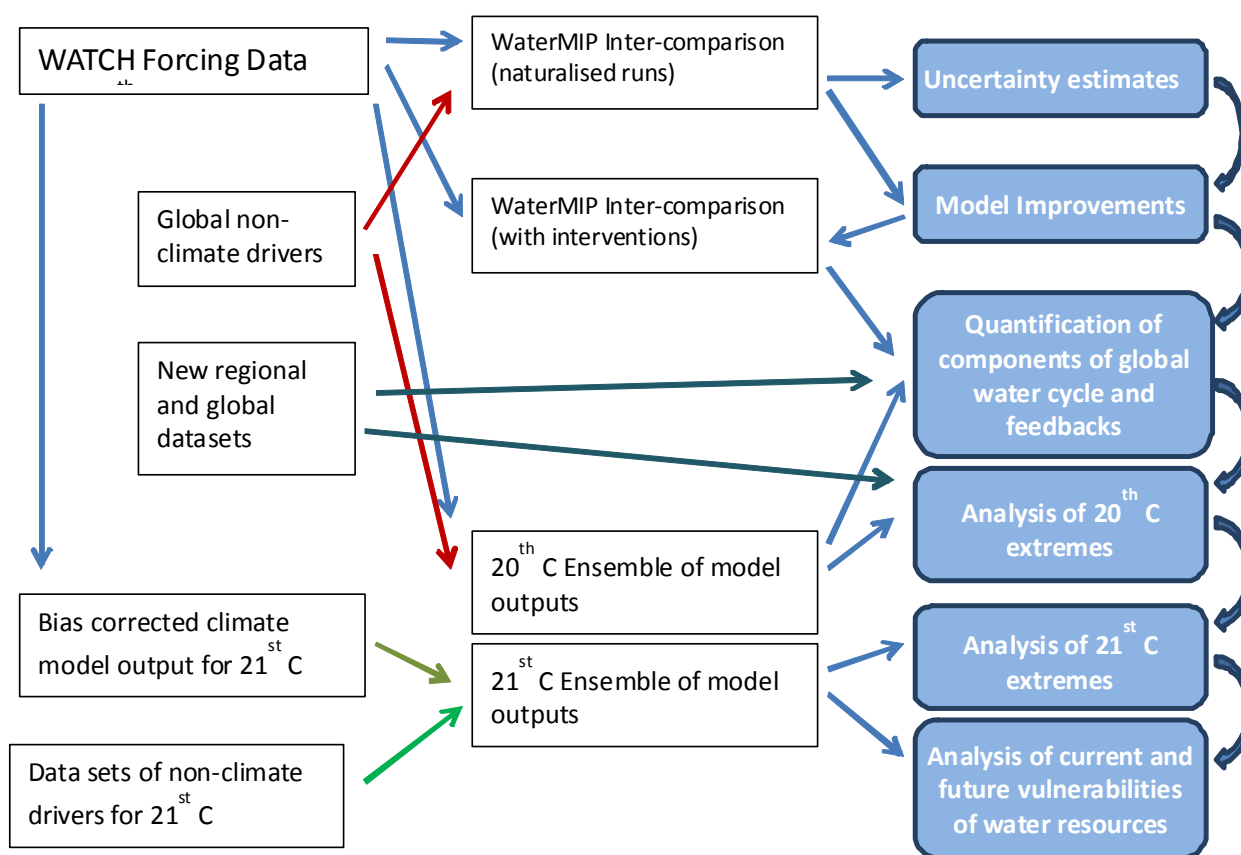**Technical Report No. 56**

EXECUTIVE SUMMARY OF THE COMPLETED WATCH PROJECT

Author names: Richard Harding, Tanya Warnaars, Graham Weedon, David Wiberg, Stefan Hagemann, Lena Tallaksen, Henny van Lanen, Eleanor Blyth, Fulco Ludwig, Pavel Kabat

Date: Sept 2011

WATCH is an Integrated Project Funded by the European Commission under the Sixth Framework Programme, Global Change and Ecosystems Thematic Priority Area (contract number: 036946). The WACH project started 01/02/2007 and will continue for 4 years.

|	
Title:	Executive summary of the completed WATCH project
Authors:	Richard Harding, Tanya Warnaars, Graham Weedon, David Wiberg, Stefan Hagemann, Lena Tallaksen, Henny van Lanen, Eleanor Blyth, Fulco Ludwig, Pavel Kabat
Contributors:	Richard Harding, Tanya Warnaars, Graham Weedon, David Wiberg, Stefan Hagemann, Lena Tallaksen, Henny van Lanen, Eleanor Blyth, Fulco Ludwig, Pavel Kabat
Submission date:	Sept 2011
Function:	e.g. This report is an output from Work Block 7; and is part of the final report of WATCH
Deliverable	WATCH deliverable : final reporting

Publishable Final Summary
Project: **WATer and global CHange**
Acronym: **WATCH IP**
Contract: **036946**
Dates   **1 Feb. 2007 – 31 July 2011**
Coordinator: **Richard Harding**
Coordinator Institute: **Natural Environment Research Council (NERC)**
Contact point: **info-watch@ceh.ac.uk**
Web site: **www.eu-watch.org**

Executive Summary

The WATCH (Water and Global Change) project is a European Union funded project to improve our understanding of the terrestrial water cycle. It has brought together scientists from 25 European research Institutions (as well as others from America and Japan) from many disciplines – hydrology, climate, water resources, remote sensing etc) to achieve this common goal.

A central focus of the project has been the development of a common modelling framework (see figure below) to allow the linkage of a large variety of spatial data sets with hydrological and water resource models. This has provided a comprehensive and consistent assessment of the water cycle (means and extremes), water resources and uncertainty.
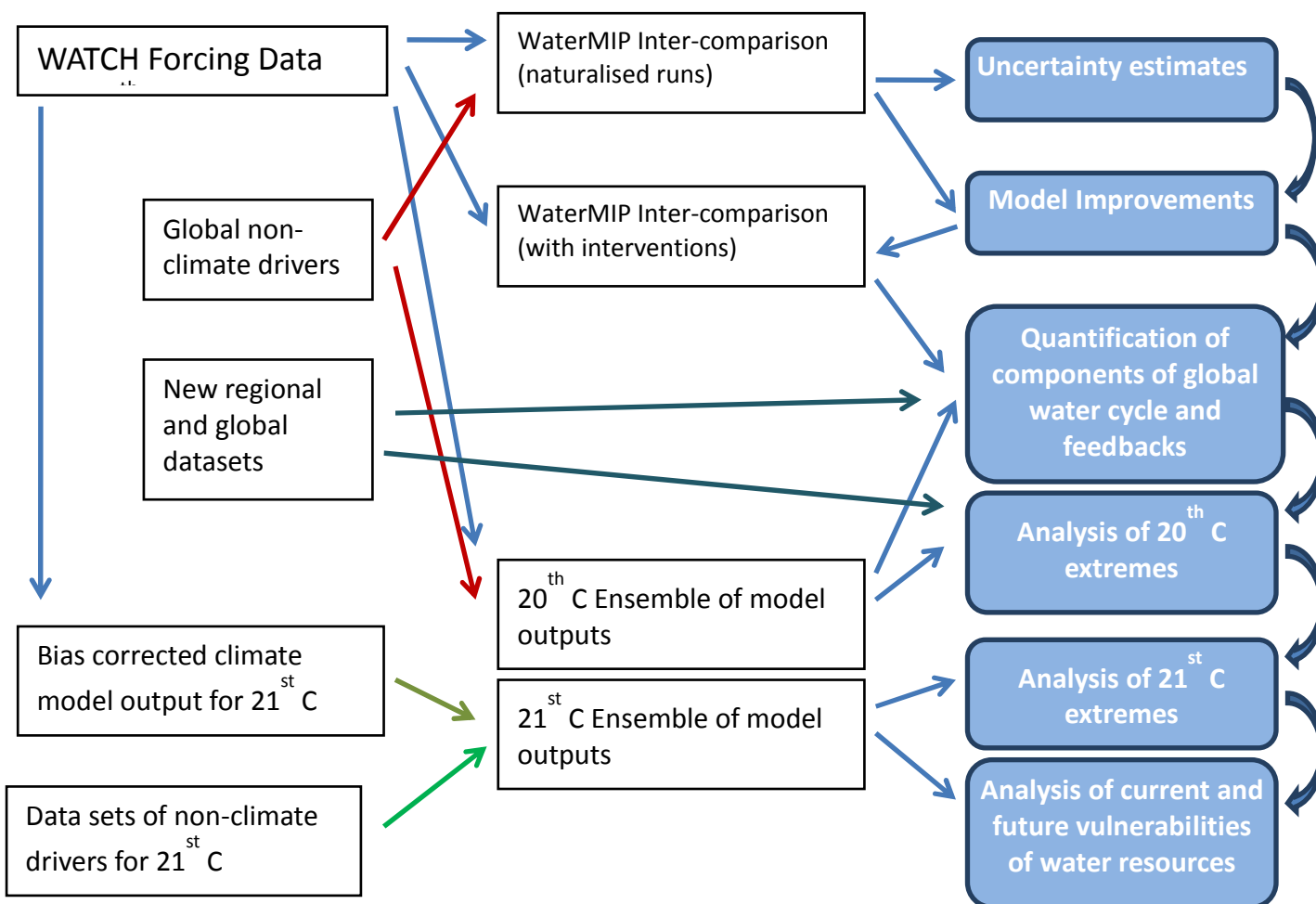
Key to the modelling framework has been the development of a consistent set of climate data for use as input. The WATCH Forcing Data covers the period 1901 – 2001 and is based on a global 0.5 degree x 0.5 degree (~ 50km x 50km) grid. It comprises eight essential climate variables. The 21st century data set – the WATCH Driving Data – covers the period 2001– 2100. It was created using a novel bias-correction methodology applied to three well-established climate models, each running for two IPCC-SRES future emissions scenarios. Both data sets are freely available to the world's research community, providing a significant new resource for future projects.

Using these data, WATCH completed an ambitious Water Model Inter-comparison Project. This led to the development of data and tools to provide a reliable multi-model approach to assessing impacts on the water cycle. The models were shown to be fit-for purpose for estimating river flows at global, continental and regional scales. This allowed the first steps to be taken towards a consistent assessment of water availability. This approach is similar to the one taken with climate studies – such as in IPCC Reports – and will reduce the need to rely on local hydrological studies that are unlikely to be representative at a global scale.

WATCH has compiled an exceptional pan-European set of observed river flow data from more than 400 stations; which have contributed to the compilation of the Flood and Drought Catalogues & Atlases as well as to a range of pan-European studies, including calculation of trends in streamflow and identification of the most extreme large-scale events. In addition, it has been used for a unique model validation. These publications capture the spatial and temporal characteristics of droughts and floods over the 20th century across Europe. They can be combined with other key data sets to produce figures for the human, economic and environmental consequences of individual historical events. WATCH has made significant progress in understanding and recording hydrological extremes in the 20th century and assessing the likely impacts of climate change in the 21st C.

WATCH has highlighted the critical importance of evaporation within the water cycle. It has produced a new global data set of evaporation from land for the period 1984 – 2007 that provides totally new insights on the importance of evaporation for the global water cycle. This breakthrough is due to the availability of high-quality satellite data, coupled with novel and innovative approaches used by WATCH researchers. Early analysis of the data indicates to support the suggestion that total global land-evaporation has reduced over the last ten years. This is contrary to the common belief that increasing temperatures, due to climate change, should cause an increase in global evaporation. The data will allow future studies of global trends, and changes in regional evaporation, across different biomes.

Overall, the model results confirm the need for land-use change to be considered alongside climate change, and any predictions of future climate ought to include the impact of land-use and land-cover changes. Until WATCH, climate and impact models had been treated separately. WATCH has shown that these models can be coupled, and that they should be coupled routinely in the future. Only then will we be able to model feedbacks, and be able to estimate the effects of future planned changes.

By combining data on water availability and water demand, WATCH has identified and quantified where there are deficits, and where water is more plentiful. Water scarcity occurs when there is not enough water available to meet the demands of agricultural, industrial, and domestic use. WATCH quantified water use in these sectors and assessed the drivers that will influence future water use. The WATCH approach to assessing water use by rainfed and irrigated agriculture makes a distinction between "blue" and "green" water;"blue" is water withdrawn from rivers, lakes, reservoirs and groundwater for use in irrigation schemes, and "green" is the moisture stored in the soil from rainfall. This approach revealed

that approximately half of the blue water that is withdrawn for use in irrigation schemes is from non-renewable or non-local water resources. Globally, the amount of water used in agriculture also far exceeds what was suggested in previous studies which considered blue water only. The consistent methods used within WATCH to derive new data sets make it easier to link them and to consider them together rather than in isolation. This promotes better understanding of the total demands that are being placed on the world's resources.

WATCH leaves a clear legacy of an increased understanding of the water cycle in a time of global change. In addition, it has created an international group of knowledgeable and experienced modellers working at the interface between hydrology and climate science. These scientists will go on to influence international research projects for years to come, underpinning the development of evidence based inter-governmental policy-making. And, they will take with them an awareness and an enthusiasm for what can be achieved by large research teams working in partnership.

1. Project Objectives

The Integrated Project (WATCH) brings together the hydrological, water resources and climate communities to analyse, quantify and predict the components of the current and future global water cycles and related water resources, evaluate their uncertainties and clarify the overall vulnerability of global water resources related to the main societal and economic sectors. The specific objectives of the WATCH project have been to:

- analyse and describe the current global water cycle, including observable changes in extremes (droughts and floods)
- evaluate how the global water cycle and its extremes respond to future drivers of global change (including greenhouse gas release and land cover change)
- evaluate feedbacks in the coupled system as they affect the global water cycle
- evaluate the uncertainties in coupled climate-hydrological- land-use model predictions using a combination of model ensembles and observations
- develop an enhanced (modelling) framework to assess the future vulnerability of water as a resource, and in relation to water/climate related vulnerabilities and risks of the major water related sectors, such as agriculture, nature and utilities (energy, industry and drinking water sector)
- provide comprehensive quantitative and qualitative assessments and predictions of the vulnerability of the water resources and water-/climate-related vulnerabilities and risks for the 21st century
- collaborate with the key leading research groups on water cycle and water resources in USA, Japan, India and other countries.
- collaborate in dissemination of its scientific results with major research programmes worldwide (through, for example: WCRP, IGBP, GSWP)

WATCH has been a collaboration between 25 funded European partners and well as a number of unfunded European and International partners, see table 1.1.

For ease of management the activities of WATCH have been split into 6 science work blocks and a management, dissemination and training activity:

Work Block 1: The Global Water Cycle of the 20th Century.
WB1 will consolidate gridded data sets, improve the hydrological representation of hydrology in hydrological models and investigate the 20th century global water cycle using a combination of models and data.

Work Block 2: Population and land use change.
WB2 will provide gridded estimates of population, land use and water requirements for the 20th and 21st centuries for use in the other Work Blocks.

Work Block 3: The Global Water Cycle in the 21st Century. *Coordinator: MPI-M*
WB 3 will produce multi-model based projections for the terrestrial components of the global water cycle for the 21st century. This will include projections globally and for two contrasting regions. A full uncertainty analysis will be provided.

Work Block 4: Extremes: Frequency, Severity and Scale.
WB4 will advance our knowledge on the impact of global change on hydrological extremes, including spatial and temporal patterns of droughts and large-scale floods.

Work Block 5: Feedbacks between Hydrology and Climate.
WB5 will provide a global and regional analysis of feedbacks between the land surface and climate system using a fusion of models and data.

Work Block 6: Assessing the vulnerability of global water resources.
WB6 will develop a unified water resources modelling and risk assessment framework, and use that generate more reliable, consolidated, quantitative assessments of the past and future states of water resources.

Work Block 7: Project management training and communication and Dissemination:
WB7 will deliver the management and organizational structures and processes to ensure the effective delivery of WATCH integrated and to maximize the benefits of this research to all stakeholders, by using the most effective knowledge transfer through the project's training and dissemination activities.

In practice these seven 'work blocks' have been strongly linked; the primary interactions are demonstrated graphically in Figure 1.1. A central tenet of WATCH has been the crossover of data and techniques between the climate and hydrological sciences. Thus new datasets suitable to run hydrological models have been produced from the climate and meteorological analyses, a new regional river flow data sets have been consolidated to provide validation, new indexes of extremes (floods and droughts) have been developed suitable for regional and global use and new hydrological model components developed for use within the global models. All these add up to a step change in our ability to analyse and understand the components of the global terrestrial water cycle for the 20th and 21st centuries.

Table 1.1: The 25 WATCH partner organisations plus associate partners

No.	Institution
1	National Environmental Research council - Centre for Ecology and Hydrology
2	Wageningen Universiteit
3	Vrije Universiteit Amsterdam
4	Danish Meteorological Institute
5	Centre National du Machinisme agricole, du Génie Rural, des Eaux et des Forêts
6	Johann Wolfgang Goethe-Universitaet Frankfurt am Main
7	The Abdus Salam International Centre for Theoretical Physics
8	UK Meteorological Office
9	Max Planck Institute for Meteorology
10	Institu for Agricultural and Forest Environment, Polish Academy of Sciences,
11	Potsdam-Institut für Klimafolgenforschung e.V. (Potsdam-Institute for Climate Impact Research)
12	Technical University of Crete
13	University of Oslo Department of Geosciences
14	Universitat de Valencia. Estudi General
15	University of Oxford
16	International Institute for Applied Systems Analysis
17	Centre National de la Recherche Scientfque/Laboratoire de Meteorologie Dynamique
18	Fundacao da Faculdade de Ciencias da Universidade de Lisboa
19	Comenius University in Bratislava (Univerzita Komenskeho v Bratislave)
20	Consejo Superior de Investigaciones Cientificas
21	University of Kassel
22	KWR WATER BV

No.	Institution
23	Observatoire de Paris
24	Vyzkumny ustav vodohospodarsky T.G. Masaryka, v. v.i. T.G. Masaryk Water Research Institute
25	Norwegian Water Resources and Energy Directorate

Associate partner Institution
ETH-Zurich (Swiss Federal Institute of Technology Zurich)
Geozentrum Riedberg Goethe-Universitaet Frankfurt a.M (Germany)
Indian Institute of Technology Delhi (India)
National Institute for Environment Studies (Japan)
Science Applications International Corporation, (NASA, USA)
University of Castilla de la Mancha (Spain)
University of New Hampshire (USA)
University of Reading (UK)
University of Tokyo (Japan)
University of Utrecht (Netherlands)

Fig. 1.1 *Structure of WATCH: six science work blocks consist of three main blocks (horizontal bars) providing an assessment of current (WB1) and future (WB3) water cycles and water resources (WB6). Cross-cutting themes (vertical bars) support these with respect to the representation of feedbacks (WB5), detection and attribution of extremes (WB4), and provision of dynamics of population, land-use change and water demands (WB2). Coherent management supported the interactions across all work blocks(WB7)*
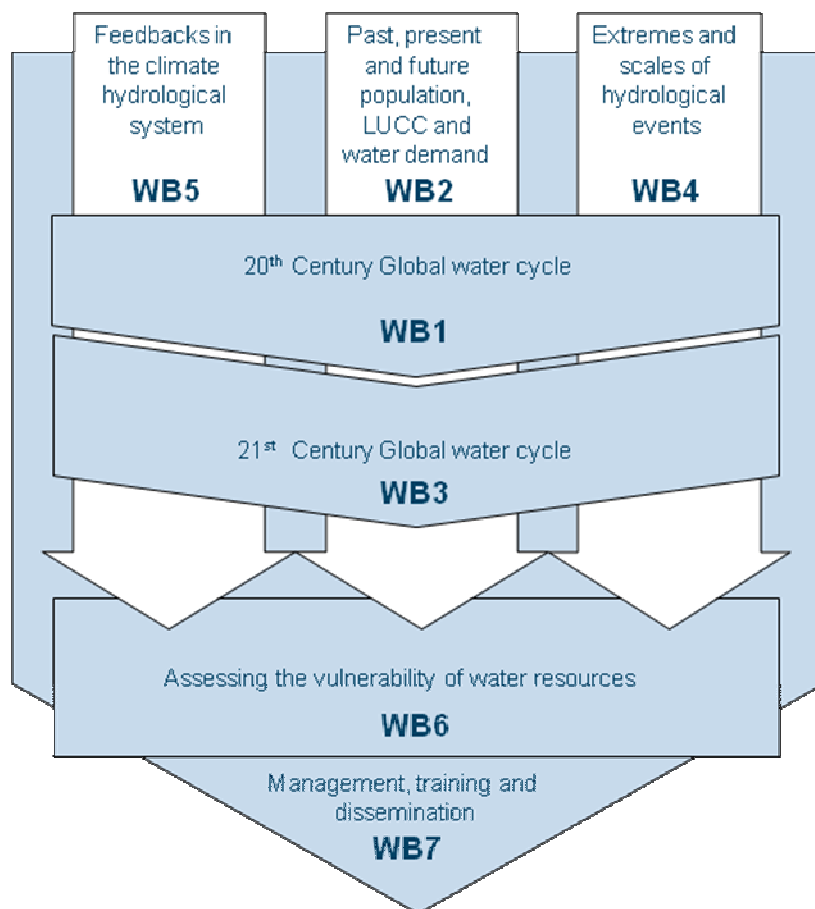
2. The Global Water Cycle of the 20th Century

An analysis of the global water cycle for the 20th C (and 21st C) requires a consistent and well found data set of the meteorological variables which drive the water cycle. The WATCH Forcing Data set has provided the underpinning for many activities across WATCH, including the WaterMIP model inter-comparison, the climate model bias correction and the 20thC analysis of extremes. It is also beginning to be used widely outside WATCH in a wide variety of modelling and simulation studies (of, for example, the carbon cycle).

WATCH forcing and driving data

The WATCH Forcing Data is a single data set of climate variables that covers the period 1901 – 2001. It has been produced by combining the Climatic Research Unit's monthly observations of temperature, "wet days" and cloud cover, plus the GPCCv4 monthly precipitation observations, and the ERA40 reanalysis products (with the addition of corrections for seasonal – and decadal – varying atmospheric aerosols needed to adjust the solar radiation components). Between 1901 and 1958 (when the ERA40 analyses are not available) a methodology based on random re-ordering ERA-40 Reanalysis data has been used. The data have been validated using point sites from the FLUXNET dataset (http://www.fluxnet.ornl.gov/) and at a small catchment level using the WATCH test basins. For more details see Weedon et al. (2011).

The WATCH Driving Data covers the period 2001 – 2100 and has been generated using three well-established climate models that have been downscaled and bias corrected. Each model was run for two different IPCC scenarios, giving six data subsets within the driving data.

All of the forcing and driving data sets cover the land surface of the Earth (excluding Antarctica) on a 0.5° x 0.5° (~50km x 50km) grid. This gives 67,420 data points. Each data set provides eight variables. These are:

- . air temperature at 2m above ground;
- . surface pressure at 10m above ground;
- . specific humidity at 2m above ground;
- . wind speed at 10m above ground;
- . downwards long-wave (infra-red) radiation flux;
- . downwards short-wave (solar) radiation flux;
- . rainfall;
- . snowfall.

The first five variables are provided at 6-hourly intervals, the remaining three variables are provided at 3-hourly intervals. The WATCH Forcing data are freely available – see WATCH Web site.

The forcing data sets have been used to run different models describing components of the Global Water Cycle. These models can be grouped into:

- Land Surface Hydrology Models (LSMs JULES, Orchidee and HTessel) (e.g. Gedney *et al.*, 2006)
- Global Hydrological Models (GHMs), such as WaterGAP (Alcamo *et al.*, 2003; Döll *et al.*, 2003), GWAVA (Meigh *et al.*, 2005), MPI-HM (Hagemann & Dümenil Gates, 2003) and WBM (Vörösmarty *et al.*, 1998)
- River Basin Hydrological Models (RBHMs), such as ECOMAG (Gottschalk *et al.*, 2001), SIMGRO/MOGROW (Querner, 1997; Querner & Van Lanen, 2001), Grid-2-Grid (Bell *et al.*, 2006).

LSHMs have their origins in the land surface descriptions within climate models. They generally close the energy balance at the land surface and describe the vertical exchanges of heat, water and, sometimes, carbon very well. More recently they have incorporated representations of lateral transfers of water (Blyth, 2001) – typically using semi-distributed models, such as TOPMODEL (Beven, 2001), PDM (Moore, 1985) or VIC (Liang et al., 1994). Increasingly LSHMs can be operated coupled into climate (or Earth System) models or in a standalone mode, driven by global or regional data sets. River basin scale hydrological models (RBHMs) close the water balance at the basin scale and have a good representation of lateral transfers but are weaker in the energy and carbon linkages. They also frequently require basin-specific, often optimised, parameters, dependent on their physically-based nature. Global Hydrological Models (GHMs) are the first attempts to produce a synthesis of the Global Hydrological Cycle. They have limited process representation, compared to the LSMs and generally use simple conceptual hydrological models to generate runoff. These contain parameters calibrated on river flows, this can be done from a large range of basins across the world (for example WaterGAP, Alcamo et al., 2003, uses basin specific parameters tuned on 11,050 river basins and MacroPDM (Arnell, 1999) uses regional model parameters tuned to a range of river basins. These models include representations of hydrological stores and interventions, such as groundwater (Döll & Florke 2005), irrigation (Döll & Siebert, 2000) and water withdrawals and dams (Döll et al, 2009). GHMs also interface to global water use models to provide global estimates of water scarcity and stress (e.g. Alcamo et al., 2003, 2007).

WATCH has provided a strong impetus and mechanism to improve both the Global Hydrology Models and Land Surface Hydrology Models. The model intercomparison project (WaterMIP - described later) has highlighted many deficiencies in individual models and provided an opportunity for modellers to compare and develop model approaches and components. Considerable progress has been made in introducing parameterisations of new processes into the WATCH hydrological and land surface models. Different models have adopted appropriate solutions to their development in terms of treatment of groundwater, crops, reservoirs and dams within a common framework for river routing. It did not prove practicable to implement all developments uniformly across the hydrological models (see WATCH Technical Report 34) though there has been considerable sharing of expertise/methodology across different modelling groups.

New parameterisations of Dams and Irrigation in LSMs

Work and testing has finished on adding representations of the effects of irrigation and dams to the JULES land surface model. A new parameterisation of dam operation was added, largely following Biemans et al. (2011). The model is built around a set of simple rules that calculate the amount of water released from a dam as a function of the demand for water from downstream areas and the amount of water stored in the reservoir behind the dam. Each dam is considered to be either primarily for irrigation supply or for "other" purposes, and separate rules govern the operation of each type. At each grid box the demand for irrigation water is calculated on a daily basis and the model tries to meet this demand, first by extracting water from the local river, then if necessary augmenting this with water from a dam release. The addition of these representations of irrigation demand and water supply mean that JULES is now more appropriate for use in studies of water resources, in particular of how the availability of water will change as the demand for water for agriculture increases over the coming century. Similarly, a reservoir management scheme has been implemented in the LPJmL model, which introduces ~7,000 reservoirs dynamically in the river routing module (Biemans et al., 2011). Specific reservoir operation rules were developed for irrigation reservoirs and other reservoirs (hydropower, navigation, flood control). Besides simulating the change in timing of river flow, it also simulates extractions of irrigation water and supply to irrigated area downstream of the reservoir. Thus it allows for a spatially explicit quantitative estimate of the water withdrawal and supply from reservoirs. Main conclusions derived from a global application of this new scheme are (Biemans et al., 2011):

- Reservoirs have significantly changed the timing and amount of rivers discharging into the ocean.
- Simulated discharge at >300 gauges with reservoirs upstream showed an improvement in 91% of the cases.
- By storing and redistributing water, reservoirs have significantly increased surface water availability in many regions.
- The continents gaining the most from their reservoirs are North America, Africa, and Asia (40% more than the availability in the situation without reservoirs).
- Globally, irrigation water supply from reservoirs increased from around 18 km^3 per year (adding 5% to surface water supply) at the beginning of the 20th century to 460 km^3 per year (adding almost 40% to surface water supply) at the end of the 20th century.

One aim of WATCH has been to establish a modeling framework for the global estimation components of the water cycle. From the outset WATCH has collaborated with the Global Water Systems Project (GWSP http://www.gwsp.org/) to bring together and compare land surface hydrology models and global hydrological models using the same driving data and a strict modeling protocol. The WaterMIP project has made global water balance estimates based on model runs from 13 models from Europe, USA and Japan at 0.5 degree spatial resolution for global land areas for a 15-year simulation period (1985-1999), Haddeland et al, 2011. The results show large variations in estimated global mean annual runoff values, with a range of nearly 30,000 km^3 $year^{-1}$, which obviously will influence any impact study based on model simulation results (see Table 2.1 and figure 2.1). Some intrinsic differences in the model simulation results are explained and attributed to model characteristics. Distinct simulation differences between land surface models and global hydrological models are found to be caused by the snow scheme. The physically based energy balance approach used by land surface models in general results in lower snow water equivalent values than does the conceptual degree day approach used by global hydrological models. For evapotranspiration and runoff processes no major differences between simulation results of land surface models and global hydrological models have been found. However, some model simulation differences can be explained by the chosen parameterization included in the

models, although the processes included, and parameterizations used, are not distinct to land surface models or global hydrological models.

Table 2.1: Participating models, including their main characteristics.

Model name[1]	Model time step	Meteorological forcing variables[2]	Energy balance	Evapotranspiration scheme[3]	Runoff scheme[4]	Snow scheme	Reference(s)
GWAVA	Daily	P, T, W, Q, LW, SW, SP	No	Penman-Monteith	Saturation excess / Beta function	Degree day	Meigh et al. (1999)
H08	6 h	R, S, T, W, Q, LW, SW, SP	Yes	Bulk formula	Saturation excess / Beta function	Energy balance	Hanasaki et al. (2008a)
HTESSEL	1 h	R, S, T, W, Q, LW, SW, SP	Yes	Penman-Monteith	Variable infiltration capacity / Darcy	Energy balance	Balsamo et al. (2009)
JULES	1 h	R, S, T, W, Q, LW, SW, SP	Yes	Penman-Monteith	Infiltration excess / Darcy	Energy balance	Cox et al. (1999), Essery et al. (2003)
LPJmL	Daily	P, T, LWn, SW	No	Priestley-Taylor	Saturation excess	Degree day	Sitch et al. (2003)
MacPDM	Daily	P, T, W, Q, LWn, SW	No	Penman-Monteith	Saturation excess / Beta function	Degree day	Arnell (1999)
Matsiro	1 h	R, S, T, W, LW, SW, SP	Yes	Bulk formula	Infiltration and saturation excess / GW	Energy balance	Takata et al. (2003)
MPI-HM	Daily	P, T	No	Thorntwaite	Saturation excess / Beta function	Degree day	Hagemann and Dümenil Gates (2003),Hagemann and Dümenil (1998)
Orchidee	15 min	R, S, T, W, Q, SW, LW, SP	Yes	Bulk formula	Saturation excess	Energy balance	De Rosnay and Polcher (1998)
VIC	Daily/ 3h	P, Tmax, Tmin, W, Q, LW, SW, SP	Snow season	Penman-Monteith	Saturation excess / Beta function	Energy balance	Liang et al. (1994)
WaterGAP	Daily	P, T, LWn, SW	No	Priestley-Taylor	Beta function	Degree day	Alcamo et al. (2003)

1: Model names written in italic are classified as LSMs, the other models are classified as GHMs.

2: R: Rainfall, S: Snowfall, P: Precipitation, T: Air temperature, Tmax: Maximum daily air temperature, Tmin: Minimum daily air temperature, W: Wind speed, Q: Specific humidity, LW: Longwave radiation (downward), LWn: Longwave radiation (net), SW: Shortwave radiation (downward), SP: Surface pressure

3: Bulk formula: Bulk transfer coefficients are used when calculating the turbulent heat fluxes.

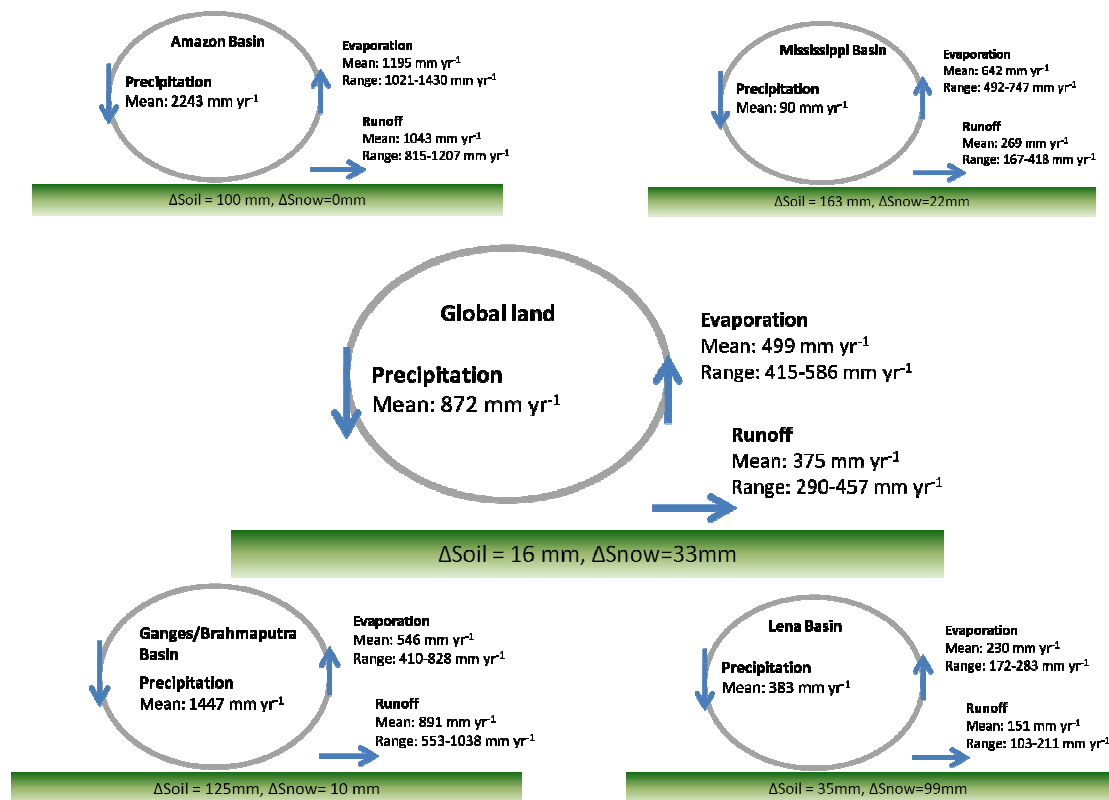4: Beta function: Runoff is a nonlinear function of soil moisture.

Figure 2.1. Components of water fluxes and storages for terrestrial land surface and four major basins representing different climate regimes, numbers taken from WaterMIP (Haddeland et al. 2011)

The WaterMIP project and WATCH Forcing Data have been the foundation of the development of the WATCH 20th Century Ensemble dataset. This contains daily averages and associated descriptors for seven land surface and general hydrological models using "naturalized runs" with the WATCH Forcing Data for every half-degree land grid box as stored in monthly full latitude-longitude grid netCDF files. The models providing daily data for the full twentieth century are: GWAVA, Htessel, LPJml, MPI-HM, Orchidee, WaterGAP and JULES. The hydrological variables involved are: snow water equivalent ("swe"), total evaporation (i.e. bare soil evaporation plus canopy evaporation/transpiration, "evap"), total soil moisture (i.e. the sum of all soil layer moisture values, "soilmoist") and surface runoff plus subsurface runoff (i.e. Qs + Qsb, "qs+qsb"). Outlier values were excluded from the Ensemble as described in WATCH Technical Report 37. These data will be analysed and reported on beyond the end of WATCH.

WATCH, in collaboration with the UNESCO-IHP FRIEND program, the European Water Archive (EWA); has developed a unique dataset of river flow observations from about 450 small basins across Europe (Stahl et al., 2010). With the support of WATCH partners additional data were obtained from the Baltic countries (NVE) and the Spanish partners supplied supplementary data from Spain. Unfortunately it had to be concluded that it is indeed impossible to obtain streamflow data from Poland and some other Eastern European countries as well as from Italy, where data collecting agencies are regional and quality control is limited (see Figure 2.2). WATCH partners have collaborated on the consolidation of the different data sets, including harmonizing of data formats. The time series were further quality controlled in response to experiences made in the initial analysis. Good data quality during low flow period is crucial for any evaluation of prediction uncertainty.
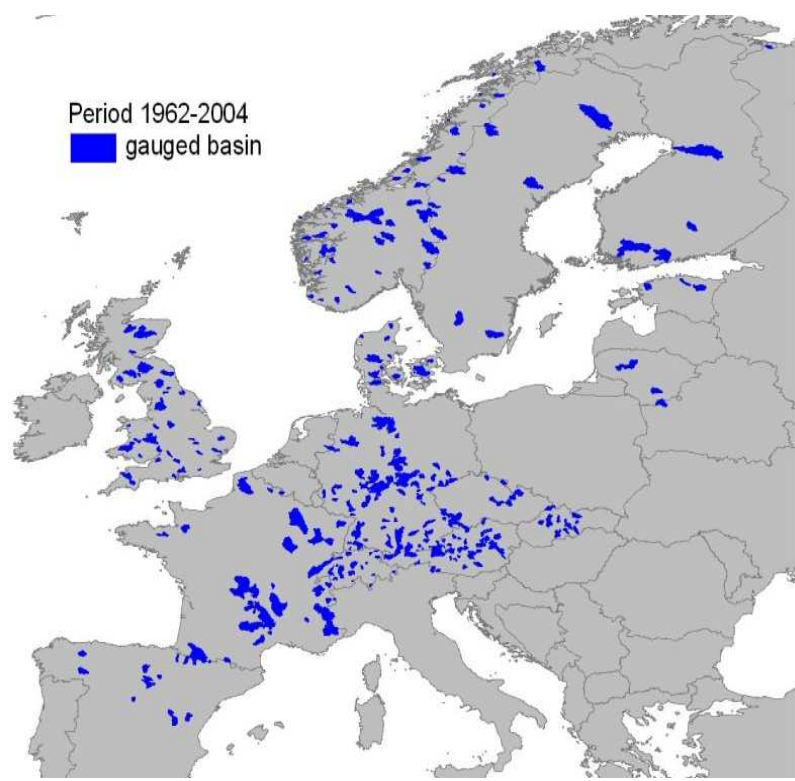
Figure 2.2 - *Overview of daily streamflow series (map shows catchment boundaries) for selected countries in Europe (EWA and additional sources).*

A multi-model ensemble of nine large-scale hydrological models was compared to the independent runoff observations from 426 small catchments in Europe. to evaluate their ability to capture key features of hydrological variability and extremes, including the inter-annual variability of spatially aggregated annual time series of five runoff percentiles derived from daily time series - including annual low and high flows (Gudmundsson et al., submitted). Overall, the models capture the inter-annual variability of low, mean and high flows well. However, high flow was on average found to be better simulated than low flow (Figure 2.3; note that absolute values in mm/day are given). Further, the spread among the models was largest for low flow (relative bias), which reflects the uncertainty associated with the representation of terrestrial hydrological processes. The large spread in model performance implies that the application and interpretation of one single model should be done with caution as there is a high risk of biased conclusions. However, this large spread is contrasted by the overall good performance of the ensemble mean, constructed as the average of all model simulations.
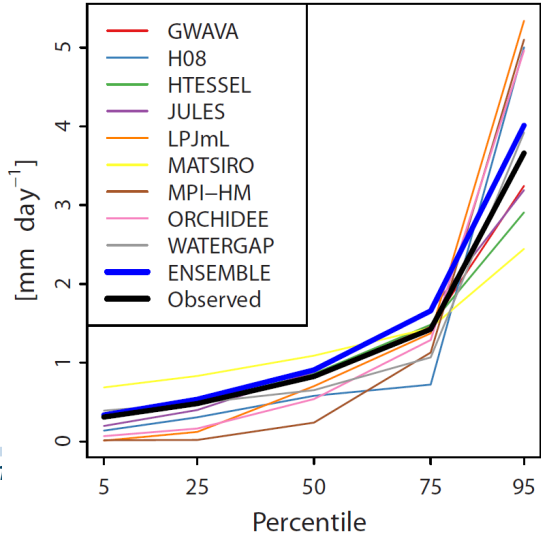

Figure 2.3 Mean runoff for the different *percentiles series (based on exceedance frequencies).*

Experiments in detection and attribution of runoff changes in the twentieth century.

Both climate and non-climate changes are likely to affect river flows. The non-climatic components likely to affect river flow through the 20th Century are the effects of:
a) atmospheric carbon dioxide on transpiration (and therefore runoff),
b) aerosols affecting the amount of shortwave radiation reaching the surface (and therefore the energy available for surface evaporation) and
c) land use through both energy and water availability.

As atmospheric CO_2 concentration increases CO_2 is able to diffuse across plant stomata more readily. Hence plants tend to close their stomata more at higher atmospheric CO_2 concentrations for a given water stress resulting in increased water use efficiency. There has also been a significant increase in global crop and pasture throughout the 20th Century.

The optimal fingerprinting technique of Tett et al, (2002) has been used. A number of simulations are carried out with different components of the model or forcing data fixed. Four separate simulations are carried out:
 a) WATCH climate forcing with no aerosols incorporated into the short wave surface radiation, land use and CO_2 set to 1901 values (control simulation);
 b) as for the control simulation but with CO_2 concentration varying throughout the 20th Century (CO_2);
 c) as for the control simulation but with land use varying throughout the 20th Century (land use); and
 d) as for the control simulation but with varying aerosols incorporated in the WATCH short wave forcing (aerosols). A fully "transient simulation" is estimated by adding the individual effects of CO_2, land use and aerosols together (i.e. assuming the system is linear).

In order to assess how well the model reproduces the observed river flow we assess how highly the modelled river flow is correlated to the observed river flow. There is generally a high correlation between modelled runoff and observed river flow for the control (i.e. "climate-only") simulation. This is especially the case over western Europe and the Central USA, indicating that the forcing data and/or observed river flow data are likely to be the most accurate over these regions.

The results show that including the changes in atmospheric CO_2, aerosols and land use all result in an increase in modelled runoff over the 20th Century relative to when only the "climate" forcing is used. These increases mainly occur over regions where there is significant runoff in the control simulation. This is to be expected as many of these runoff changes are a result of modifications to evaporation. Over arid regions these changes tend to lead to an increase in soil moisture only. Land use change has a more limited impact on runoff than aerosol or CO_2 changes.

References

Alcamo, J., P. Döll, T. Heinrichs, F. Kaspar, B. Lehner, T. Rösch, and S. Siebert, 2003: Development and testing of the WaterGAP 2 global model of water use and availability. *Hydro. Sci. J.*, **48**, 317-333.

Alcamo, J., M. Florke, and M. Marker, 2007: Future long-term changes in global water resources driven by socioeconomic and climatic change. *Hydrol. Sci. J.*, **52**, 247–275.

Arnell, N. W., 1999: A simple water balance model for the simulation of streamflow over a large geographic domain. *J. Hydrol*., **217**, 314-335.

Beven, K.J., 2001: Rainfall-runoff modeling: The Primer. *John Wiley, Chichester, UK.*

Blyth, E.M., 2001. Relative influence of vertical and horizontal processes in large-scale water and energy balance modelling. *IAHS Publ.* **270**, 3-10

Biemans, H., I. Haddeland, P. Kabat, F. Ludwig, R. W. A. Hutjes, J. Heinke, W. von Bloh, and D. Gerten, 2011, Impact of reservoirs on river discharge and irrigation water supply during the 20th century, *Water Resour. Res*., 47, W03509, doi:10.1029/2009WR008929.

Döll, P. and M. Flörke, 2005: Global-scale estimation of diffuse groundwater recharge. *Frankfurt Hydrology Paper 03, Institute of Physical Geography, Frankfurt University*

Döll, P. and S. Seibert, 2000: Global modeling of irrigation water requirements. *Water Resour. Res.* **38**, 1037, doi : 10.1029/2001WR000355.

Döll, P., K. Fiedler, and J. Zhang, 2009: Global-scale analysis of river flow alterations due to water withdrawals and reservoirs. *Hydrology and Earth System Sciences*, **13,** 2413-2432.

Gedney, N., P. M. Cox, R. A. Betts, O. Boucher, C. Huntingford, and P. A. Stott, 2006: Detection of a direct carbon dioxide effect in continental river runoff records. *Nature* **439**, 835–838.

Gudmundsson, L., Tallaksen, L. M., Stahl, K., Dumont, Clark, D., Hagemann, S., Bertrand, N., Gerten, D., Hanasaki, N., Heinke, J., Voß, F. & Koirala, S., submitted, 2011. Comparing large-scale Hydrological Models to Observed Runoff Percentiles in Europe. *J. Hydrometeo.*

Haddeland, I., D.B. Clark, W. Franssen, F. Ludwig, F. Voss, N.W. Arnell, N. Bertrand, M. Best, S. Folwell, D. Gerten, S. Gomes, S. N. Gosling, S. Hagemann, N. Hanasaki, R.J. Harding, J. Heinke, P. Kabat., S. Koirala, T. Oki, J. Polcher, T. Stacke, P. Viterbo, G.P. Weedon , P. Yeh, 2011. Multi-Model Estimate of the Global Water Balance: Setup and First Results. *J. of Hydrometeorology*, accepted.

Liang, X., D. P. Lettenmaier, E. F. Wood and S. J. Burges, 1994: A simple hydrologically based model of land surface water and energy fluxes for general circulation models. *J. Geophys. Res.* **99** (D7), 14415-14428.

Moore, R.J. 2007. The PDM rainfall-runoff model. *HESS*, **11**, 483-499

Stahl, K., Hisdal, H., Hannaford, J., Tallaksen, L. M., van Lanen, H. A. J., Sauquet, E., Demuth, S., Fendekova, M., and Jódar, J. (2010) Streamflow trends in Europe: evidence from a dataset of near-natural catchments, *Hydrol. Earth Syst. Sci*., **14**, 2367-2382.

Tett SFB, Jones GS, Stott PA, Hill DC, Mitchell JFB, Allen MR, Ingram WJ, Johns TC, Johnson CE, Jones A, Roberts DL, Sexton DMH, Woodage MJ (2002) Estimation of natural and anthropogenic contributions to 20th century temperature change. J Geophys Res 107:doi 10.1029/2000JD000028

3. Non- Climate drivers to changes in the Global Water Cycle

Spatial driver datasets, i.e. population, land cover and use, and sectoral water demands are essential to drive and inform large-scale hydrology and water resource models. In the first year of WATCH, the population datasets were completed along with current land use datasets. In the second year datasets on past and future land cover and land use, along with supporting datasets were developed and work began on datasets of sectoral water. In the third year, the focus was on updating, enhancing, and refining the datasets developed already and further developing the datasets of sectoral water uses. In the final year, the datasets of sectoral water uses were completed and delivered. Work also continued to improve and refine datasets, while responded to more specialized requests for data by project partners for use with their own models. Highlights of achievements during the year are listed below:

- The report describing the methodology used for spatially explicit estimates of past and present manufacturing and energy water use was finalized and made available as Technical Report 23.
- The report on projections of future sectoral water uses was made available, Technical Report 46.
- The final future land use scenario under the SRES B1 socio-economic scenario was completed, with the data made available at the website IIASA has used to distribute the other data it has made available for WATCH: http://www.iiasa.ac.at/Research/LUC/External-Watch/WATCHInternal/WATCHData.html.
- GAEZ3.0, the new global, spatial agricultural assessment has been completed, with the co-funding provided by FAO and IIASA. The data available includes:
  - land resources: soils terrain, and land cover shares.
  - agro-climatic resources, consisting of many agriculture specific climatic indicators.
  - agricultural suitability and potential yields for 92 land utilization groups under multiple management levels.
  - downscaled actual yields and production of more than 20 crop types; and
  - yield gaps between the potential yields at various levels of input and management and the actual downscaled yields of these same crops.

  The methodologies have been documented and an internet portal has been set up to access the terabytes of data and documentation at: http://www.iiasa.ac.at/Research/LUC/GAEZv3.0/.

- an index of crop production changes in the future scenarios to provided for water resource assessment (WB6).

- The methodology to downscale regional, national and sub-national agricultural statistics to grid-cell level has been revised and completed. Results of the downscaling are included in the GAEZ Portal mentioned above.
- The Global Reservoir and Dam (GRanD) database version 1.1 was released and made available along with the technical documentation.

4. The 21st Century Water Cycle

The focus of studies of 21st C water cycle have been on:

- the construction of the 21st century climate forcing data,

- the production of the naturalized global hydrological model simulations and their analysis,

- the impacts of the statistical bias correction on the projected climate change signals and associated uncertainties,

- the evaluation of regional climate model simulations over the Indian subcontinent, and

- investigating effects of anthropogenic influence on the terrestrial water cycle, such as imposed by land use change and irrigation.

Climate Models routinely produce large regional biases, particularly in precipitation. These biases are not only in the mean precipitation but also in its distribution in time. This is important for the application of hydrological models because of the substantial non-linearity of runoff generation. One established method to account for these biases is the bias correction methodology for daily precipitation. WATCH has developed new bias correction routines and applied them to global simulations for 21st C. Using the newly available WATCH hydrological forcing dataset as observation, daily precipitation and mean, maximum and minimum daily temperature have been corrected.

Bias correction – additive, linear or exponential

Given the diverse nature of observed precipitation climatology over the entire globe and for all seasons and the diverse nature of the climatological bias for different climate models, the main challenge was to devise an algorithm to select for every grid point, period and model the best possible type of correction, be it additive, linear or exponential. Figure 4.1 shows how the different choices of correction are mapped onto the globe when bias correcting the monthly decadal climatology of daily precipitation from the ECHAM5/MPIOM model.
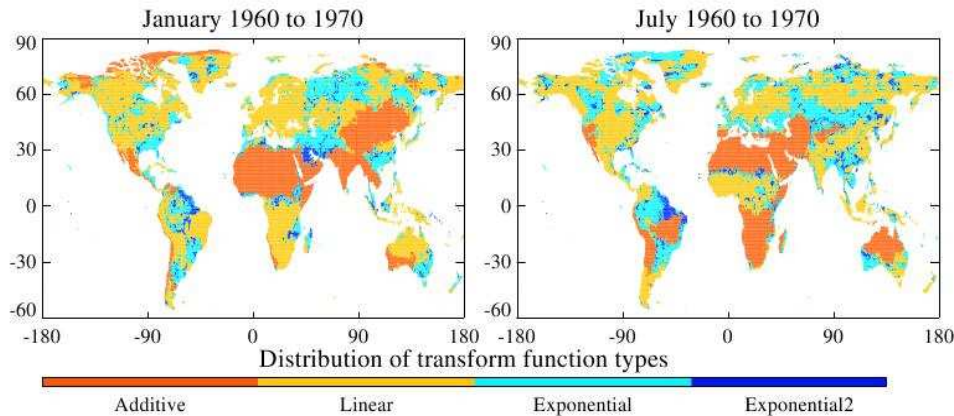
Figure 4.1: *Distribution of the choice of bias correction type over the globe for the month of January and July for daily precipitation from the ECHAM model. A simple additive correction is preferred when there are few wet days or when the mean precipitation is to low (red area). A linear correction is the standard choice (yellow). The exponential form is chosen when there is a strong discrepancy between the amount of drizzle (light blue and dark blue). The two choices of exponential correction differ only in how the curve fitting is done.*

The bias correction of the temperature variables (always linear) could not be carried out independently because this resulted in large relative errors in the amplitude and skewness of the daily temperature cycle. Instead, linear combinations of the temperature variables, which minimize interdependencies, are corrected and then used to reconstruct the required variables. The bias correction methodology and the algorithm for choice of correction type were distributed in the form of script and IDL code for ready application to all members of the WATCH community.

Data from three GCMs from the WATCH partners have been bias corrected: ECHAM5/MPIOM from MPI-M; CNRM-CM3 from CNRM; and LMDZ-4 from IPSL. These data have been finalized and stored on the WATCH ftp server at IIASA. For each GCM, the bias corrected data comprise a control period for current climate (1960-2000 using the WATCH Forcing data) and two SRES scenarios, B1 and A2, for the future climate of the 21st century (2001-2100).

The bias corrected 21st C data (The WATCH Driving Data) have been used to produce an ensemble of hydrological model outputs. Together with the WATCH community it was decided that the transient hydrology model simulations should follow the protocol defined within the WATCH WaterMIP.

The following GHMs provided simulation results for the full set of available forcing data, i.e. for all GCMs the 20th century control period as well as the future period (2001-2100) for both scenarios: Gwava,

LPJmL, MacPDM, MPI-HM, VIC and WaterGAP. For H08, HTESSEL and JULES, a subset of these simulations is available, comprising at least the control and A2 scenario periods from ECHAM5/MPIOM and CNRM-CM3. Note that all GHM runs are naturalized runs, i.e. direct anthropogenic influences on the hydrological cycle are not considered. In this respect, another subset of simulations was provided by the Orchidee model which also takes into account the effect of irrigation.

In order to identify areas with greatest change in the land-surface water balance, several analyses were conducted and published. From these results, catchment based maps of changes in available water resources can be highlighted, which identify areas that are vulnerable to projected climate changes with regard to water availability. In this respect available water resources are defined for various catchments around the globe as the total annual runoff (R) minus the mean environmental water requirements. According to Smakhtin et al. (2004), environmental water requirements (EWR) for a specific catchment can be roughly approximated by 30% of the total annual catchment runoff. Let us assume that these requirements obtained from the current climate simulations (1971-2000) will not significantly change until the end of the 21st century, and then the projected change in available water resources (ΔAW) can be determined as:

$$\Delta AW = (R_{Scen} - EWR) - (R_{C20} - EWR) / (R_{C20} - EWR) = (R_{Scen} - R_{C20}) / (R_{C20} - EWR)$$

Here, R_{C20} and R_{Scen} are the mean annual runoff for the current climate (1971-2000) and future scenario periods, respectively, and $EWR = 0.3 R_{C20}$. Figure 3 shows ΔAW for the period 2071-2100 according to the A2 scenario for a selection of about 90 catchments around the globe. Here, ΔAW was calculated from the multi-model ensemble mean runoff values averaged over the simulations from the 8 GHMs and the 3 GCMs, i.e. 24 simulations for the current and future climate each. Several regions can be identified were the available water resources are expected to significantly decrease (more than 10%), figure 4.2. These regions comprise Central, Eastern and Southern Europe, the catchments of Euphrates/Tigris in the Middle East, Mississippi in North America, Xun Jiang in Southern China, Murray in Australia, and Okawango and Limpopo in Southern Africa. But giving the large uncertainty induced by the choice of a GCM, it cannot be neglected that some regions might be affected by a significant future reduction in available water resources if this is even projected based on only one GCM. These results and some more details were published as WATCH technical report 45.
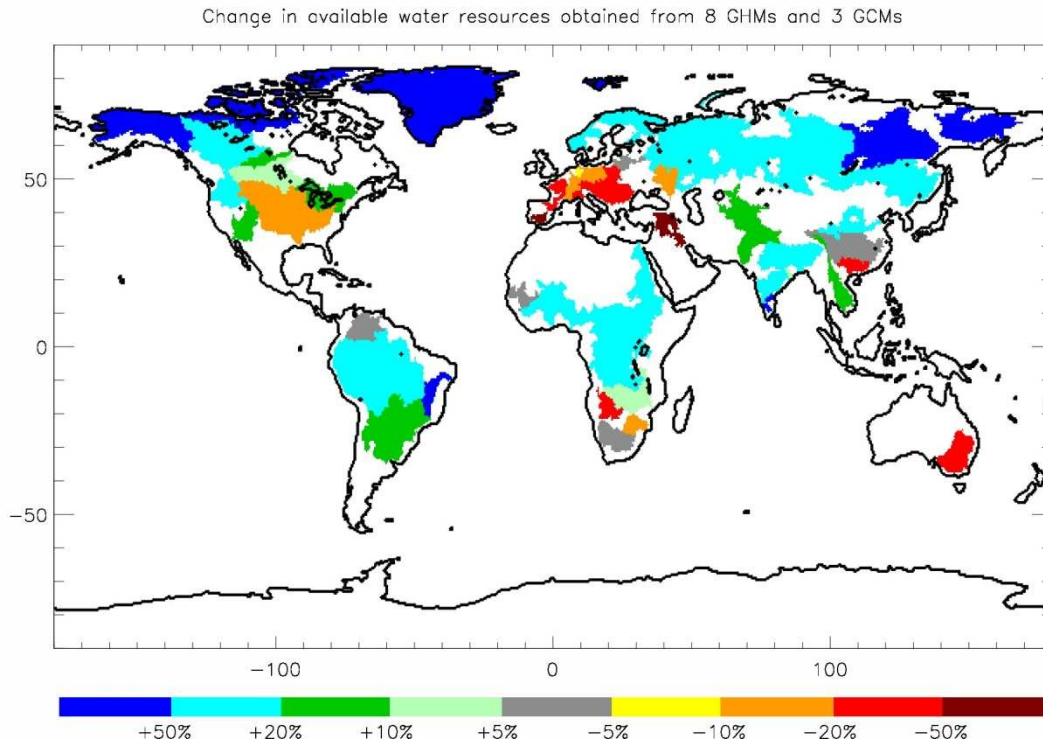
Figure 4.2: A2 changes (2071-2100 compared to 1971-2000) in available water resources over selected large-scale catchments projected by the 8 GHM ensemble averaged for all 3 GCMs

The regional model (REMO model) has been used for sensitivity simulations focusing on the impact of irrigation on the hydrological cycle over India under future climate conditions. Three 15-year time slices were conducted with a preceding 2-year spin up with and without irrigation over the South Asian domain at 0.5° (about 50 km) resolution. The model used GCM forcing data from an ECHAM5/MPIOM simulation (ECHAM5 henceforth) following the A1B scenario:

1. (1983) 1985-1999 Control

2. (2033) 2035-2049 Scenario I

3. (2083) 2085-2099 Scenario II

The results of the control simulations show that REMO has done a good job in downscaling the ECHAM5 data. The orographically induced precipitation highs over the Western Ghats and foothills of Himalaya are represented better in the REMO model due to its higher resolution as compared to ECHAM5. Moreover the rain shadowed area on the east of Western Ghats and high over the central India are also well simulated by the model. However, REMO shows the similar acute temperature bias of more than 5°C as was present in ECHAM5 simulation over northwestern India and Pakistan region.

In order to represent the irrigation in REMO, we have adopted the same methodology as presented by Saeed et al. (2009) with increasing the soil wetness at each time step to a critical value so that potential evapotranspiration may occur. As in their study, we have again observed the removal of the warm and dry biases over the regions of northwestern India and Pakistan, thereby showing the better simulation of these variables with the inclusion of representation of irrigation in the REMO model.
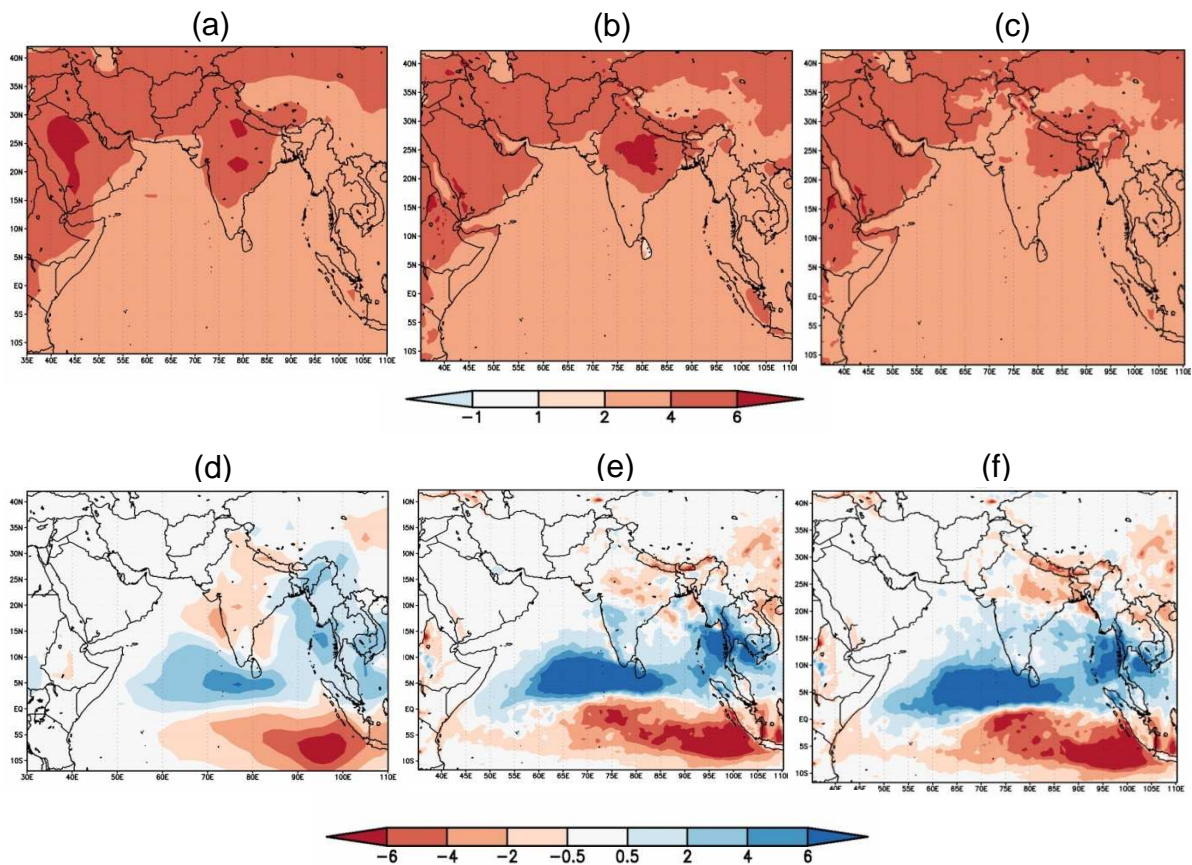
Figure 4.3. Scenario II (2085-2099) minus Control (1985-1999) for 2m temperature in °C (above panel) and Precipitation in mm/day (lower panel). The results of ECHAM5 (a and d), REMO without irrigation (b and e) and REMO with irrigation (c and f) are presented.

For the climate change simulations, the results of the Scenario II (2085-2099) minus control (1985-1999) are presented in the figure 4.3. Here, it is shown for the projected changes in 2m temperature that ECHAM5 and REMO without irrigation project an increase of more than 4°C in general and more than 6°C over the central Indian region. Whereas, the REMO simulation with irrigation projects much less warming as compared to the other two simulations, with a temperature increase ranging from 2°C to 4°C. For precipitation, both REMO versions with and without irrigation show similar climate change signals, with a decrease of precipitation over the northern Indian region and an increase in precipitation over the southern peninsular. Here, the signal projected by both REMO versions is different from that of ECHAM5 which shows a decrease of precipitation over the whole of South Asia except for Bangladesh and northeastern India, where the model projects an increase.

The present study highlights the role played by irrigation in attenuating the climate change signal over the South Asian region. Thus, it can be concluded that the irrigation within the 20th century may have already masked recent climate change signals over this region. The difference in the signals of 2m temperature between both versions of REMO (with and without irrigation) illustrates the importance of the representation of irrigation for carrying out any study over the South Asian region using climate models. The results are published as part of the WATCH technical report 47.

References

Saeed, F., S. Hagemann, and D. Jacob, 2009: Impact of irrigation on the South Asian summer monsoon. Geophys. Res. Lett., 36, L20711, doi:10.1029/2009GL040625.
Smakhtin, V., Revenga, C., Döll, P. , 2004). A pilot global assessment of environmental water requirements and scarcity. Water International, 29(3), 307-317.

5. Floods and Droughts: frequency, severity and scale

Changes in hydrological extremes (floods and droughts) are arguably the most important and visible consequences of climate change. While there has been considerable anecdotal evidence of the changing severity of extremes there have been very few systematic studies of past and future changes. The WATCH project has provided a unique opportunity to provide this across Europe and worldwide. The development of a powerful data base of observations from over 400 small catchments across Europe and the gridded data set of driving data and modelled flow data provides a massive resource to study the 20th and 21st century extremes and our uncertainties in how we represent and predict future flows.

Methodologies that quantify the space-time development of drought have been developed for the regional, continental and global scale (e.g. Corzo Perez et al., 2011a; Hannaford et al., 2011; Stahl & Tallaksen, 2010; Tallaksen et al., 2011). These have been applied to both observations and simulations from large-scale models (global hydrological models and land surface models). The combined observed streamflow dataset of the European Water Archive and the WATCH project described in Section 2 has provided the basis for the analyses in Europe.

Drought in the 20th Century

Drought can cause serious problems across much of Europe. Many droughts are localised and short, but others are widespread and cause environmental and social effects that cross national boundaries. The European Drought Catalogue (spanning 1961 – 2005) defines for 23 homogenous regions in Europe, time series of regional streamflow deficits; see figure 5.1 and Hannaford et al. (2011). This enabled a characterisation of major drought periods, in terms of duration, seasonality and spatial coherence in the various regions. An example of the catalogue is given for two contrasting regions in figure 5.2. A technical report presents the catalogue plots (like those shown in figure 5.2) for all twenty-three European regions, along with a commentary (Parry *et al.*, 2011).
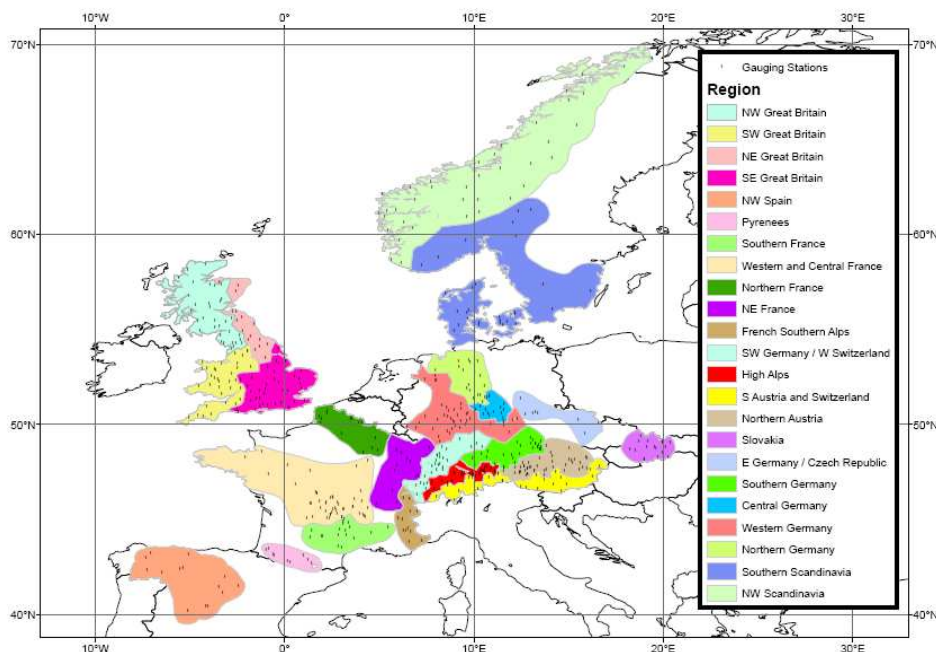

Figure 5.1   Regions used in the Drought Catalogue for Europe (Parry et al., 2011).
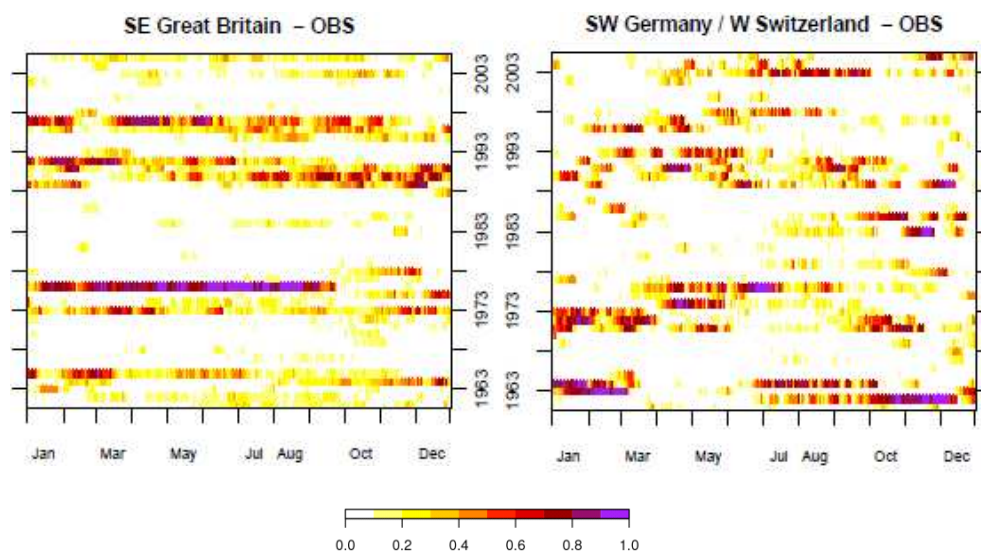
Figure 5.2: Drought catalogue derived from observed river flow gauges for two contrasting regions of Europe: Southeast Great Britain and Southwest Germany and West Switzerland. Month of the year are showed on the x axis, years on the y-axis. Colour shows the Regional Deficiency Index, a measure of the proportion of the region experiencing a flow deficiency (from Parry et al., in press.).

The drought catalogue data has also been used to examine the spatio-temporal evolution of large-scale European droughts. A Regional Drought Index (RDI) has been aggregated to a monthly basis, and has been used to show the month-by-month spatial evolution of major historical droughts, along with a parallel indicator of meteorological drought, the Regional Standardized Precipitation Index. These were also analysed alongside pressure and temperature anomaly plots and large-scale drivers such as the North Atlantic Oscillation and the East Atlantic/West Russia pattern, to examine the causes behind these major, pan-European events (Parry *et al.*, in revision). Finally, the catalogue data is being used as a benchmark dataset against which outputs of Global Hydrological Models and Land Surface Models can be tested.

The low-frequency components of observed monthly river flow have been analysed for the small catchment dataset in Europe. The low-frequency components, defined as fluctuations on time scales longer than one year, were analysed both with respect to their dominant space-time patterns as well as their contribution to the variance of monthly runoff. The analysis of observed streamflow and corresponding time series of precipitation and temperature, showed that the fraction of low-frequency variance of runoff is on average larger than, and not correlated to, the fraction of low-frequency variance of precipitation and temperature. However, it is correlated with mean climatic conditions and is on average lowest in catchments with significant influence of snow. Furthermore, it increases (decreases) under drier (wetter) conditions and is consistently lower in responsive catchments, with a high variability of daily runoff. The dynamics of low-frequency runoff follows well known continental-scale atmospheric features, whereas the proportion of variance attributed to low-frequency fluctuations is controlled by catchment processes and varies with mean climatic conditions (Gudmundsson *et al.*, HESSD 2011a).

A multi-model ensemble of nine large-scale hydrological models was compared to independent runoff observations from 426 small catchments in Europe to evaluate their ability to capture key features of hydrological variability in space and time. It was found that the location and timing of runoff deficits agree largely among the different models, which suggests a strong influence of the common forcing. However, severity and variability within the drought affected area varied among models and also

compared to the observations. This can partly be related to the conceptualization of hydrological processes in the different models (Tallaksen et al., 2011).

The average magnitude, amplitude as well as the timing of the mean annual cycle was assessed using monthly runoff data (Gudmundsson et al., in revision). Three regime classes were identified; RC1: snow dominated with a winter minimum and spring maximum, RC2: spring maximum and autumn minimum (eastern Europe) and RC3: winter maximum and summer minimum (central and western Europe). The study revealed large uncertainties associated with modeling runoff (figure 5.3). At the local (grid-cell) scale differences between observed and simulated runoff can be large, and contrasted by a relatively good regional average performance. Model performance varied systematically with climatic conditions and was best in regions with limited snow influence.
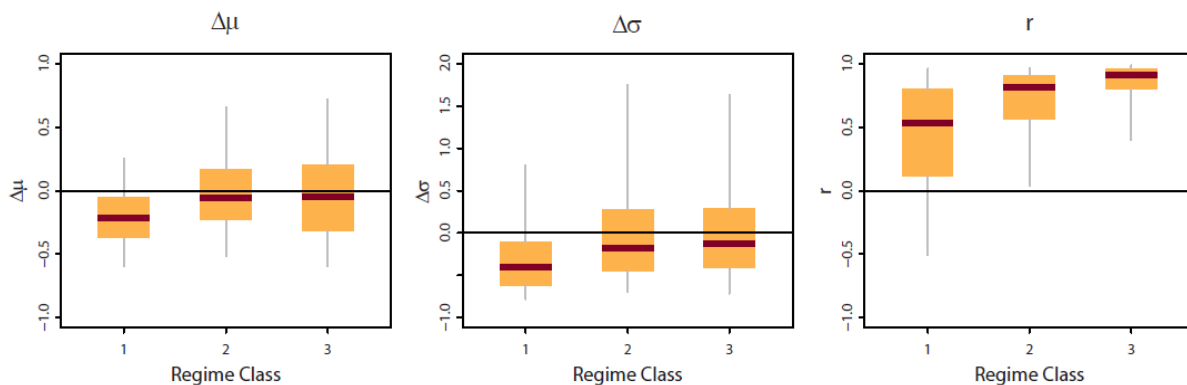

Figure 5.3. Average model performance for each regime-class as measured by the relative difference in mean (Δμ), the relative difference in standard deviation (Δσ) and the correlation (r). The dark horizontal bar is the median, the box covers the 25 to 75 percentile and the gray whiskers the 5 to 95 percentile.

Various trend detection studies have been performed to identify possible changes in historical streamflow series. This included an assessment of hydrological change (annual mean, monthly mean and low streamflow) in small basins at the sub grid scale of climate models based on the newly assembled and updated streamflow data set for Europe (Stahl et al., 2010). Figure 5.4a shows a regionally coherent picture of observed annual streamflow trends, with negative trends in southern and eastern regions, and generally positive trends elsewhere. In a follow-up study trend maps for annual and monthly runoff, and high and low flows across the whole of Europe (filling the white spaces on the map) are presented based on an ensemble of eight large-scale hydrological models. Modelled trends were validated against trends from 293 discharge records showing that the ensemble mean provides the best representation of trends. Estimates of change are particularly reliable for annual runoff, winter runoff, and high flows. The new trend maps reveal valuable details of a pronounced gradient between positive (wetter) trends in the Northwest and negative (drier) trends in the Mediterranean and in the Southeast (Figure 5.4b), and provide a considerable improvement over previously published maps of observed trends covering only parts of Europe (Stahl et al., 2011; Stahl et al., 2011, GRL in revision). The broad, continental-scale patterns of change are mostly congruent with the hydrological responses expected from future climatic changes, as projected by climate models.
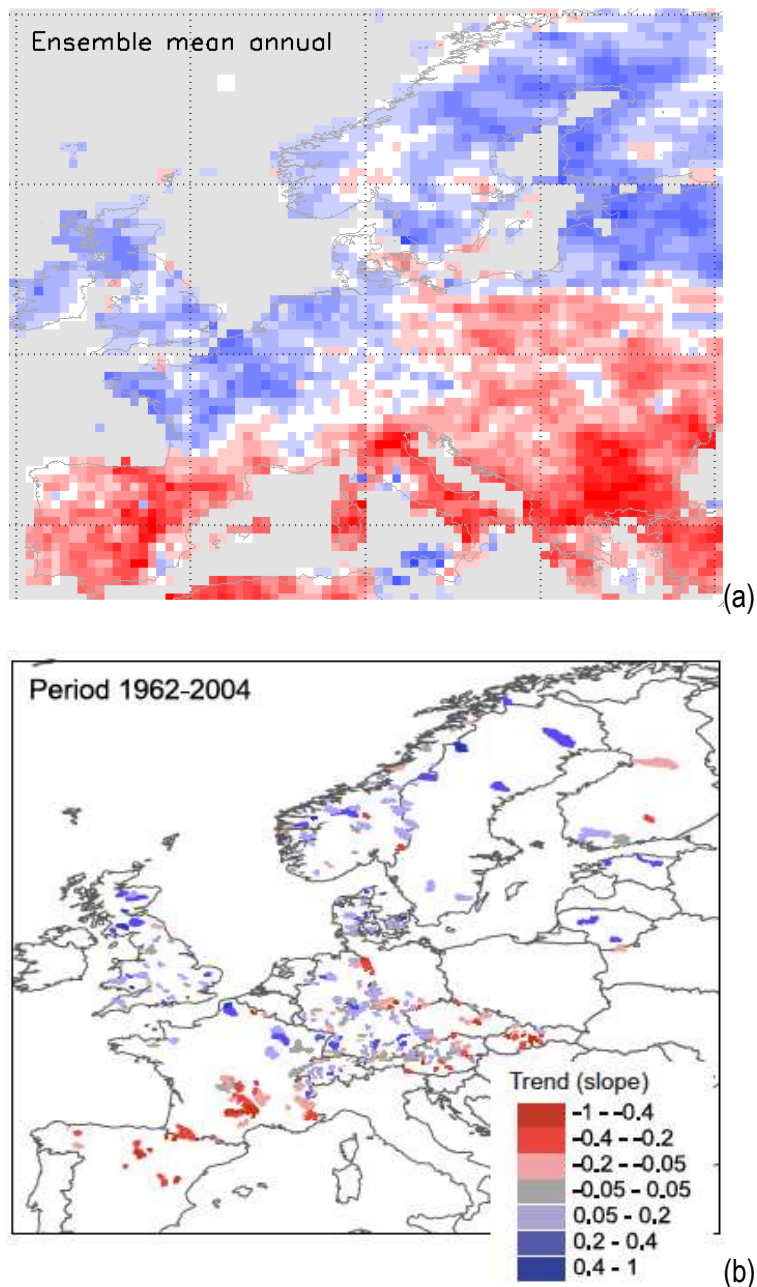
Figure 5.4.: Trends in annual runoff in Europe: a) observed and b) as simulated by a multi-model ensemble of eight large-scale hydrological models (from Stahl et al., 2011).

One key question in the WATCH project was to assess to what level do large-scale models (GHMs and LSMs) capture drought propagation as found through observations and detailed modelling (RBHMs) using the WATCH test basins: the Glomma (Norway), Upper-Elbe (Czech Republic), Upper-Guadiana (Spain); Upper-Nitra (Slovakia), Crete (Greece). These studies have been complemented with work in the Pang (UK) and Malawi (Africa). Therefore, drought propagation was explored in by intercomparing drought in different hydrometeorological variables among nine large-scale models and a RBHM (i.e. HBV). Furthermore, the multi-model ensemble mean was included. The outcome of these studies has been summarized in van Loon *et al.* (2011). Figure 5.5 provides an example from this comprehensive study. It shows for two drought events in the Upper-Metuje, the drought in precipitation, soil moisture, subsurface runoff and total runoff. The times series of the multi-model ensemble mean is given, as well as the variable threshold and the spread of the nine large-scale models.
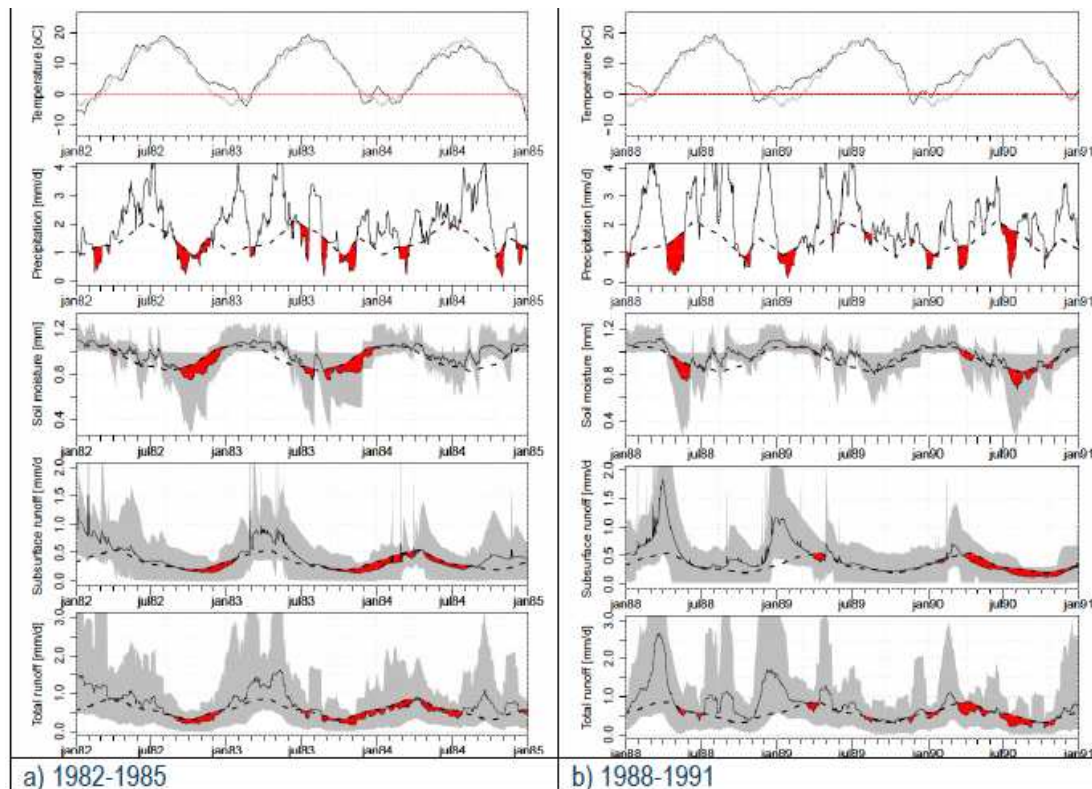
Figure 5.5. Drought in different hydrometeorological variables for two events in the Upper-Metuje, Czech Republic. Droughts are in red, the solid line gives the multi-model ensemble mean, the dashed line is the variable threshold, and the gray-shaded area shows the spread of the nine large-scale models (GHMs and LSMs)) (Van Loon et al., 2011)..

Van Loon *et al.* (2011) conclude that the main features of drought propagation are reproduced by all models in a number of selected river basins in Europe, i.e.:

- meteorological droughts are combined into a prolonged hydrological drought (pooling);
- meteorological droughts are attenuated when catchment storage is high at the start of the event (attenuation);
- a lag occurs between meteorological, soil moisture and hydrological drought (lag);
- droughts get longer moving from meteorological to soil moisture to hydrological drought (lengthening).

Differences among the models can be large (see spread, figure 5.5). In all river basins, meteorological droughts were most frequent. Soil moisture drought and hydrological droughts occurred less and had a longer duration. However, some problems still occur in basins with substantial snow accumulation (e.g. Narsjø basin) and basins with large storage in aquifers or lakes (e.g. Upper-Metuje & Upper-Sázava basin), where the ensemble mean is still too flashy. In these basins not all of the above features are correctly reproduced by the ensemble mean and especially attenuation of the drought signal is not reproduced in basins with storage. In general, the ensemble mean of these nine large-scale models gives a reasonable representation of drought propagation in contrasting basins in Europe. This is probably because flashy and smooth hydrographs of very different large-scale models are averaged out (van Loon *et al.*, 2011).
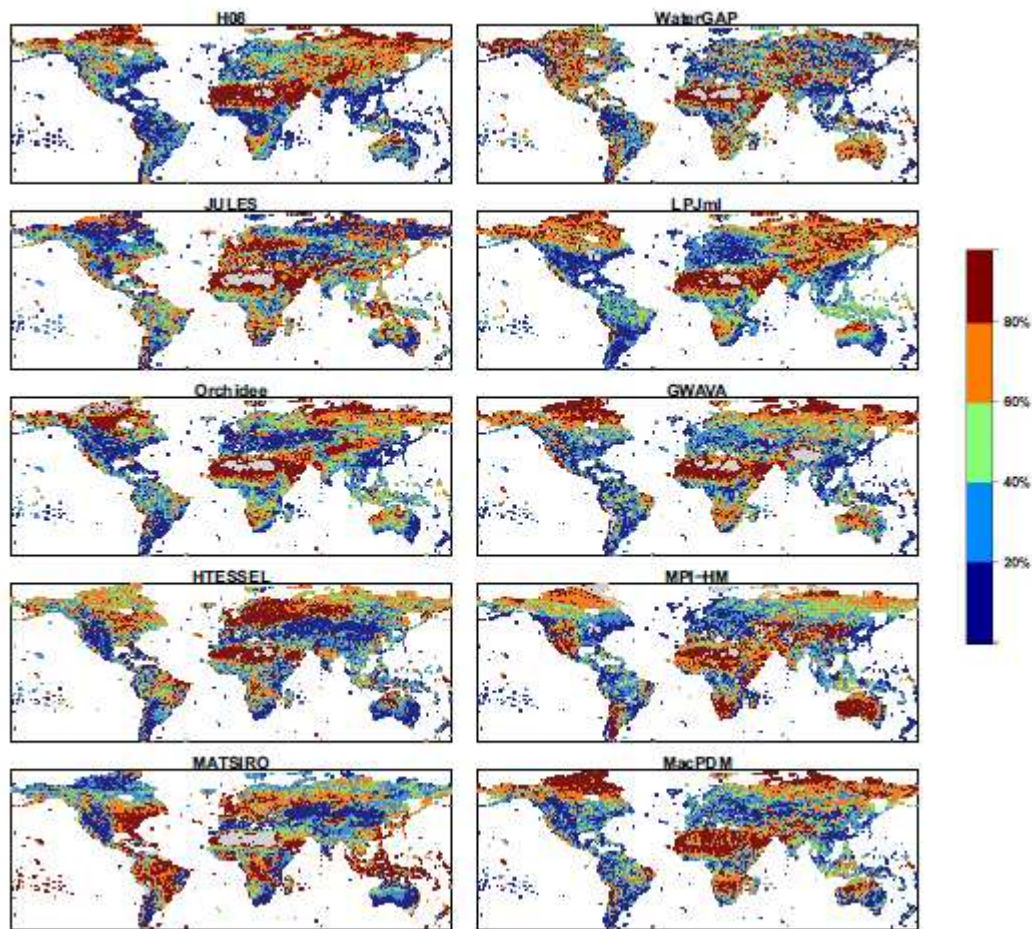
Figure 5.6   Average drought duration (expressed as percentile of the average drought duration of all land grid points) for five LSMs (left panel) and five GHMs (right panel), period 1963-2000 (Van Huijgevoort et al., 2011).

.

Global distribution of general drought characteristics (drought number, average drought duration, average deficit volume) derived from the large-scale models were compared. These characteristics show that the models give substantially different results when comparing absolute values. For example, the average number of drought for the whole globe varies from 94 to 131 for the LSMs and from 87 to 122 for the GHMs over the period 1963-2000. Therefore a relative measure was introduced for each land grid point and model, i.e. as percentile of drought numbers of all land grid points. Figure 5.6 shows the global distribution of average drought duration as percentiles for the ten large-scale models. Similar drought patterns among the models are observed when relative numbers are utilized. Areas with a high runoff, and thus also a high variability in runoff, have many short drought events. In contrast the driest areas in the world only have a few drought events of very long duration. Largest differences between the average duration occur in cold arid regions, which is associated with the diverse snow modelling schemes of the large-scale models (Van Huijgevoort et al., 2011).

Gridded time series of hydrometeorological variables from some large-scale models are also available for the first part of the 20th century (1906-1957), included a multi-model ensemble mean (six models). The NCDA approach was used to assess global hydrological drought for the whole 20th century based on runoff simulations of two global hydrological models (WaterGAP and GWAVA), two land surface models (HTESSEL and Orchidee), and the ensemble mean. Preliminary trend studies led to the investigation of the influence of thresholds of different time periods on hydrological drought. It appears

that the time window used to compute the threshold per land grid point substantially affects the outcome. Three types of time windows were defined: (i) whole 20th century, (ii) two periods (1906-1957 and 1958-2000), and (iii) seven sliding, overlapping 40-year periods (1906-1940, 1911-1950, 1921-1960, …., 1961-2000). In the final drought analysis the thresholds of the seven sliding time windows were used and the global area in drought was determined for the first and the second part of the century (1906-1957 and 1958-2000). Most models agree on a minor increase in the median of the area in drought for the second part of the 20th C (see also above). Plots of the monthly evolution of the global area in drought show this in more detail (Figure 5.7).
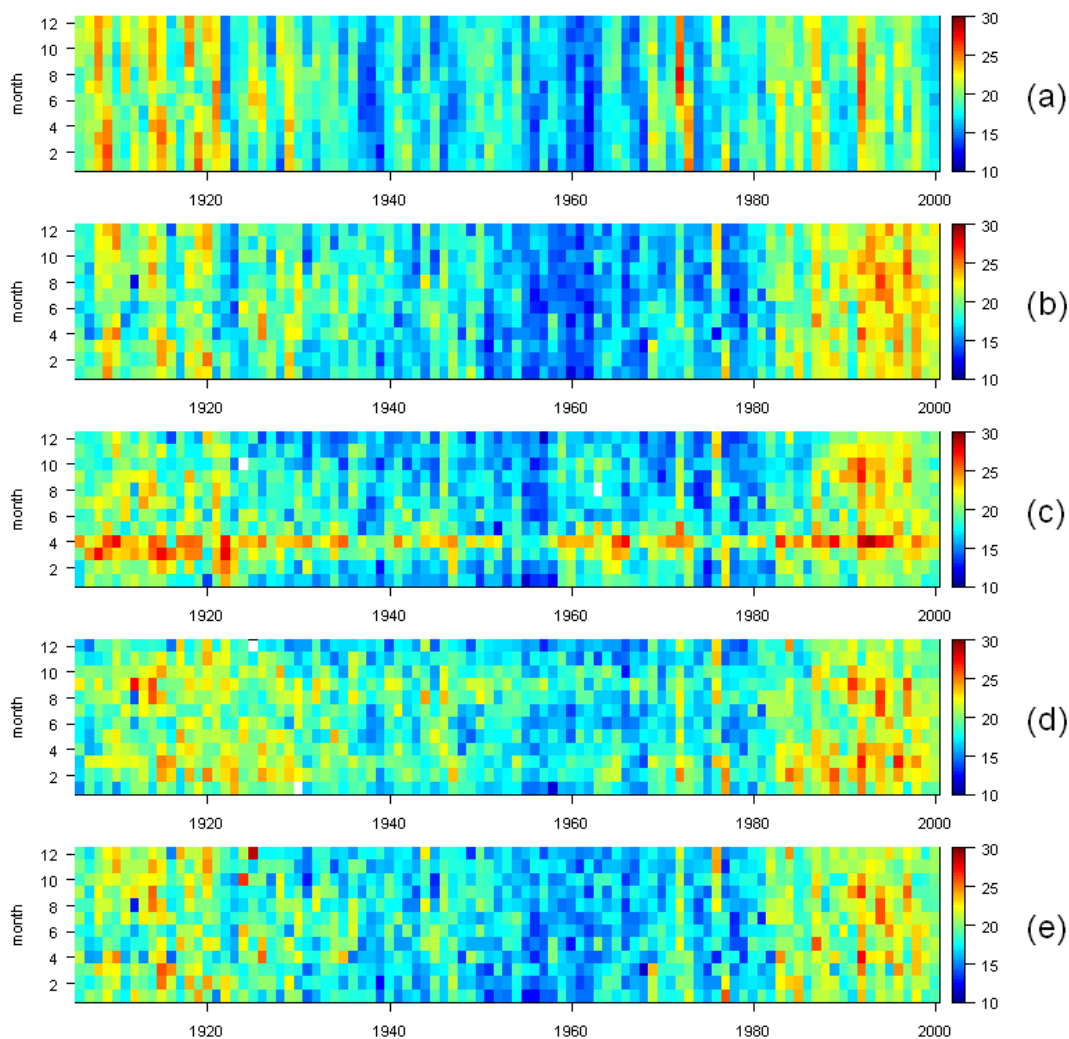

Figure 5.7   Percentage area of the globe in drought: (a) WaterGAP, (b) GWAVA, (c) HTESSEL, (d) Orchidee, and (e) multi-model ensemble mean (Estifanos et al., 2011)..

The area is larger in the first and last part of the 20th C. The first part is definitely affected by the low data availability that restricted bias correction of the WFD. The dry year 1992 clearly shows up in most models. Some models cause typical persistent drought patterns, e.g. HTESSEL in March and April, which likely is associated with simulation of snow melt. Similar plots are made for each of the continents that reveal rather clear temporal patterns for Asia and Africa and only weak patterns for Europe. The results of this study are summarized in a WATCH Technical Report (Estifanos *et al.*, 2011).

Floods in the 20th Century
The Flood Catalogue describing the major large-scale floods in the 20th century with their main physical aspects (frequency, severity, scale) is included in a WATCH sponsored IAHS book on "Changes in flood

risk in Europe" (Kundzewicz, Z.W. (Ed.)). Figure 5.11 provides an example from Chapter 5 "Changing floods in Europe".
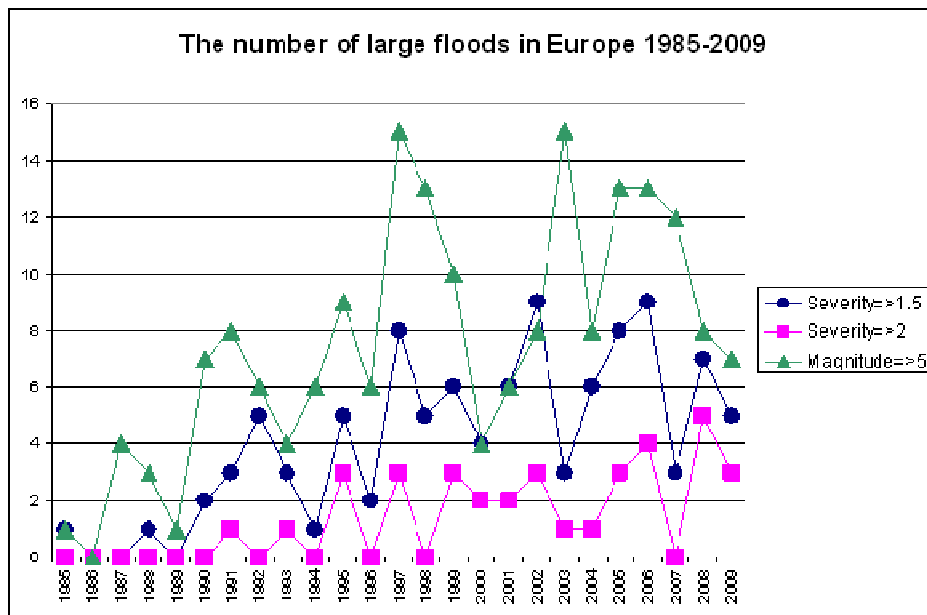

Figure 5.11.   Changing floods in Europe (Pinskwar et al., 2011).

Regional High Flow Indices (RHFIs) were derived from gridded total runoff (sum of surface and subsurface runoff) simulated by the WaterMIP global hydrological models for the same 23 regions of Europe selected for the European High Flow catalogue (Prudhomme *et al*. in press)

Interest in attributing the risk of damaging weather-related events to anthropogenic climate change is increasing. Yet climate models used to study the attribution problem typically do not resolve the weather systems associated with damaging events such as the UK floods of October and November 2000. Occurring during the wettest autumn in England and Wales since records began in 1766, these floods damaged nearly 10,000 properties across that region, disrupted services severely, and caused insured losses estimated at £1.3 billion. Although the flooding was deemed a 'wake-up call' to the impacts of climate change at the time, such claims are typically supported only by general thermodynamic arguments that suggest increased extreme precipitation under global warming, but fail to account fully for the complex hydrometeorology associated with flooding.

A multi-step, physically based 'probabilistic event attribution' framework showed that it is very likely that global anthropogenic greenhouse gas emissions substantially increased the risk of flood occurrence in England and Wales in autumn 2000. Several thousand seasonal-forecast-resolution climate model simulations of autumn 2000 weather were made, both under realistic conditions, and under conditions as they might have been had these greenhouse gas emissions and the resulting large-scale warming never occurred. Results are fed into a precipitation-runoff model that is used to simulate severe daily river runoff events in England and Wales (proxy indicators of flood events). The precise magnitude of the anthropogenic contribution remains uncertain, but in nine out of ten cases our model results indicate that twentieth-century anthropogenic greenhouse gas emissions increased the risk of floods occurring in England and Wales in autumn 2000 by more than 20%, and in two out of three cases by more than 90%, figure 5.8. See Pall et al (2011) for more details.

Attributable risk of severe daily river runoff for England and Wales autumn 2000.
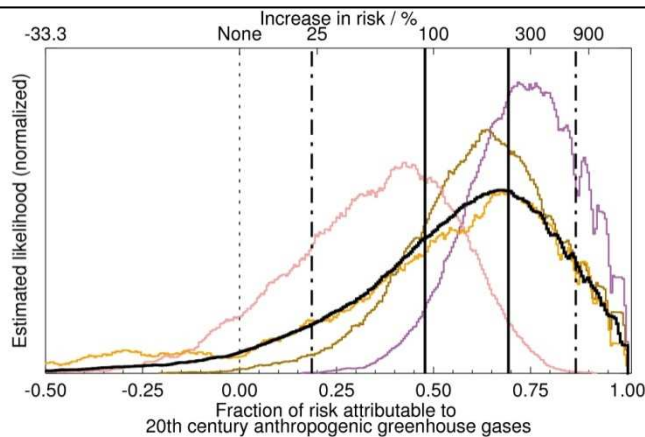
Figure 5.8. Histograms (smoothed) of the fraction of risk of severe synthetic runoff in the A2000 climate that is attributable to twentieth-century anthropogenic greenhouse gas emissions. Each coloured histogram shows this fraction of attributable risk (FAR) with respect to one of four A2000N climate estimates. The aggregate histogram (black) represents the FAR relative to the full A2000N climate, with the dot-dashed (solid) pair of vertical lines marking 10th and 90th (33rd and 66th) percentiles. Top axis is equivalent increase in risk.

Runoff regime in the 21st Century

The effect of changing CO_2 levels on the variability of global runoff was analyzed. Runoff variability was characterized using the coefficient of variation (i.e. the standard deviation divided by the mean) derived from monthly runoff, the mean annual cycle of runoff, and monthly runoff anomalies. The coefficient of variation of monthly runoff captures the total runoff variability disregarding the time scale and generating processes. Changes in the coefficient of variation of the mean annual cycle are related to changes of hydrological processes such as snow accumulation and melt as well as evapotranspiration, which influence both the timing as well as the magnitude of annual low and high flows statistics - such as the annual maximum or the annual minimum. The variability of runoff anomalies is in turn closely related to the intensity and number of rainfall-runoff events.

Model uncertainty was approached using a multi-model ensemble of eight large-scale models (GHMs and LSMs) most of them being forced with three different global circulation models, resulting in 23 ensemble members. Changes in runoff variability were assessed by comparing the thirty year control period (1971 - 2000) to the 2071 – 2100 time interval. Significance of the changes was assessed for each grid-cell individually using a signed rank test that takes model uncertainty into account (Gudmundsson *et al.*, 2011b). Significance is reported at the $p<0.01$ (Figure 5.14). Distinct global patterns are found in the control period (Figure 5.15, top panel) and runoff variability is highest in dry regions with low runoff and lowest in humid areas. Values larger than one indicate that runoff fluctuations are, on average, larger than the monthly runoff rate. The A2 emission scenario triggers significant changes in runoff variability (Figure 5.15, bottom panel). Runoff variability is predicted to decrease at northern latitudes, whereas an increase is predicted at mid latitudes (northern and southern hemisphere). The spatial patterns in change in runoff variability are discussed with respect to previously reported changes in mean runoff (Chen *et al.*, 2011). The decreasing runoff variability in the northernmost regions can likely be related to the diminishing importance of snow on runoff regimes in a warming climate. The increasing runoff variability at the mid latitudes suggest that increasing evaporation rates in a warming climate lead to an increase in runoff variability.

Further details of the study, including the calculation of significance, are given in (Gudmundsson *et al.*, 2011b). Changes in future runoff variability are investigated in a further study using a time scale dependent analysis (Gudmundsson *et al.*, 2011c).
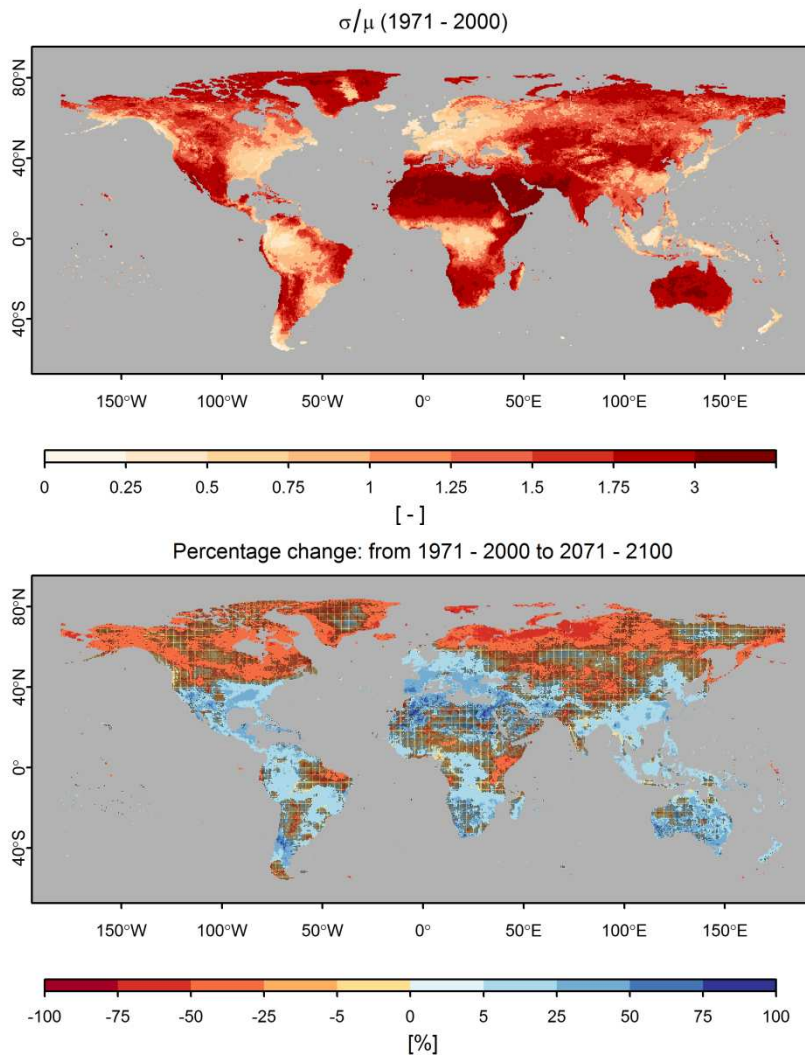

Figure 5.15.   Changes in total runoff variability. Top panel: Coefficient of variation of monthly runoff for the 1971 – 2000 control period. Bottom panel: Change (%) in the coefficient of variation of monthly runoff. Hatched areas indicate that the changes cannot be distinguished significantly from zero (p < 0.01) (Gudmundsson et al., 2011b).

Droughts in the 21st Century
The outputs of three climate models (ECHAM5, IPSL and CNRM) run under control and future emission scenarios were used, after a bias-correction procedure, was used to drive the WATCH GHMs. To produce the regional drought index (RHI) the moving threshold, which defines whether a flow is under deficit or not, was established for the control runs and used for both control and future period. This enables to assess whether the current characteristics of droughts (as defined as the proportion of a region under a river flow deficit) would significantly change in the future.

Figure 5.9 shows an example of RDI time series generated by three hydrological models (JULES, WATERGAP and MPI-HM) using the WATCH forcing data and using time series simulated by the three different climate models under historical greenhouse gases concentrations. The RDI generated by different hydrological models from the same input data show different characteristics, with MPI-HM

generating short events, while JULES and WATERGAP generate in this region much longer, spatial coherent events. In contrast, the difference due to the climate models is much more subtle. For this region, this would indicate that the uncertainty due to climate modelling (after bias correction) is smaller to that due to global hydrological modelling in reproducing droughts.

Figure 5.10 shows the results from the same model combinations for a future scenario assuming the A2 SRES emission scenario. As the threshold used to define the deficit was established from the control simulation, a change in the number and magnitude of the event would suggest that the change in the climate signal impacts on the drought generation in this region. For all three hydrological models, CNRM shows a strong change signal, with dryer late summer and autumn resulting in flow being systematically lower than the control threshold during several months while drought events nearly disappear from late winter to spring, suggesting an actually increase in runoff on those seasons. The same reduction of winter and spring event is suggested by ECHAM5, while IPSL arguably shows the weakest signal. While the way the three hydrological models generate drought episodes remain markedly different from each other, they all indicate similar signal of change in the drought occurrence when run with the same climate models. This would suggest that the uncertainty in climate model projection (i.e. different signal of change between IPSL and CNRM) remains important.
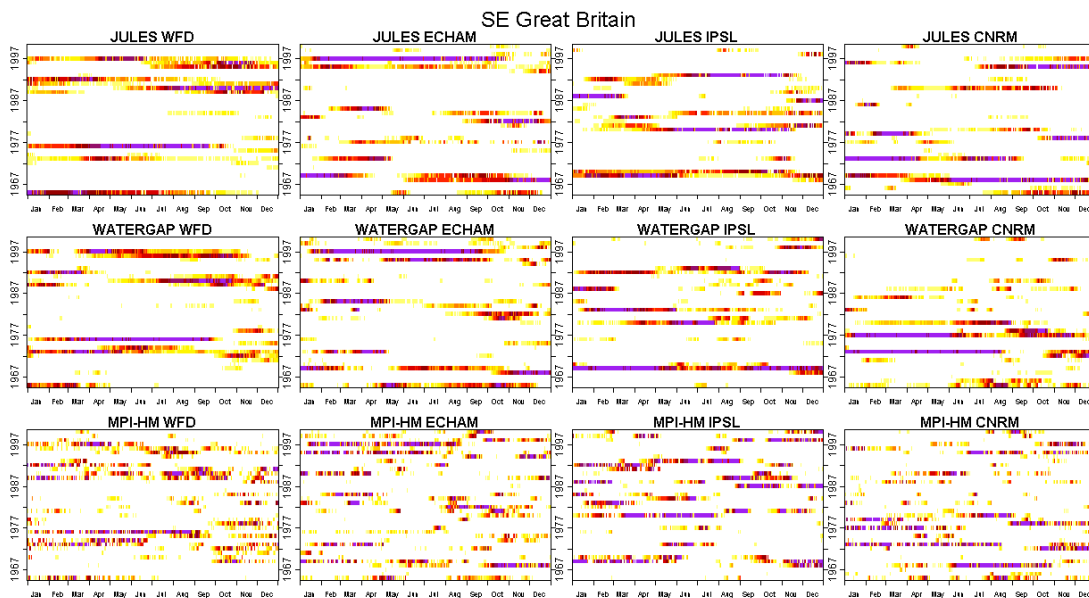

Figure 5.9: Regional Deficiency Index for Southeast Great Britain for the 20th century simulated with JULES (top), WATERGAP (middle) and MPI-HM (bottom) using observed (WATCH Forcing Data, 1957-2001), left) and bias-corrected control climate modelled by ECHAM (left), IPSL (middle) and CNRM (right)
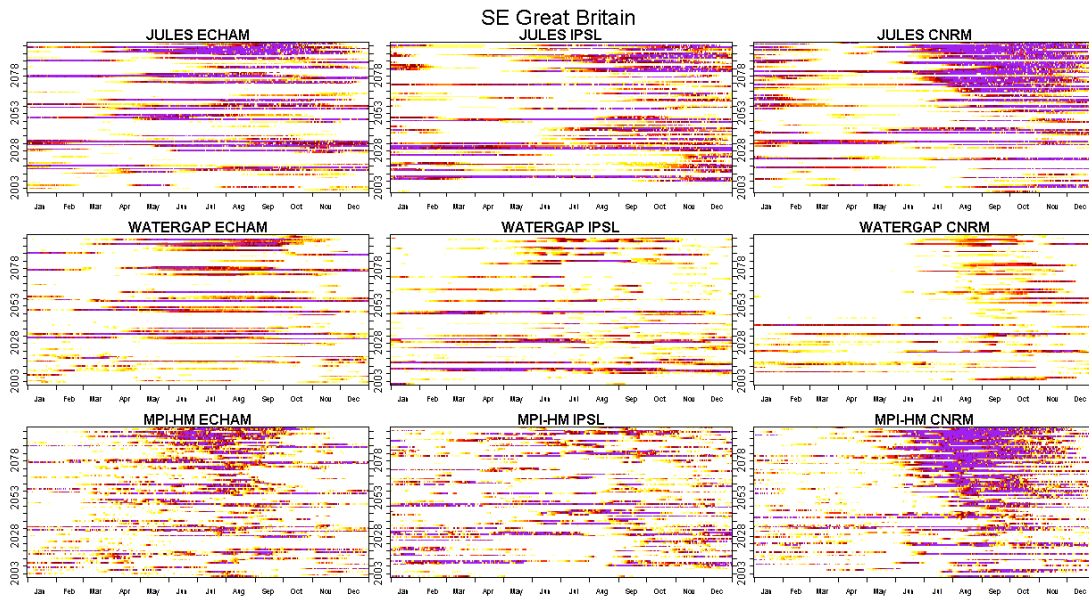
Figure 5.10: Regional Deficiency Index for Southeast Great Britain simulated under the A2 SRES emission scenario for 2070-2099 with JULES (top), WATERGAP (middle) and MPI-HM (bottom) using observed (WATCH Forcing Data, left) and bias-corrected climate modelled by ECHAM (left), IPSL (middle) and CNRM (right)

Future drought has also been explored at the global scale using a multi model ensemble of nine large-scale models (GHMs and LSMs), which are being forced with downscaled and bias-corrected (precipitation and temperature) from three different global circulation models for two emission scenarios (A2 and B1). Figure 5.x gives, as an example for three large-scale models, the number of global droughts for six forcings, which allowed: (i) to evaluate to what level GCMs can reproduce the current climate (CTRL) relevant for drought assessment, (ii) to explore impact of climate change, and (iii) explore influence of GCMs and emission scenarios.
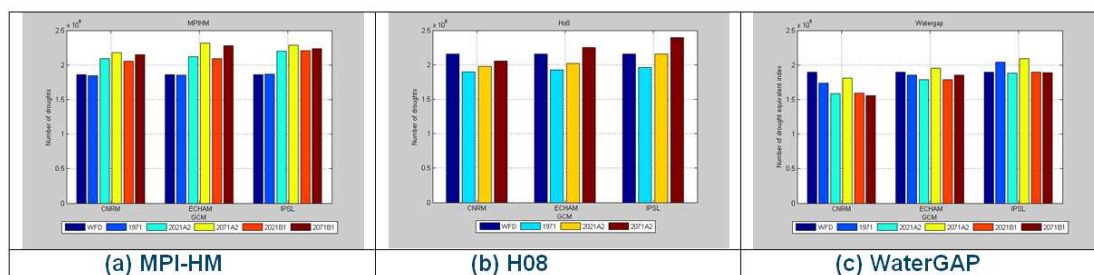

| (a) MPI-HM | (b) H08 | (c) WaterGAP |

Figure 5.x   Number of global droughts obtained from three large-scale models that were forced by: (i) WATCH Forcing Data 1971-2000 (WFD), (ii) GCM CRTL 1971-2000 (1971), (iii) GCM A2 forcing 2021-2050 (2021A2), (iv) GCM A2 forcing 2071-2100 (2071A2), (v) GCM B1 forcing 2021-2050 (2021B1), and (vi) GCM B1 forcing 2071-2100 (2071B1). The roman numbers give the order of the bars. H08 has not been forced with B1 emission scenario (Corzo Perez et al., 2011b).

Figure 5.x (left) shows that the number of droughts obtained from MPI-HM for WFD and the control period of all three GCMs are more less similar, which implies that the forcing of the GCMs can well reproduce the observed climatology (i.e. WFD) relevant for drought studies (small model uncertainty). For H08 the number of droughts with WFD as forcing are higher than with the forcings of all three GCMs (Figure 5.x, middle). WaterGAP does not have a consistent pattern (Figure 5.x, right), it depends on which GCM forcing (larger model uncertainty). MPI-HM reveals that the number of drought is expected to increase in the 21st century, and that the number by the end of the century is higher than in the midst.

The impact projected by ECHAM and CRNM is higher than for IPSL (climate uncertainty). The difference in increase of the number of droughts between the A2 and B1 emissions scenarios is rather small, although it is higher for A2 than B1 as expected (scenario uncertainty). H08 gives a similar climate change pattern for A2 as MPI-HM, although the change in the number of droughts in the future climate (compared to the CTRL) are similar to, or even smaller than, the differences between the WFD and the GCMs for the control period. WaterGAP projects a clear increase in the number of droughts by the end of 21st C compared to the middle of the century for the A2 scenario. However, the number seems to decrease until the mid of the century. The signal for the B1 scenario is less clear and dependent on the GCM. With the CRNM forcing there is a minor decrease from the mid to the end of the century, whereas for ECHAM the opposite is the case and IPSL does not show a change. WaterGAP also has deviations in the future number of droughts (as compared to the CTRL) that are similar to, or even smaller than, the differences between the WFD and the GCMs for the control period. Further details of the study, including the correction procedure for arid grid points and an additional part addressing the distribution of the drought durations, are given by Corzo Perez et al.. (2011b).

Floods in the 21st Century

Figure 5.12 shows the RHFI time series generated for West and Central France by three hydrological models (JULES, WATERGAP and MPI-HM) using the WATCH forcing data, a gridded observed time series as input and climate time series simulated by three different climate models under historical greenhouse gases concentrations. The uncertainty due to the global hydrological models is noticeable, with long, spatially coherent regional high flow events simulated by JULES most of the year except in summer when they tend to be much shorter. In contrast, WATERGAP simulates long (but not very spatio coherent) regional high flow events in the summer and short ones in the winter and spring. MPI-HM simulates very short events all year round. While different climate model inputs do not markedly change the characteristics of the simulated regional high flow indices for JULES and MPI-HM, WATERGAP is very sensitive to the climate input, with results using ECHAM5 very similar to those from WFD, but when run with IPSL or CNRM climate, the regional high flow events become much longer all year round, albeit less spatio coherent. Note that the bias correction procedure was designed, for each grid, to modify the monthly distribution of precipitation and temperature so they match as much as possible that of the WFD. However, the temporal sequencing (i.e. number of consecutive wet days) or the spatial pattern (the extent of wet areas during a day) remains unchanged from the original global climate model simulations. Such spatio-temporal characteristics of precipitation events will have a very strong impact on the runoff generation, as they will influence the soil moisture and the infiltration capacity, and by consequence, on the timing of high flow anomalies and the spatial coherence of those anomalies. The generated RFHI time series suggest that the hydrological processes included within WATERGAP are more sensitive to such sequencing than those of JULES and MPI-HM.
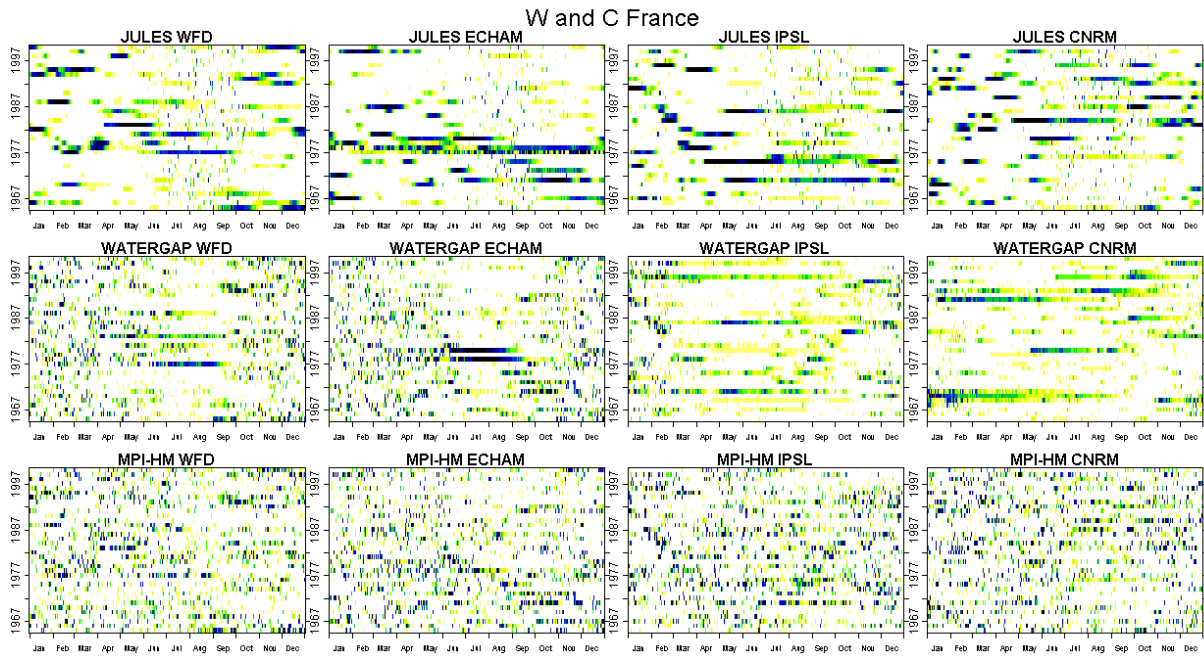
Figure 5.12: Regional High Flow Index for West and Central France for the 20th century simulated with JULES (top), WATERGAP (middle) and MPI-HM (bottom) using observed (WATCH Forcing Data, 1957-2001), left) and bias-corrected control climate modelled by ECHAM (second left), IPSL (middle) and CNRM (right)
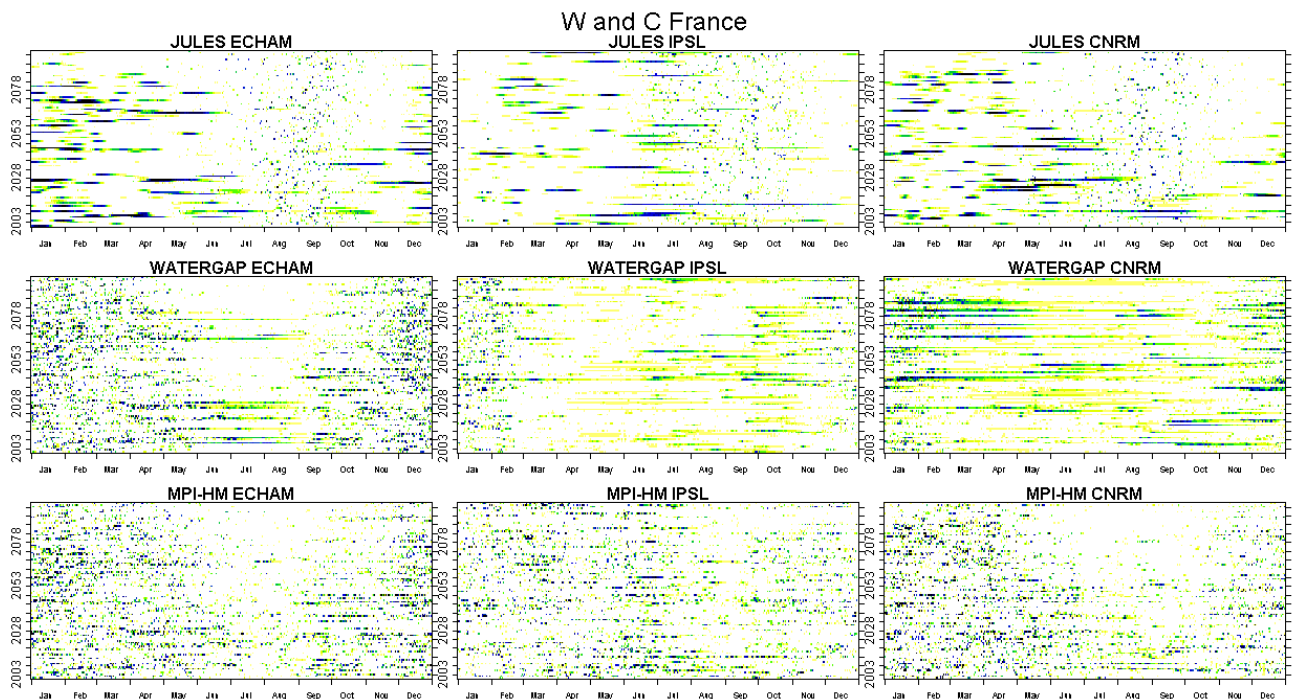

Figure 5.13: Regional High Flow Index for West and Central France simulated under the A2 SRES emission scenario for 2070-2099 with JULES (top), WATERGAP (middle) and MPI-HM (bottom) using bias-corrected climate modelled by ECHAM (left), IPSL (middle) and CNRM (right)

Figure 5.13 shows the results from the same model combinations for a future scenario assuming the A2 SRES emission scenario. As the threshold used to define the deficit was established from the control simulation, a change in the number and magnitude of the event would suggest that the change in the

climate signal impacts on the regional high flow generation in this region. All three climate models suggest a slight reduction in the number of RHFI events, in particular during autumn and winter. This would suggest a decrease in runoff by the end of 21st century. While the signature is slightly different for each climate model-hydrological model combination, the uncertainty in the signal is small for this region.

Climate change is expected to lead to shifts in the global hydrological cycle, resulting in regional changes in runoff quantity and greater variability in seasonal flows. This will potentially lead to significant changes in flood frequencies and magnitude altering regional flood growth curves. Flood frequency entails estimating the frequency of occurrence for a given peak flow, using a probability distribution fitted to an observed series of annual flood maxima. Assessing modelled runoff data for future periods against baseline conditions allows a comparison to be made between flood frequency curves, indicating whether extreme flood events will potentially become more common. An analysis of annual maximum series of peak flow was undertaken on the outputs of the WaterMIP global hydrological models JULES and WATERGAP run using the WATCH Forcing Data for the period 1963-2001, as benchmark data, and using the ECHAM5 model (control and 2070-2099 future under A2 SRES emission scenario).

For each period the annual maximum series (AMS) of peak flow were extracted based on a water-year from October to September, and a generalised extreme value (GEV) distribution fitted to the data using the method of L-moments. The steepness of the individual growth curves were quantified as the ratio between the 50-year and the 5-year flood as estimated from the GEV distributions.

Future changes in the growth curve were calculated: a decrease indicates that the difference between average and extreme flood events diminishes, while an increase shows a greater difference, perhaps suggesting an amplification of the extremes. Figure 5.14 shows the changes as simulated by WATERGAP run with ECHAM5 with increases in red and decreases in blue. While for most of Europe, the growth curve is projected to decrease or remain unchanged, Mediterranean and southern central European countries see their extreme floods increasing more that less extreme events.
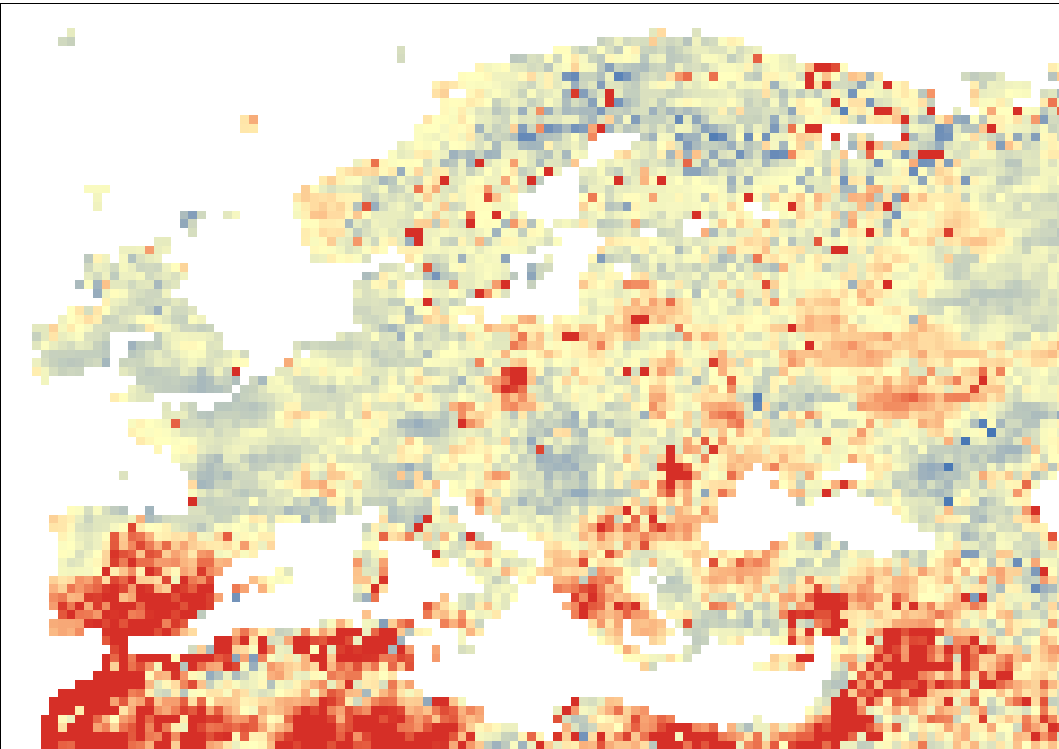
Figure 5.14: Change in the flood frequency growth curve between baseline (1965-1994) and future (2070-2099) periods as simulated by WATERGAP using ECHAM5 bias-corrected climate model input run under the A2 SRES emission scenario

Epilogue

WATCH has made significant progress in understanding and recording hydrological extremes in the 20th century and has provided the clearest evidence yet that it is possible to model these both on a European and global scale for the 21st Century. The WATCH forcing and driving data sets, in combination with the WATCH global hydrological models, provide an excellent global overview. However, it is clear the models need to be improved further, and WATCH has demonstrated that such improvements are accelerated by the availability of comprehensive and up-to-date observed data. Europe has a dense network of river flow measuring sites, but the data from these sites needs to be made more readily available, preferably through a single outlet. A system is already in place for flood warning at JRC in Ispra. This network could be expanded – an evenly spread network of 500 stations would be a starting point - to include sites that are suitable for drought studies.

References

Chen, C. *et al.* (2011). Projected hydrological changes in the 21st century and related uncertainties obtained from a multi-model ensemble. WATCH Technical Report Number 45.

Corzo Perez G.A., van Huijgevoort, M.H.J., Voss, F. & van Lanen, H.A.J. (2011a) On the spatio-temporal analysis of hydrological droughts from global hydrological models. Hydrol. Earth Syst. Sci. 15: 2963-2978, doi:10.5194/hess-15-2963-2011.

Corzo Perez, G.A., van Lanen, H.A.J., Bertrand, N., Chen, C., Clark, D., Folwell, S., Gosling, S., Hanasaki, N., Heinke, J. & Voβ, F. (2011b) Drought at the global scale in the 21st Century. WATCH Technical Report No. 43.

Estifanos *et al.* (2011), Multi-model analysis of drought at the global scale: differences in hydrological drought between the first and the second part of the 20th century. WATCH Technical Report No. 40

Gudmundsson, L.; Tallaksen, L.M.; Stahl, K. & Fleig, A.K. (2011a) Low-frequency variability of European runoff. *Hydrol. Earth Syst. Sci.*, 15, 2853-2869.

Gudmundsson, L., Wagener, T., Tallaksen, L.M. & Engeland, K. (in revision) Seasonal Evaluation of nine Large-Scale Hydrological Models Across Europe. Submitted to Water Resour. Res.,

Gudmundsson, L., Tallaksen, L.M. & Stahl, K. (2011b) Projected changes in future runoff variability - a multi model analysis using the A2 emission scenario. WATCH Technical Report Number 49.

Gudmundsson, L., L. M. Tallaksen, *et al.* (2011c). Projected changes in future runoff variance - a time scale dependent analysis. AGU fall meeting 2011, San Francisco, USA.

Hannaford et al. (2011) Examining the large-scale spatial coherence of European drought using regional indicators of precipitation and streamflow deficit, Hydrol. Process. 25 (7), 1146 – 1162.

Pardeep Pall**,** Tolu Aina**,** Dáithí A. Stone, Peter A. Stott, Toru Nozawa, Arno G. J. Hilberts, Dag Lohmann & Myles R. Allen. 2011. Anthropogenic greenhouse gas contribution to flood risk in England and Wales in autumn 2000. *Nature,* 470, 382–385

Parry, S., Prudhomme, D., Hannaford, J. & Williamson, J. (2011) Objective low flow catalogue for Europe. WATCH Technical report 33.

Parry et al. (in press) "Multi-year hydrological droughts in Europe: analysis of development and causes". Hydrology Research.

Prudhomme *et al.* (2011) How well do large-scale models simulate regional hydrological extremes? Journal of Hydrometeorology, WATCH Special Collection.

Stahl, K. & Tallaksen, L.M. (2010) RCM simulated and observed hydrological drought: a comparison of the 1976 and 2003 events in Europe (2010). In: Global Change: Facing Risks and Threats to Water Resources (Proc. of the Sixth World FRIEND Conference, Fez, Morocco, October 2010), IAHS Publ. 340, 150-156.

Stahl, K., Tallaksen, L.M., Gudmundsson, G. and Christensen, J.H. (2011) Streamflow data from small basins: a challenging test to high resolution regional climate modeling. *J. Hydromet.* **12(5)**, 900-912.

Stahl, K., Tallaksen, L.M., Hannaford, J. & van Lanen, H.A.J. (2011) Filling the white space on the map: recent European runoff trends from multi-model data. Submitted to GRL.

Tallaksen, L., Stahl, K. & Wong, G. (2011) Space-time characteristics of large-scale droughts in Europe derived from streamflow observations and WATCH multi-model simulations. WATCH Technical Report 48.

Van Huijgevoort, M.H.J., Hazenberg, P., van Lanen, H.A.J., Bertrand, N., Clark, D., Folwell, S., Gosling, S., Hanasaki, N., Heinke, J., Stacke, T. & Voβ, F. (2011) Drought at the global scale in the 2nd part of the 20th Century (1963-2001). WATCH Technical Report No. 42.

Van Loon *et al.* (2011), Propagation of drought through the hydrological cycle. WATCH Technical Report No. 31.

6. Evaporation and feedbacks

Climate change is only one of the drivers that will affect the water cycle in the future. Human activities – particularly deforestation – are changing large areas of the globe. This change – generally to shorter vegetation of crops and pasture – affects the overall surface energy balance and partition of energy into evaporation. This, in turn, has the potential to change not only river flows, but also large-scale weather patterns and hence rainfall. Engineering projects such as hydro-electric and irrigation schemes cannot be ignored, and the scale of these will only increase in response to a growing and an increasingly wealthy world population. Finally increasing CO_2 levels are likely to increase vegetation growth and water use efficiency which may directly affect evaporation.

There is an ongoing debate about the potential effects that increasing atmospheric CO_2 concentration has already had on the global water cycle and on river discharge in particular (Gedney et al. 2006; Pell & McMahon 2006; Piao et al. 2007; Kundzewicz et al. 2007; Huntington 2008). To contribute to this debate, we applied the global vegetation and hydrology model LPJmL to quantify the contribution of risen CO_2 concentration relative to the contributions of changing precipitation, temperature, land use and irrigation to worldwide trends in river discharge (Q) over the past century. In addition we repeated the seminal Gedney et al (2006) study, but this time including a dynamic vegetation model, so that both increased abundance as well as reduced transpiration could be simulated.

Both the models showed that rising CO_2 levels had the effect of decreasing the runoff in some dry-lands, indicating increased transpiration due to expanding vegetation, and increased runoff in parts of the northern hemisphere, indicating dominance of the transpiration-reducing physiological CO_2 effect. These spatial differences are due to the regional variations in the contrast of structural and physiological plant responses to increased CO_2. There is general agreement between the patterns simulated by JULES and LPJmL although exact regions of reduction differ. This is probably due to difference in simulated soil moisture stress and vegetation growth. The JULES model with dynamic vegetation resulted in a slightly smaller increase in global runoff of about ~1200 km3/yr (3.2%) by 1995. Thus, even if dynamical vegetation responses are included, JULES still simulates that increasing CO_2 has a noticeable positive impact on runoff over the 20th century. The LPJmL model shows the same tendency, but the magnitude of the CO_2 effect is smaller in that model (405 km3/yr, or 1.1%, over the period 1901–1995).This result supports Gedney et al.'s (2006) finding that the rise in CO_2 increased global runoff over 1960–1994 and supports the analysis of Huntington [2008], who showed that the magnitude of CO_2-induced reductions in transpiration was secondary in size to the changes in precipitation (see Gerten et al 2008 and WATCH technical report 3 for more details).

WATCH has developed a satellite based methodology to estimate daily evaporation. The approach uses the Priestley and Taylor evaporation equation in combination with an independent Gash-based rainfall interception model, and soil water and stress modules (see Box). In general, the results show high correlation with FLUXNET in situ observations both at daily (R=0.83) and monthly (R=0.9) timescales. Moreover, no systematic bias for specific vegetation types or rainfall conditions has been detected. By overlaying the evaporation data set on land cover data, we can see that 30% of global land evaporation comes from tropical forests. If you add savannah to this, the figure rises to over 50%.

Twenty-year time series of global evaporation

The model, known as GLEAM (Global Land surface Evaporation: the Amsterdam Methodology), is designed to maximize the use of satellite-derived observations to create a spatially coherent estimate of the evaporative flux over land. For this reason, parameterisations are chosen that have global validity; whenever possible, constant parameters are preferred over those which vary across the globe. As a consequence, the methodology distinguishes only three sources of evaporation based on the land surface type: (1) bare soil, (2) short vegetation, and (3) vegetation with a tall canopy. The snow and ice sublimation is estimated for the pixels covered in snow through a separate routine. The contribution of lakes and rivers is not modelled; the predicted evaporation therefore refers only to the land fraction of the total surface area of each grid cell. The land evaporation (E) of each grid-box is the sum of the evaporation modelled for each of the three land surface types (s), weighted by their fractional coverage (a):

$$E = \sum_{s=1}^{3} E_s a_s \qquad (1)$$

The global model is composed of four modules. In the first module, the evaporation of intercepted rainfall from forest canopies is calculated. A separate module describes the water budget that distributes the incoming precipitation (rain and snow) over the root-zone. In a third module, the stress conditions are parameterised as a function of the root-zone available water and dynamic vegetation information. Finally, the evaporation from each of the three surface components is calculated based on the PT equation, the modelled stress, rainfall interception. The figure below gives an overview of the structure of GLEAM.
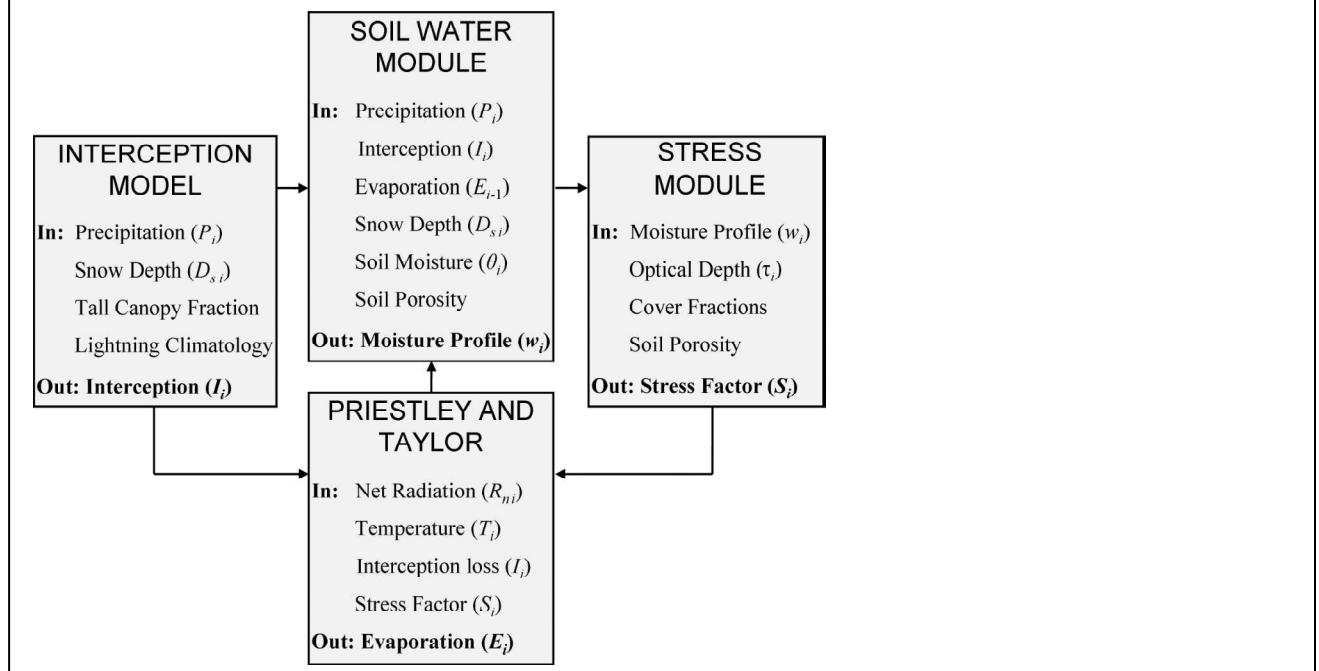
An average annual land evaporation of 67.9×10^3 km^3 is estimated for the period 2003–2007, which represents 58% of the incoming precipitation. South America, Asia and Africa are found to contribute together to 73% of the Transpiration contributes to 80% of global land-surface evaporation. Canopy interception loss is estimated as 11% and plays a major role in the long-term partition of rainfall and the volume of runoff generated in forested ecosystems, see Table 6.1.

Table 6.1: Annual precipitation (P), evaporation (E) and water available for runoff (P-E) divided by continents for the period 2003-2007. The contribution of rainfall interception loss (I) to E is also presented

Continent	P	E			P − E			I		
	mm	mm	10^3 km^3	%P	mm	10^3 km^3	%P	mm	10^3 km^3	%P
Africa	930	545	16.2	59	385	11.4	41	38	1.1	4
Antarctica	199	21	0.3	11	177	2.5	89	0	0.0	0
Asia	648	388	16.8	60	260	11.3	40	38	1.7	6
Europe	638	369	3.5	58	269	2.6	42	54	0.5	9
N. America	665	413	9.5	62	252	5.8	38	42	1.0	6
Oceania	795	519	4.6	65	276	2.5	35	50	0.4	6
S. America	1712	967	17.0	56	745	13.1	44	144	2.5	8
Total	799	463	67.9	58	336	49.0	42	50	7.2	6

The final GLEAM evaporation product is described in detail by Miralles et al.2010, 2011a, 2011b. The daily 0.25 degree Evaporation dataset spans a period from 1984 till 2007 and is free available on the following ftp site 130.37.78.12 (user: adaguest, pwd: downloader) .
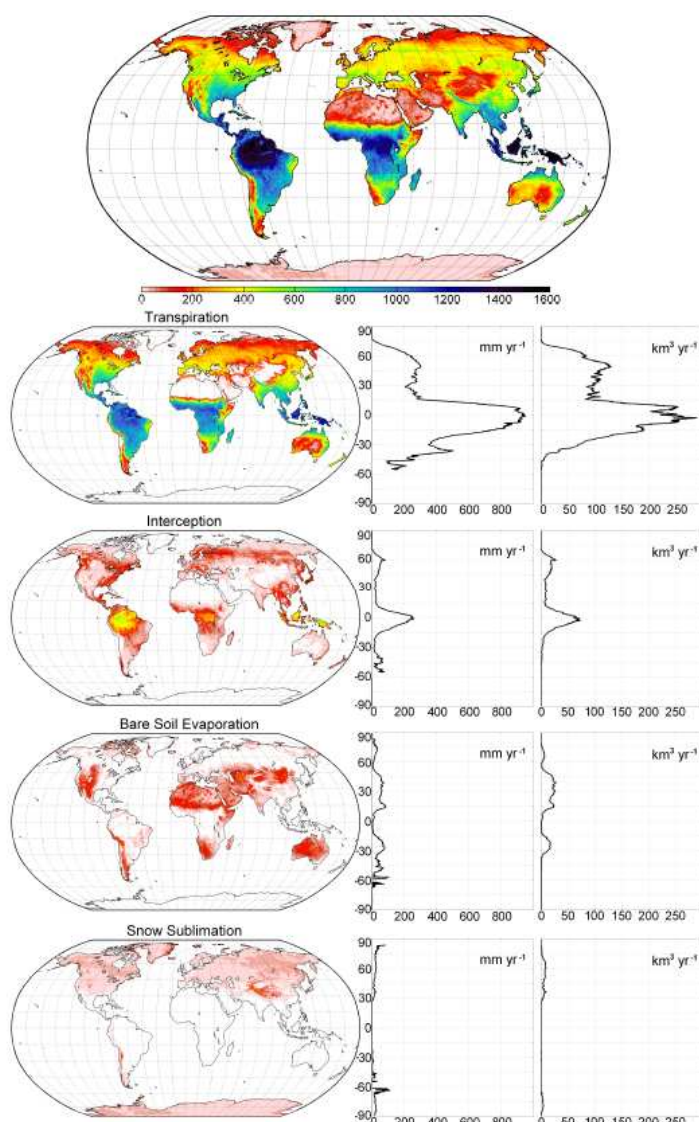

Figure 6.1. Decomposition of 2003-2007 average annual evaporation (mm) into its contributing fluxes. The latitudinal profiles are shown in units of mm yr-1 and km3 yr-1

WATCH Evaporation from VU contributed to the ground breaking report on observed global evaporation trends, published in Nature (Jung et al, 2010). Acceleration or intensification of the hydrological cycle with global warming is a long-standing paradigm in climate research, but direct observational evidence of a positive trend in global evaporation is still lacking (Huntington T.G. 2006). A combination of global land surface observed evaporation products were assessed at monthly time steps and the results suggest that the rate of land ET increased from the early 1980s to the late 1990s with a linear trend of 7.161mm per year per decade for 1982–1997 (P,0.01 according to the Mann–Kendall test). The positive trend shown in Fig. 6.2 is consistent with the expected 'acceleration' of the hydrological cycle caused by an increased evaporative demand associated with rising radiative forcing and temperatures. Indeed,

interannual variability in temperature correlates well with evaporation variability from 1982 to 1997 (Pearson's correlation coefficient 0.84, P,0.01). However, this trend disappears after the last big El Niño event in 1998.

GLEAM shows a similar trend with a similar increase over the first period and a decline in the last part. We are cautious regarding the robustness of this recent evaporation slowdown, given that the ensemble median is based on only relatively few models towards the end. Distinguishing land-evaporation response due to atmospheric demand from that due to terrestrial moisture-supply limitation is a classic ecohydrological problem. Evaporation responds to changing atmospheric demand, for example to changing radiation, or to changing vapour-pressure deficit, which is often associated with temperature, if there is sufficient moisture supply. In contrast, if the soils are too dry, evaporation becomes restricted by soil moisture. We analysed the spatial pattern of evaporation-trend changes and found that the largest regional contributions to the declining trend in global evaporation since 1998 originate from the Southern Hemisphere in Africa and Australia. The largest trend declines seem to have occurred in regions in which evaporation is limited by moisture
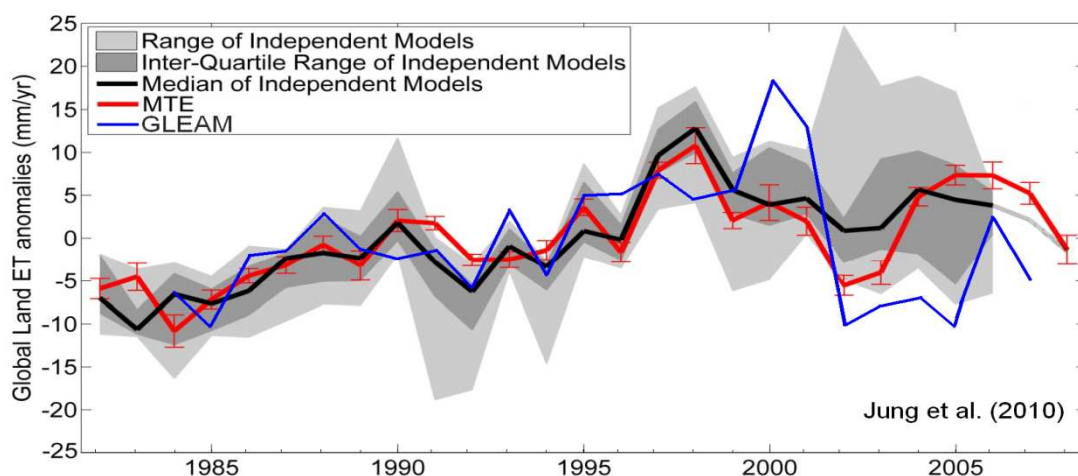

Figure 6.2: Annual global land ET anomalies based on MTE, GLEAM and an ensemble of up to nine independent process-oriented models. Error bars indicate one s.d. within the MTE (from Jung et al., 2010)

Changing soil moisture is likely to influence rainfall but only when soil moisture is limiting evaporation and where the atmospheric conditions are right. Studies have been undertaken to try to identify regions of the world where there is a detectable influence of soil moisture on rainfall. We have used satellite datasets of soil moisture and 3-hourly precipitation to examine evidence of feedbacks. Specifically, our analysis focuses on local afternoon rainfall maxima and the differences in antecedent soil moisture between these maxima and nearby minima. We find that in many semi-arid regions of the world (Africa, Australia, US Great Plains), rain maxima tend to occur more frequently over locally dry soils than would be expected purely by chance (at the 10% level, pink to red pixels in figure 6.3). Conversely, regions where rain is favoured over locally wet soils (blue pixels in figure) are much less numerous. This analysis suggests that when considering conditions across the globe, afternoon convection is favoured by drier rather than wetter soils locally i.e. a negative soil moisture – precipitation feedback. Evidence to support this somewhat surprising result comes from a recent study (Taylor et al 2011) for the Sahel region, where more spatially detailed datasets revealed a pronounced preference for convective initiation close to strong soil moisture gradients, with subsequent storm development on the dry side of the gradient.
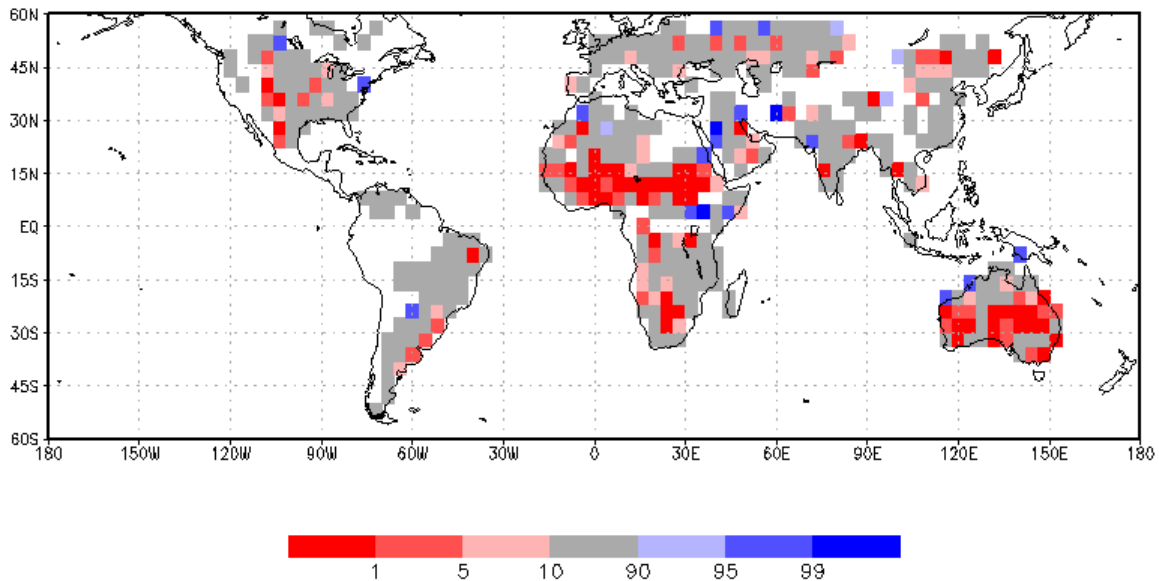
Figure 6.3. Afternoon rain events from the CMORPH dataset (Joyce et al 2004) for the period Jan 2003-Jul 2010 are analysed using soil moisture derived from the AMSR-E sensor (Owe et al 2008). For every afternoon rain event in the 4x4 degree boxes shown, differences in antecedent soil moisture over the local rainfall maximum and minimum were averaged. The shading shows the likelihood [%] of finding the observed mean soil moisture difference based on random resampling. The red shades (probability less than 10%) indicate a strong preference for rain to fall on locally dry soils, the blue shades for rain on locally wet soils. White areas are plotted where there are insufficient data to perform the calculation, whilst the probability for grey boxes lies within the range 10-90%. Overall, 29.7% of the shaded grid boxes are red compared to 4.9% blue.

Feedback from irrigated land to water cycle

The northern Indian subcontinent (the Ganges and Indus river basins) has the highest percentages of irrigated land of an extensive region anywhere in the world. This makes this region a useful test case to understand feedbacks between irrigated land and climate. Two lines of research have been followed. First, a trajectory analysis investigated the fate of irrigated water after evaporation. Second, an inter-comparison of regional climate models was carried out to analyse atmospheric effects of irrigation.

For river basins of Ganges and Indus, the fraction of evaporation that falls again as precipitation in the same river basin (the moisture recycling) can be determined. Furthermore, the seasonal variance of moisture recycling and the fraction of precipitation that originates from evaporation from the same river basin can be quantified. Using a quasi-isentropic moisture tracking scheme, evaporation from land surfaces in India is tracked through the atmosphere until precipitation brings it back to the land surface. The moisture tracking scheme is forced with ERA interim reanalysis data from 1990-2009. With the information about the atmospheric paths of water vapour, the distance between evaporation and precipitation location is determined. Thus, the fraction of evaporation that falls again as precipitation (or recycles) within a certain length scale is derived.

Results show a strong annual cycle in the recycling ratio. For the Ganges basin, the recycling ranges from 5% during the winter months (Nov-Mar) to 60% during the June-July-August (JJA) season. The comparison of irrigated and non-irrigated areas in the Ganges basin shows that there is more evaporation from the irrigated area during March until August. During the pre-monsoon months, up to 70% of the additional evaporation due to irrigation recycles within the Ganges basin.

The importance of basin moisture recycling for precipitation shows an annual cycle as well (see figure below). An annual average of 4.5% of precipitation originates from water evaporating in the Ganges basin. During the winter monsoon, all precipitation originates from sources outside the basin. During March-April-May (MAM) and Oct-Nov, 10% of the precipitation originates from evaporation within the basin. During the summer monsoon season, the large influx of moisture from the Indian Ocean dominates the precipitation and recycling is 5% of precipitation. Irrigation has the largest effect on the atmospheric part of the water cycle during May to September. During this period, recycling of evaporation from irrigated areas contributes about 2% more precipitation than recycling of evaporation from non-irrigated areas.
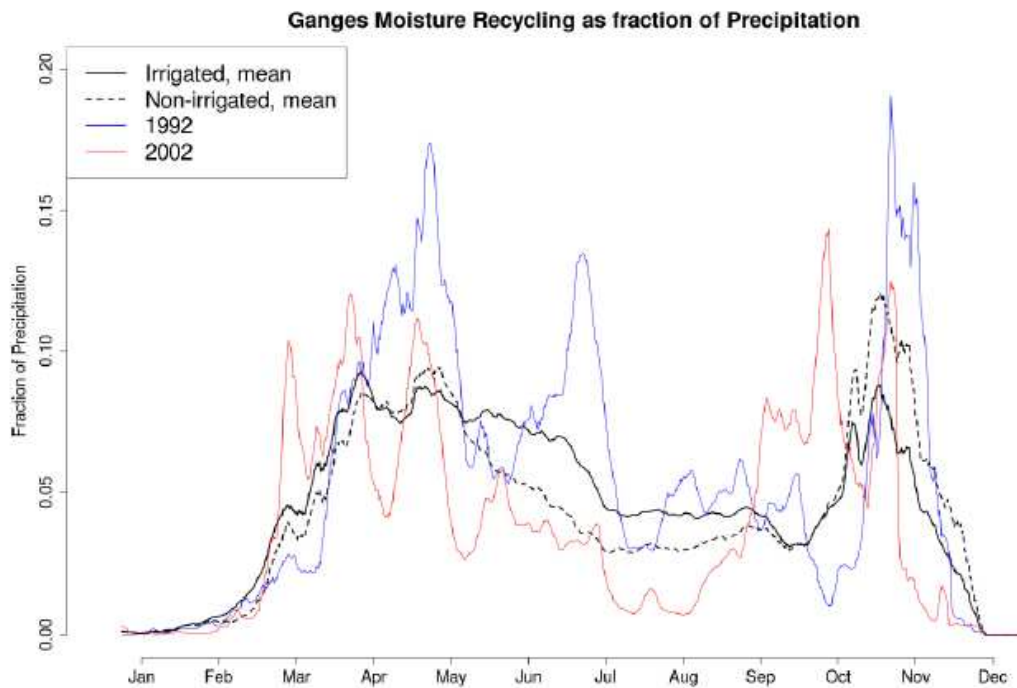

Figure 10: Relative importance of evaporation recycling compared to total precipitation in the Ganges basin, annual mean cycle for 1990–2009 for irrigated and non-irrigated parts of the basin and basin mean for two extreme years.

A WATCH irrigation intercomparison of Regional Climate Models has been undertaken. The ability of four regional climate models (RCMs) to represent the Indian monsoon was studied in a consistent framework for the period 1981–2000 using ERA40 reanalysis as lateral boundary forcing data. During the monsoon period, the RCMs are able to capture the spatial distribution of precipitation with maximum over the central and west coast of India, but with important biases at the regional scale on the east coast of India, in Bangladesh and Myanmar. Most models are too warm in the north of India, compared to the observations. This has an impact on the simulated mean-sea-level pressure from the RCMs, being in general too low compared to ERA40. Those biases perturb the land-sea temperature and pressure contrasts, which drive the monsoon dynamics and, as a consequence, lead to an overestimation of wind speed, especially over the sea. The timing of the monsoon onset of the RCMs is in good agreement with that obtained from observationally based gridded datasets, while the monsoon withdrawal is less well simulated. In summary, the spread at the regional scale between the RCMs indicates that important feedbacks and processes are poorly, or not taken into account, in the state-of-the-art regional climate models.

Across the 5 models participating in the IrriMIP activity considerable variations have been found in nearly all relevant variables and processes. Despite very similar algorithms determining the introduction of (irrigation) water when the soil moisture falls below a certain threshold, there is considerable variation in the introduced water accumulated over the seasons and sub-regions. For some models the evaporation enhancement seems to correlate with the irrigation water, for others the effect appears non-linear (e.g. RAMS) and in one model (HadRM) the evaporation is reduced following irrigation. The effective response of evaporation to soil moisture increases varies with its precise parameterisation and that of the vegetation. In addition, there are feedbacks in the land-atmosphere system that affect the surface evaporation. For instance, the HadRM response is modulated by an increase of cloudiness following irrigation which reduces the available energy at the surface, with negative consequences for evaporation (and even vegetation productivity). In the other models the (variously) increased evaporation always leads to opposite effects, i.e. reductions of moisture convergence and reduced cloudiness. However, the exact balance between the two determines whether irrigation ultimately leads to increased precipitation or to reduced rainfall. Some models also show a shift (delay) in the monsoon initiation following (pre-monsoon) irrigation.

The effects of humans changing the use of large areas of the Earth's surface are highly complex. Within regions it can be unclear as to the overall effect they are having, but WATCH has demonstrated that these changes should not be ignored. Climate models need to develop methods to represent the changes in land use, and they need to represent human activities such as irrigation. Until now we have treated climate and impact models separately. Climate models have been the providers of input data to the impact modellers. We must now aim to couple the models routinely. Impact models must not just receive data from the climate models, but also provide data to them in return. Only then will we be able to model feedbacks, and be able to estimate the effects of future planned (and unplanned) changes.

References

Gedney, N., P. M. Cox, R. A. Betts, O. Boucher, C. Huntingford, and P. A. Stott (2006), Detection of a direct carbon dioxide effect in continental river runoff records, *Nature, 439,* 835–838.

Gerten, D., Rost, S., von Bloh, W., Lucht, W. 2008. Causes of change in 20th century global river discharge. *Geophysical Research Letters*, Vol. 35, L20405, 5 PP doi:10.1029/2008GL035258

Huntington, T. G. Evidence for intensification of the global water cycle: review and synthesis. J. Hydrol. 319, 83–95 (2006).

Huntington, T. G. (2008), CO2-induced suppression of transpiration cannot explain increasing runoff, *Hydrol. Proc, 22,* 311–314.

Jung, M., Reichstein, M., Ciais, P., Seneviratne, S., Sheffield, J., Goulden, M., Bonan, G., Cescatti, A., Chen, J., de Jeu, R., Dolman, A. J.,

Joyce RJ, Janowiak JE, Arkin PA, Xie P. 2004. CMORPH: A Method that Produces Global Precipitation Estimates from Passive Microwave and Infrared Data at High Spatial and Temporal Resolution. *J. Hydromet.* 5: 487-503.

Kundzewicz, Z. W., et al. (2007), Freshwater resources and their management. In: *Climate Change 2007: Impacts, adaptation and vulnerability* (Eds. Parry, M. L., O. F. Canziani, J. P. Palutikof, P. J. van der Linden, and C. E. Hanson), Cambridge University Press, Cambridge and New York, 173–210.

Miralles, D. G., Crow, W. T., and Cosh, M. H.: Estimating spatial sampling errors in coarse-scale soil moisture estimates derived from point-scale observations, J. Hydrometeorol., 11, 1423–1429, 2010a.

Miralles, D. G., Gash, J. H., Holmes, T. R. H., de Jeu, R. A. M., and Dolman,A. J.: Global canopy interception from satellite observations, J. Geophys. Res.-Atmos., 115, D16122, 2010b.

Miralles, D. G., Holmes, T. R. H., de Jeu, R. A. M., Gash, J. H., Meesters, A. G. C. A., and Dolman, A. J.: Global land-surface evaporation estimated from satellite-based observations, Hydrol. Earth Syst. Sci., 15, 453–469, 2011a.

Miralles, D. G., de Jeu, R. A. M., Gash, J. H., Holmes, T. R. H., and Dolman, A. J.: Magnitude and variability of land evaporation and its components at the global scale, Hydrol. Earth Syst. Sci., 15, 967–981, 2011b.

Peel, M. C., and T. A. McMahon (2006), Continental runoff: A quality-controlled global runoff data set, N*ature, 444,* E14.

Piao, S., P. Friedlingstein, P. Ciais, N. de Noblet-Ducoudré, D. Labat, and S. Zaehle (2007), Changes in climate and land use have a larger direct impact than rising CO2 on global river runoff trends, *Proc. Nat. Acad. Sci., 104,* 15242–15247.

Rost, S., D. Gerten, A. Bondeau, W. Lucht Owe M, de Jeu R, Holmes T. 2008. Multisensor historical climatology of satellite-derived global land surface moisture. *Journal of Geophysical Research-Earth Surface* 113.

Taylor CM, Gounou A, Guichard F, Harris PP, Ellis RJ, Couvreux F, De Kauwe M. 2011. Frequency of Sahelian storm initiation enhanced over mesoscale soil-moisture patterns. *Nature Geosci* 4: 430-433. DOI: 10.1038/ngeo1173

7. Assessing the vulnerability of Global water resources

The methods and data sets developed in WATCH allow us to make estimates of past and future global water availability. But, it is only when we bring this together with the demand for water that we can begin to identify and quantify where there are deficits – where water scarcity is a problem – and areas where water might be more plentiful. Water scarcity occurs when there is not enough water available to meet the demands of agricultural, industrial, and domestic use. To identify such areas, WATCH has quantified water use in these sectors and has assessed the drivers that will influence usage in the future.

Underpinning the WATCH studies of Global water resources has been the development of the WATCH modelling framework (see figure 7.1). This has enabled global and hydrology models to be run easily for the 20th and 21st centuries and (through the WaterMIP protocols) provided estimates of uncertainty and a route for model development.

Figure 7.1. Visualization of the Watch modelling framework
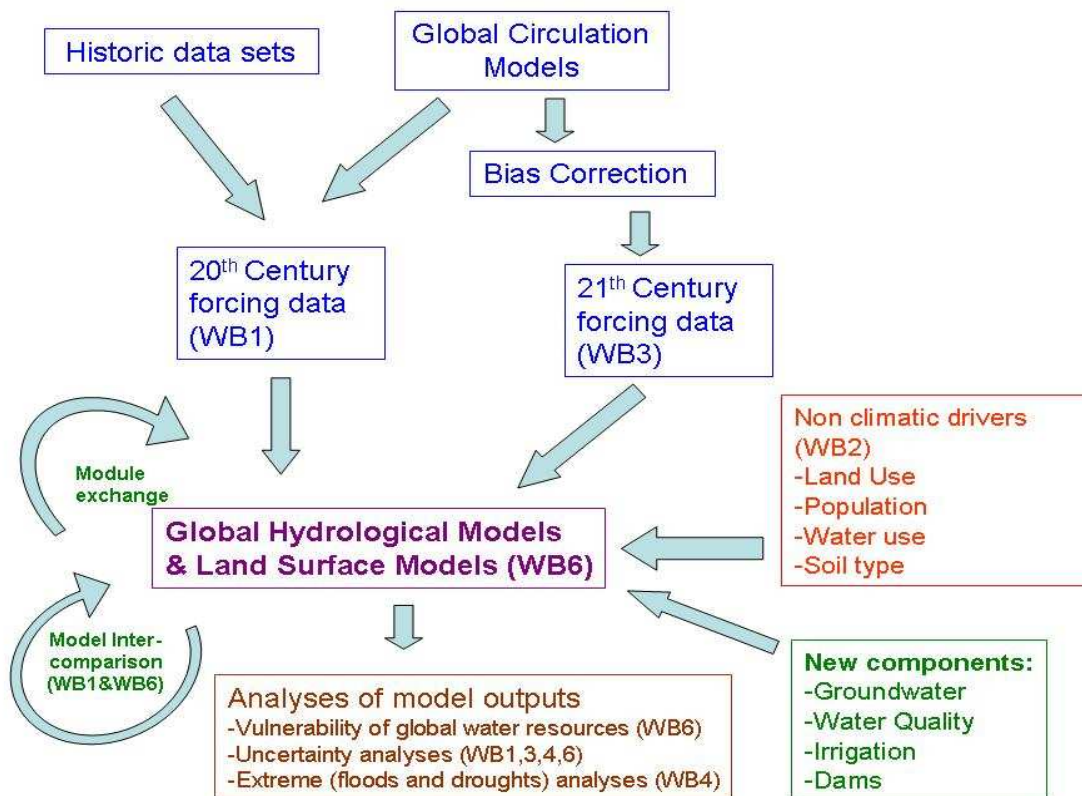
The WATCH test basins (Guadiana basin, Crete Island, Nitra river basin, Glomma & Laagen river basins, Elbe river basin) have been used to answer the question: to what extent are the global data sets useful for application in small Basins in Europe. The main conclusion (Huijgevoort et al. 2011) is that in most of the Basins it is possible to use the "Watch Forcing Data (WFD)" set and the 21st Century WATCH Driving data for water resources and drought analyses (see for example figure 7.2). There was a good correlation between locally measured rainfall and temperature and the data in the WFD. Also there were little differences in water availability and drought frequencies when either local climate data or global data sets were used.
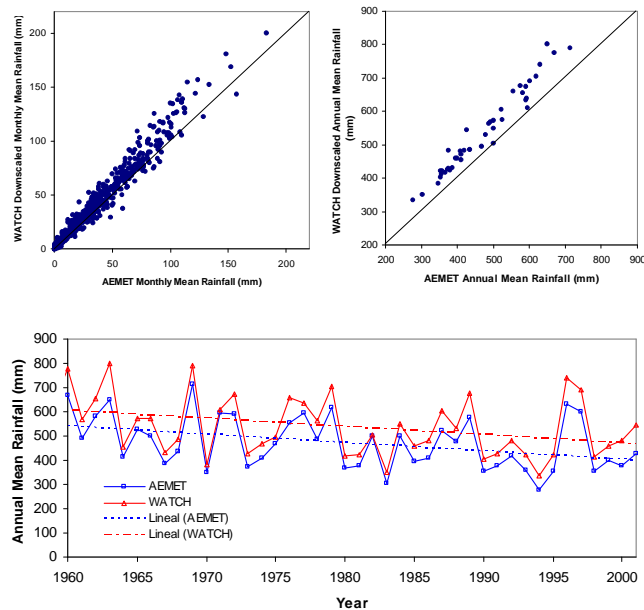
Figure 7.1. Mean monthly precipitation (up-left) and annual precipitation (up-right) from Watch Forcing Data (WFD) Vs observed mean monthly precipitation (AEMET) in the Upper Guadiana Basin. The averaging period is 1950-2000. (down) Annual cumulated precipitation time evolution in both WFD and AEMET data series for the period 1960-1990 in the Upper Guadiana basin.

Historic and future water demand of the agricultural, domestic, and industrial sectors have been developed by WATCH. Spatially detailed scenarios of population and economic activity coupled with the WATCH Forcing and Driving Datasets are used to calculate scenarios of future water use for human and economic activities that investigate the impact of demographic and economic changes, new water-saving technologies, competition for water from other sectors, and climate change. Spatial downscaling of past (from statistical data) and projected water-related activities provide locations and estimates of water use, moreover, hot spots of water abstractions become visible. Spatially explicit information is given for past, present and future water withdrawals and consumption for all sectors in form of gridded data sets which were made available to WATCH partners.

Scenarios on the future of domestic and industrial water uses are based on projected economic developments and population and urbanisation trends provided by WATCH partners. Assumptions regarding water use efficiencies were taken from other global scenario assessments, i.e. UNEP's – Global Environment Outlook (GEO-4, Rothman et al. 2007) or the Millennium Ecosystem Assessment Carpenter et al. 2005, Alcamo et al. 2005). Studies of domestic water use have confirmed that consumption and vulnerability of people to the availability of water vary significantly between income and age groups. Scenarios of domestic water use are formulated on the basis of current trends and projected economic development, and forecasted population distributions and urbanisation trends. This activity is reported in Technical Reports No. 17, 23 and 46.

In order to quantify past, present and future water use the WaterGAP model (Alcamo et al. 2003, Döll et al. 2003, Flörke and Alcamo 2004) has been applied. WaterGAP was used to compute both water use and availability on a global scale. It consists of two main components: a Global Hydrology Model to simulate the terrestrial water cycle and a Global Water Use Model to estimate water withdrawals and consumption. The Global Water Use Model consists of five modules to determine both water withdrawals and water consumption in the domestic, thermal electricity, manufacturing, irrigation, and livestock sectors. In this context, Water withdrawals indicate the total amount of water used in each sector while the consumptive water use indicates the part of withdrawn water that is lost to

evapotranspiration, consumed by industrial products or humans. For most water use sectors, only a small amount of water is actually consumed, whereas a large proportion of the extracted water withdrawn is returned, (usually with reduced quality) to the environment for subsequent use. Water demand for industrial uses is rapidly increasing and taking up a larger and larger share of global freshwater resources. Freshwater demand of the 20th Century was described in WATCH Technical report No. 23., Projections for water use in the 21st century following two different pathways into the future are described in detail in WATCH Technical report 46..

Total global water withdrawals on a grid cell level were calculated for the past, present and future using the methods described above (Figure 7.3). Current water withdrawals are especially high in densely populated regions such as Japan, Korea, coastal China, India, Pakistan, Western and Central Europe, and in North America, as well as parts of Latin America and Australia. Intensely irrigated areas in for example Northern China, Central Asia, the Middle East, and the Western United States also show high water withdrawals. Some of these hot sports are already visible in the 1960s, especial in Europe, North America, South-east Asia, and Australia. In the 1960s Water withdrawals, were much less pronounced in South America and Africa compared to current time.

For the future water use and demand two different pathways were selected, the SRES A2 and B1 scenarios. The A2 scenario shows a further increase in water withdrawals until the year 2050. For the B1 scenario water withdrawals are similar to current demands or in some regions even reduce to more efficient irrigation and reduced cooling water withdrawals.. However, due to an increase in GDP per capita an increase in water withdrawals is expected in Western and Eastern Africa under the B1 scenario conditions. The A2 scenario is characterized by a rapidly growing population and neglect of water conservation which cause much higher withdrawals. In some regions slower economic growth tends to reduce the increase. On the other side, the B1 scenario (and Policy First) assumes widespread adoption of integrated water management strategies, with strong emphasis on demand management and conservation. These developments, together with slower population growth rates, lead to slower increases in overall water use.

In order to address uncertainty related to climate change projections in WATCH, bias-corrected transient time series of precipitation and temperature were generated for the time period 1958 to 2100 (see Technical Report No 22, Piani et al. 2010 a, b, Hagemann et al. 2011). The output is a range of future projections generated globally at 0.5 x 0.5 arc degree spatial resolution using the three different Global Climate Models (GCMs) forced by the IPCC SRES A2 and B1 emission scenarios. To cover the uncertainty in climate related data the climate output from these GCMs was selected to drive the hydrological simulations used for identifying vulnerable regions (hot spots).

In order to identify vulnerable regions where the fulfilment of human water demand is at risk or may become at risk in the future the "water stress" concept is used. With this approach the average conditions of water resources can be easily compared. Here, water stress is a measure of the amount of pressure put on water resources and aquatic ecosystems by the users of these resources, including households, industries, thermal power plants and agricultural users. For calculating past, present and future water stress the withdrawals-to-availability ratio is used (w.t.a.). Generally speaking, the larger the volume of water withdrawn, used, and discharged back into a river, the more it is degraded and/or depleted, and the higher the water stress. At the same time, increasing water stress will intensify the competition for water between different sectors and between society and ecosystem requirements (Raskin et al., 1997; Alcamo et al., 2003a). A drainage basin is assumed to be under low water stress if w.t.a. ≤ 0.2; under medium water stress if 0.2 < w.t.a. ≤ 0.4 and under severe water stress if w.t.a. > 0.4.

Water stress includes both, the pressure on water resources caused by climate change and by the impacts of socio-economic driving forces, i.e. leading to increased water abstractions. Total and sectoral water withdrawals are comprehensively described above and the average water resources available in drainage basins for the past, present and future were calculated for the 1960s (represented by the time period 1956-1985), present (represented by the time period 1971-2000), and 2050s (represented by the time period 2036-2065).

Withdrawals-to-availability ratio for the river basins of the world are shown in Figure 7.4. In principal river basins classified to be under "severe water stress" are mainly located in regions where total water withdrawals are highest and/or in arid areas. For the year 2000, this includes large parts of India, Northern China, Central Asia, a few river basins in North Africa and Europe, Western Latin America, a large part of the Western United States, Northern Mexico, and south-east Australia. In poorer countries a level of severe water stress indicates an intensive level of water use that likely causes the rapid degradation of water quality for downstream users and absolute shortages during droughts. Also, in both developing and industrialized countries a level of severe water stress indicates strong competition for water resources during dry years between households, industry and agriculture.

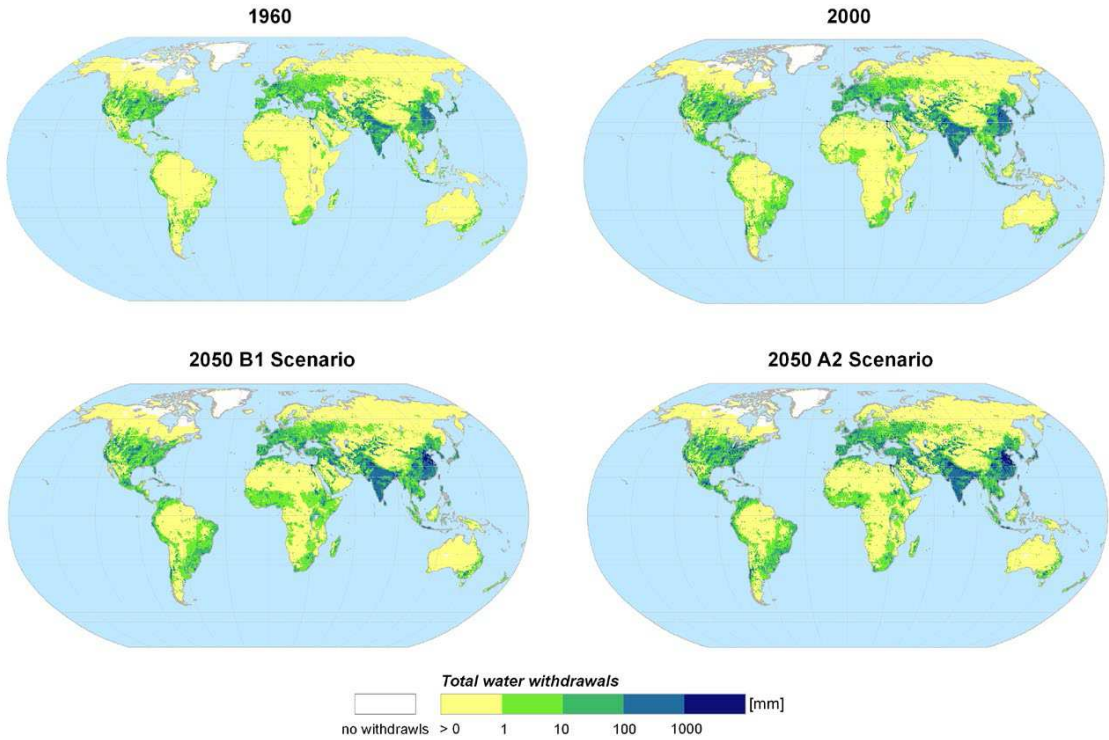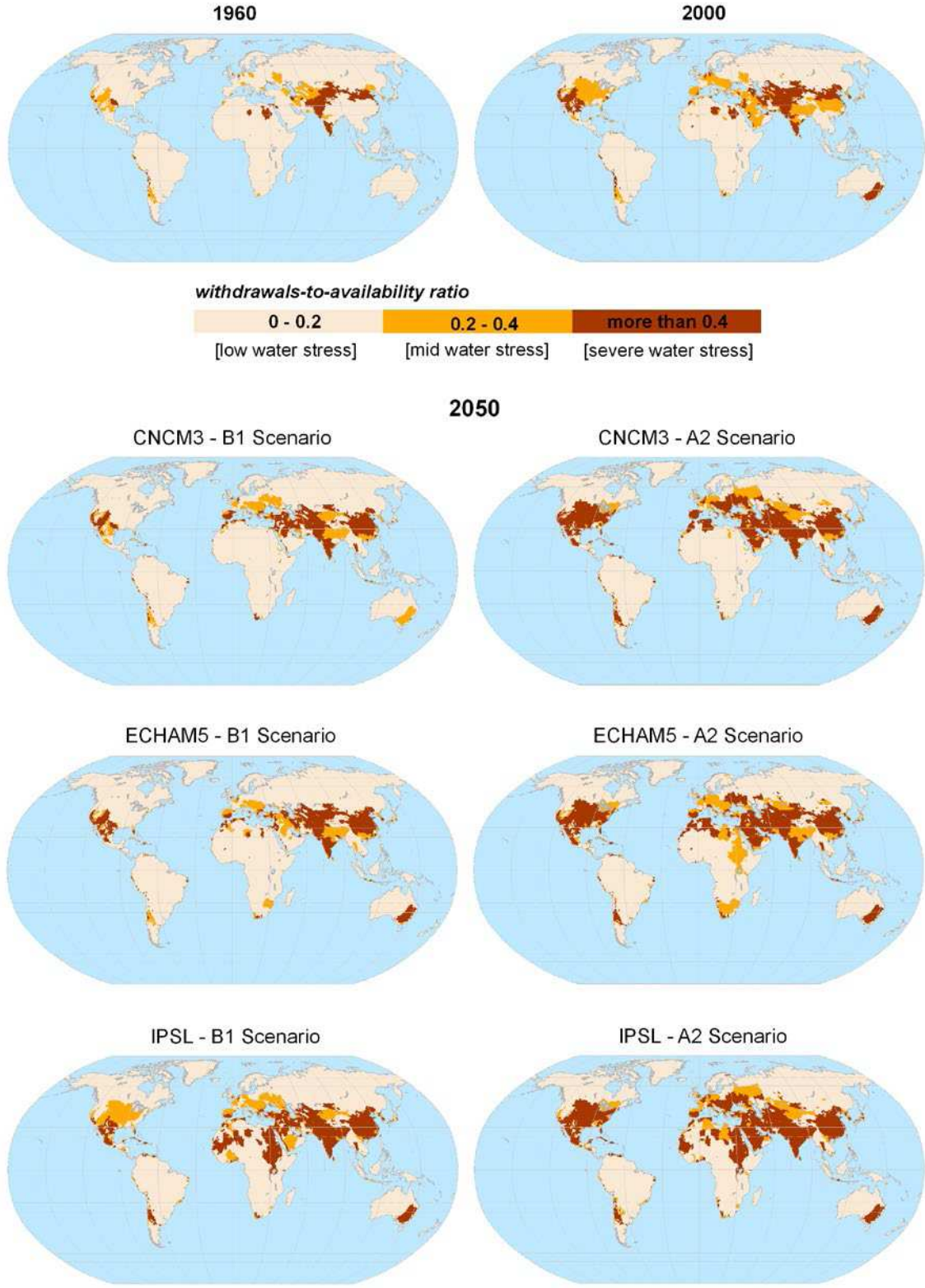*Figure 7.3. Past, present and future total water withdrawals.*

Figure 7.4. Water stress for the past, present and future. Future climate input was calculated by three different GCMs.

A further set of – global – simulations to quantify irrigation effects in the future has been performed at PIK using the LPJmL global vegetation and water balance model. The objective of these simulations was not to estimate impacts of irrigation, dam construction, land use changes or other anthropogenic activities upon the water cycle, but to assess the impacts of climate change on irrigation requirements (from which conclusions about required changes in irrigation needs and related feedbacks to the water cycle can be qualitatively deduced).

Calculation methods are based on Rost et al. (2008) who describe in detail the irrigation module embedded in the LPJmL model used in this study. Overall features of LPJmL and particularly its crop modelling procedures are described in detail in Bondeau et al. (2007), while the land use dataset used here – present and historical constructions of irrigated and rainfed crop areas and pastures, with rainfed and irrigated crop areas held constant at the year 2000 values in the future – are characterised in Fader et al. (2010). Climate inputs, i.e. monthly CRU TS 3.0 temperature, precipitation and cloudiness up to year 2000 (Mitchell & Jones 2005; http://badc.nerc.ac.uk/data/cru/) here disaggregated to daily values, and 19 GCMs for the subsequent transient simulation period up to year 2100 (CMIP3 participants; https://esg.llnl.gov:8443/home/publicHomePage.do), were the same as in Gerten et al. (in press). All simulations were performed at 0.5° x 0.5° spatial resolution, and the underlying processes (water and carbon stocks and balances, vegetation dynamics) were simulated at daily time steps, though aggregated in this report to annual totals averaged over 30-yr time slices ("present", 1971–2000; "2080s", 2070–2099). A full account of the present results along with more detailed explanations of processes underlying the simulated changes in irrigation requirements are provided by Konzmann (2011) and will be published in a forthcoming paper (Konzmann et al., in preparation).

In a first step, the LPJmL model was applied to quantify the present net irrigation requirements (NIR), defined as the amount of "blue" water from rivers, lakes, reservoirs and aquifers needed to ease water limitation of crops on areas currently equipped for irrigation. NIR is computed as a function of potential evapotranspiration, atmospheric CO_2 concentration, soil moisture, crop water limitation, duration of the growing period of the 11 major crop functional types considered (which can shift in response to climatic changes), and irrigation efficiency as estimated for each country (Bondeau et al. 2007; Rohwer et al. 2007; Rost et al. 2008; Konzmann 2011). NIR is different from gross irrigation requirement, which is the amount of water that actually needs to be withdrawn – this amount is always higher, because part of the withdrawn water is lost on its way to the field, as determined by the irrigation efficiency. As a result, present (1971–2000 average) NIR was found to be 1029 km^3 yr^{-1} globally (gross irrigation requirements, 2709 km^3 yr^{-1}), which agrees well with earlier studies. As shown in Fig. 7.5 (upper map), highest NIR values per 0.5° grid cell occur in regions where irrigation areas cover large fractions of total grid cell area, particularly in northern India, parts of Pakistan, parts of the western U.S., and along several river stretches such as the lower Nile. Highest values per irrigated area (Fig. 7.5, lower map) are typical for most subtropical and tropical irrigation areas on all continents, mostly because atmospheric irrigation demand (potential evapotranspiration) is high in these regions compared to temperate zones.
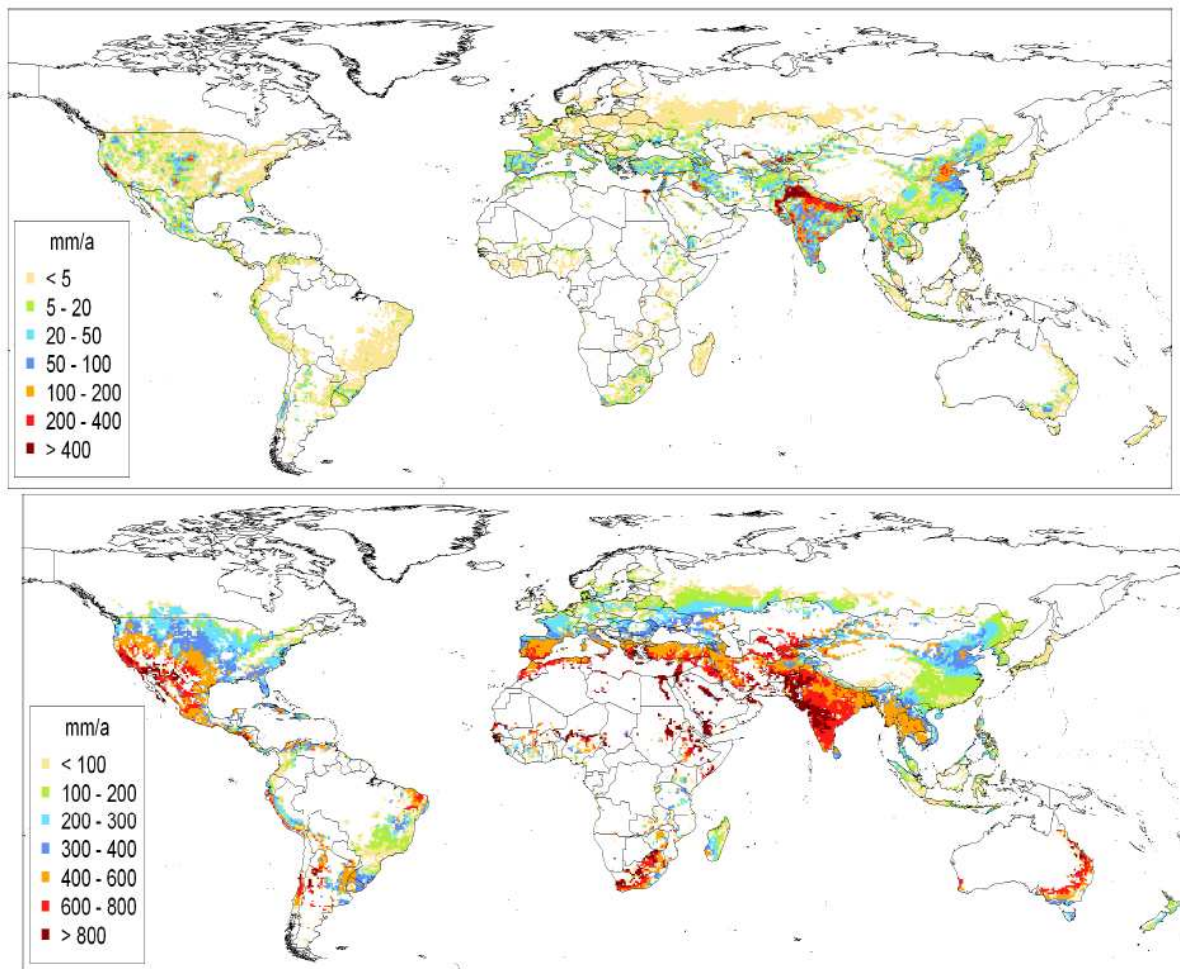
Figure 7.5: LPJmL-simulated annual net irrigation requirements (NIR, in mm yr–1), averaged over the period 1971–2000. Top: values per grid cell (incl. non-irrigated areas) highlighting the areal extent of irrigation areas; bottom: values per irrigated area in a grid cell, highlighting the climatic effect.

A key issue in the assessment of water resource vulnerability is water quality. WATCH has developed the first global model of surface water quality. This is a development of the WaterGAP model and the compilation of the data for running and testing the model. A first version of the water quality model has been completed for the conservative tracer TDS (total dissolved salts) and the non conservative parameter BOD (Biological Oxygen Demand). Now the model is able to link BOD and TDS loadings from grid cells to river flow. For the routing through river basins an exponential equation is used. The decay and retention coefficients during the transport process along the river take into account river length, variable stream velocity, and cross sectional area. The model results have been tested against measured data in 14 European river basins along the river length for different data input conditions and dates (see example for Danube in March 2000, Figure 7.6). Additionally the extension of the water quality model for the parameter: total coliform bacteria has been started. Also the temperature dependency of decay rates for BOD and total coliform bacteria has been studied, including a simple approach for water temperature based on mean air temperature (simple linear regression).

In cooperation with the SCENES project the necessary point source and diffuse loading information was further prepared as input data for water quality modelling. In order to estimate the loading information a big amount of different data has to be kept up to date. This requires a frequent recalculation of the

loading information. For this reason a MySQL database with calculation tools was setup. It consists of several tables split up by input and calculation data with country and grid cell information.
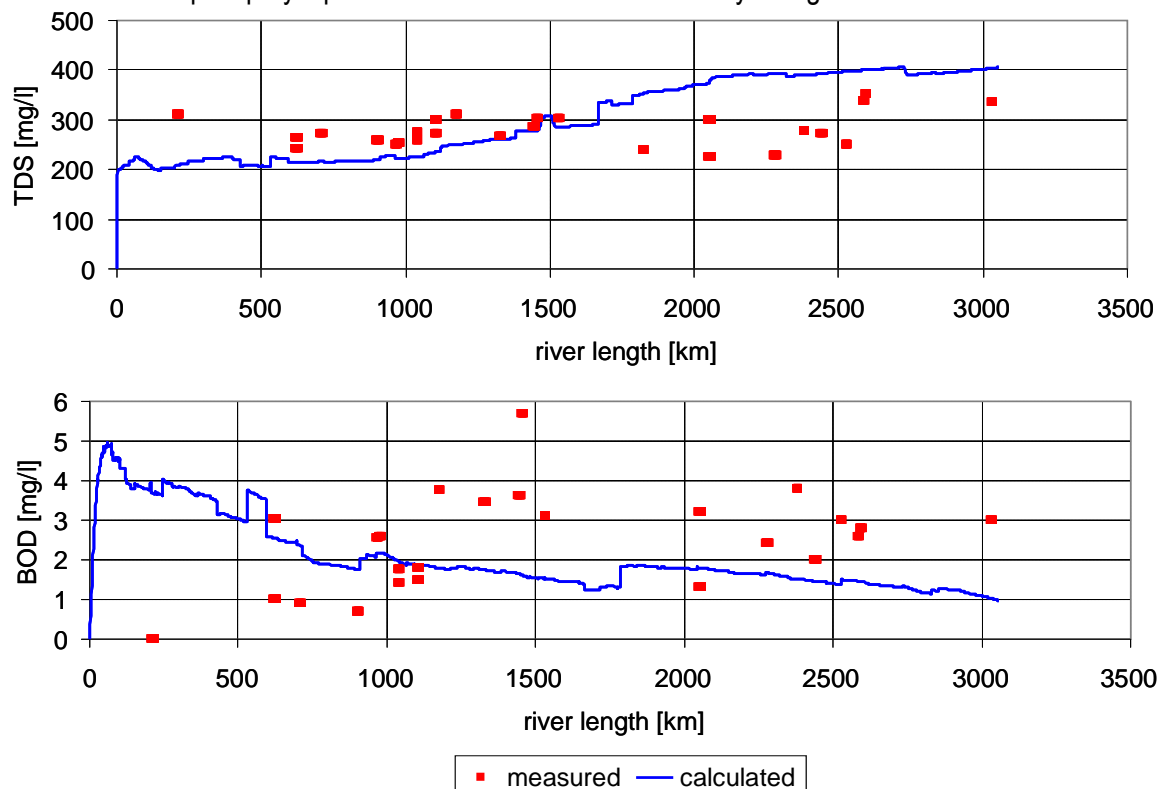

Figure 7.6: TDS and BOD concentration Danube river basin March 2000.

A detailed report for the water quality module developed in this task and a plan for linkage to the overall modelling framework is given within the Technical Report No. 18 ('Preliminary water quality module: State of development and plan for linkage to the overall modelling framework').

The vulnerability of past, current and future resources is a complex interaction of physical, social, economic and political factors. WATCH, and this report, has focused primarily on the physical aspects. The other influences on future water resources are equally, if not more, important. However, any more comprehensive analysis must be based on the physical accounting of what is available and what is (and will be) extracted. Thus the methodologies, data and models from WATCH should provide a sound basis for future analyses.

References

Alcamo, J. and Henrichs, T. (2002). Critical regions: A model based estimation of world water resources sensitive to global changes. Aquatic Sciences, 64, 1-11.

Alcamo, J., Döll, P., Henrichs, T., Kaspar, F., Lehner, B., Rösch, T. and Siebert, S. (2003). Development and Testing of the WaterGAP 2 Global Model of Water Use and Availability, Hydrological Sciences Journal, 48(3), 317–337.

Alcamo, J., van Vuuren, D., Ringler, C., Cramer, W., Masui, T., Alder, J., and Schulze, K. (2005). Changes in nature's balance sheet: model-based estimates of future worldwide ecosystem services. Ecology and Society 10(2): 19. [online] URL: http://www.ecologyandsociety.org/vol10/iss2/art19/ (18 January 2011)

Alcamo, J., Flörke, M. and Märker, M. (2007). Future long-term changes in global water resources driven by socio-economic and climatic changes. Hydrological Sciences, 52(2): 247-275.

Bondeau, A., Smith, P., Zaehle, S., Schaphoff, S., Lucht, W., Cramer, W., Gerten, D., Lotze- Campen, H., Müller, C., Reichstein, M., Smith, B. 2007. Modelling the role of agriculture for the 20th century global terrestrial carbon balance. *Global Change Biol.* 13, 679–706.

Carpenter, S., Pingali, P., Bennett, E., and Zurek, M., (eds.) (2005). Scenarios of the Millennium Ecosystem Assessment, Island Press, Oxford.

Cosgrove, W. and Rijsberman, F. (2000). World Water Vision: Making Water Everybody's Business. World Water Council, Earthscan Publications, London, p. 108.

Döll, P., Kaspar, F. and Lehner, B. (2003). A Global Hydrological Model for Deriving Water Availability Indicators: Model Tuning and Validation. J. Hydrol., 270, pp. 105-134.

Fader, M., Rost, S., Müller, C., Bondeau, A., Gerten, D. 2010. Virtual water content of temperate cereals and maize: Present and potential future patterns. *J. Hydrol.* 384, 218–

231

Flörke, M. and Alcamo, J. (2004). European Outlook on Water Use, Technical Report prepared for the European Environment Agency. Kongens Nytorv. 6. DK-1050. Copenhagen, DK URL: // http: scenarios.ewindows.eu.org/reports/fol949029, 2011.

Hagemann, S., Chen, C., Härter, J.O., Heinke, J., Gerten, D., Piani, C. (2011). Impact of a statistical bias correction on the projected hydrological changes obtained from three GCMs and two hydrology models. J. of Hydrometeorology, early online release, doi: 10.1175/2011JHM1336.1

Konzmann, M. 2011. *Modellbasierte Analyse von Klimawirkungen auf den globalen Bewässerungsbedarf unter Berücksichtigung von 19 Klimamodellen.* Master thesis at the Department of Geography, Humboldt University of Berlin, 148 pp.

Mitchell, T.D., Jones, P.D. 2005: An improved method of constructing a database of monthly climate observations and associated high-resolution grids. *Int. J. Climatol.* 25, 693-712.

Piani, C., Haerter, J., and Coppola, E. (2010a). Statistical bias correction for daily precipitation in regional climate models over Europe, Theoretical and Applied Climatology, 99, doi:10.1007/s00704-009-0134-9.

Piani, C., Weedon, G., Best, M., Gomes, S., Gomes, P., Hagemann, S., and Haerter, J. (2010b). Statistical bias correction of global simulated daily precipitation and temperature for the application of hydrological models, Journal of Hydrology, 395, 199-215. doi:10.1016/j.jhydrol.2010.10.024

Rothman, D., Agard, J. and Alcamo, J. (2007). The Future Today, in UNEP, 2007: Global Environmental Outlook 4: Environment for Development. United Nations Environment Programme, Nairobi. pp. 395-454.

Rohwer, J., Gerten, D., Lucht, W. 2007. Development of functional irrigation types for improved global crop modelling. *PIK Report* 104, 91 pp.

Rost, S., Gerten, D., Bondeau, A., Lucht, W., Rohwer, J., Schaphoff, S. 2008. Agricultural green and blue water consumption and its influence on the global water system. *Water Res. Res.* 44, W09405.

Vörösmarty, C.J., Green, P., Salisbury, J., and Lammers, R.B. (2000). Global Water Resources: Vulnerability from Climate Change and Population Growth. Science 289, 284-288.

8. Dissemination, training and outreach

Throughout the life of WATCH there has been an active programme of dissemination, training and outreach. The scientific developments have been published in a wide variety of peer reviewed scientific papers (over 200). The centrepiece of these has been the WATCH special collection published in the Journal of Hydrometeorology (editors: Richard Harding and Tanya Warnaars, http://journals.ametsoc.org/page/WATCH). In addition to the peer-reviewed papers the detail of WATCH research is available in the WATCH Technical reports.- this series now numbers over 50 and are available through the WATCH web site (http://www.eu-watch.org/).

WATCH has also had a strong presence at a number of international conferences. In particular the annual meetings of the European Geophysical Union (2009-2011) where two sessions (HS2.11Hydrological extremes: from droughts to floods; HS2.9 Hydrological change: Regional hydrological behaviour under transient climate and land use conditions) have been co-ordinated by WATCH PIs. In the 2011 EGU we also ran a dedicated WATCH splinter group meeting titled: Global Changes in Water Resources and Extremes: results from the WATCH project.
Additionally the 2010 World Water Week in Stockholm was an opportunity for WATCH to reach an audience beyond the research community. Substantial interest was generated at the WATCH sponsored side event titled: *Impacts of Climate Change on Water Quantity and Quality*.

The data sets produced by WATCH will provide a valuable resource to the entire community in the future. Already we've made the WATCH Forcing Data available to a number of groups across Europe and USA. The data sets are now freely available at the ftp site at IIASA (for details see the WATCH website) in the future we hope to provide a more user friendly web portal and download system.

Table of main WATCH data available on IIASA ftp site, a more detailed description is available via the CEH information gateway (https://gateway.ceh.ac.uk/)

Name	Brief description	Geographical range	Time period	Storage location	File format	Access restrictions
HWSD v1.1	Harmonized World Soil Database, developed by IIASA, with additional support from FAO, ISSCAS, ISRIC, and JRC.	Global	2000	http://www.iiasa.ac.at/Research/LUC/External-World-soil-database/HTML/	binary interleave by line (*.bil) and Access Database (*.mdb)	Available to all on the internet for academic purposes.
WATCH sectoral water use	gridded 20th and 21st century data for domestic, electricity production, manufacturing, and agricultural water use information from CESR.	Global	1900-2100	WATCH ftp site: ftp://ftp.iiasa.ac.at/Workblock2/sectoral_water_uses/	NetCDF	
WATCH land use and cover	gridded land use and cover information from IIASA for the year 2000 divided into 8 categories with 2 additional categories for protected areas	Global	2000	http://www.iiasa.ac.at/Research/LUC/External-Watch/WATCHInternal/WATCHData.html	ASCII grid	
WATCH future land use projections	IIASA's gridded projections of land use from 2000 to 2100 for SRES scenarios A2(r) and B1	Global	1990 - 2100	http://www.iiasa.ac.at/Research/LUC/External-Watch/WATCHInternal/WATCHData.html	ASCII grid	
WATCH population	IIASA's Gridded population projections for SRES	Global	1990-2100	http://www.iiasa.ac.at/Research/LUC/External-Watch/WATCHInternal/	ASCII and ARCGIS	

Name	Brief description	Geographical range	Time period	Storage location	File format	Access restrictions
projections	scenarios A2(r) and B1			WATCHData.html		
GLWD	Global Lakes and Wetlands Database, by Lehner and Döll	Global		http://www.worldwildlife.org/science/data/item1877.html	ARCGIS	
GRanD	Global Reservoir and Dam Database	Global		http://www.gwsp.org/85.html	ARCGIS	
TIR_LST	Land Surface Temperature maps at 0.1° spatial resolution and 10-day temporal resolution (WATCH Tech rep 9)	global land	1981-2001	WATCH FTP /WorkBlock1/	netCDF	Nil
ETD	Daily Evapotranspiration maps at 0.1° spatial resolution and 10-day temporal resolution	global land	1981-2001	WATCH FTP /WorkBlock1/	netCDF	Nil
WATCH Forcing Data	Forcing data half-degree sub-daily and daily (WATCH Tech Rep 22)	global land (exc. Antarctica)	1901-2001	WATCH FTP /WATCH_Forcing_Data/	netCDF	Nil
20th Century Ensemble Product	Ensemble average of 7 model outputs, half-degree, daily (WATCH Tech Rep 37)	global land (exc. Antarctica)	1901-2000	WATCH FTP /WorkBlock1/	netCDF	Nil
20th Century Ensemble data	Output from MPI-HM full 20th century (see also WB4 extremes data)	global land (exc. Antarctica)	1901-2000	WATCH FTP /WorkBlock1/	netCDF	Nil
Forcing comparison output	Output from H08, JULES, MPI-HM and LPJml using alternative forcing data (ncc, gswp2, Princeton)	global land (exc. Antarctica)	1986-1995	WATCH FTP /WorkBlock1/	netCDF	Nil
Evaporation	Total land-surface evaporation	Global	1984-2007	server: 130.37.78.12	ASCII	user: adaguest pass: downloader
Transpiration	Plant transpiration	Global	1984-2007	server: 130.37.78.12	ASCII	user: adaguest pass: downloader
Interception	Tall Canopy Interception	Global	1984-2007	server: 130.37.78.12	ASCII	user: adaguest pass: downloader
Bare soil evaporation	Direct evaporation from soil	Global	1984-2007	server: 130.37.78.12	ASCII	user: adaguest pass: downloader

Up until now the primary vehicle of dissemination to the wider scientific and policy communities has been through many presentations by the WATCH PIs and co-ordinators. This is currently being augmented by a specially commissioned WATCH Outreach Report and associated web sites (http://www.eu-watch.tv/), see box below.
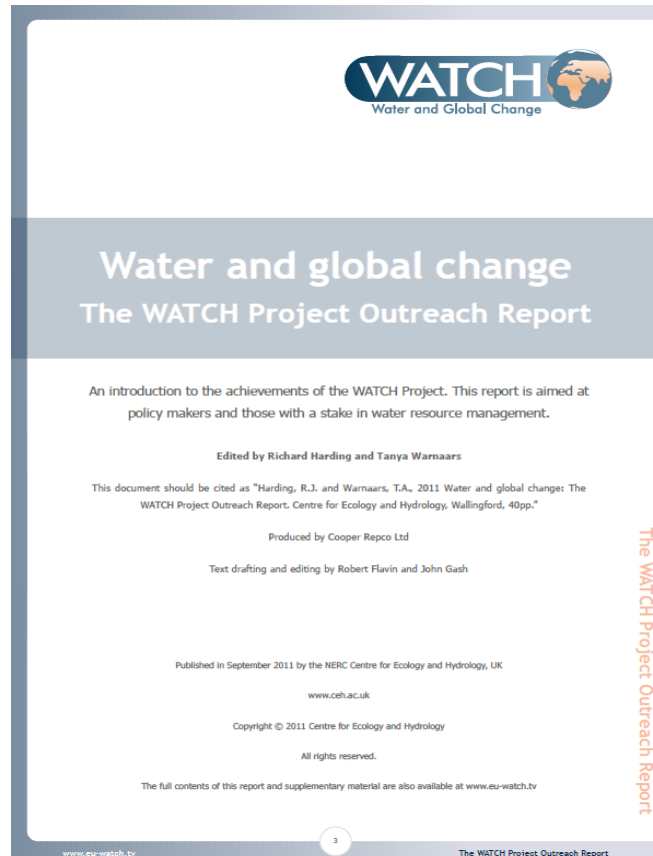
A major theme of WATCH has been the bringing of different communities together as part of this, we have been very aware of the absolute necessity of training the next generation of climate and water scientists. WATCH has run two series of Summer Schools. The first has been for high school students (15 to 18 years), who are just entering the world of scientific research and the second for post graduate and post doctoral students, who will need the interdisciplinary skills fundamental to WATCH and future environmental research.

The summer schools for high school students were held at the United World College of the Adriatic on Climate Change and the Water Cycle during June 2008 and 2010. Thirty-eight students from 11 different countries participated in a 1 week series of lectures and debates from WATCH scientists and guest speakers. Topics included: introduction to the climate system, the hydrological cycle, ethics of climate change and more.

At the end of the course students wrote a short independently researched and referenced essay on one of a series of suggested topics. The schools consisted of lectures, films and discussions and project work. During the closing ceremony a selection of students presented their essays to fellow students and lecturers. The ceremonies were also attended by local authorities along with the directors of the most important science research centres of Trieste. The overall feedback from the students was positive with many expressing an interest of learning more about climate change and water as well as being inspired to implement changes to their daily routines.

A series of post-graduate summer schools have also been held:

- Hydrology, Drought and Global Change was held in Trieste from 22 to 27 June 2008 (details in technical report 8)

- Water and Global change held in Oxford 4 to 8 July 2011 (details in technical report 50)

In addition to these formal events training events WATCH has support a large number of PhD students (30 students at 10 partner institutions) who have fully participated in the WATCH general Assemblies and internal workshops.

The emphasis on these post graduate courses and summer schools has been to include students from a wide range of countries, from Europe and developing regions. In addition WATCH has co-organised workshops in Beijing (jointly with the RCUK[1] and MAIRS[2] projects, titled "Climate Change and Global Water Cycle" in Beijing China from 24-26 November 2008) and Delhi India: (jointly with the FP7 HighNoon project, titled "Future of Water Resources in India under a Changing Climate" May 2009).

Throughout its duration WATCH has been strongly dedicated to communicating the role of modelling the water cycle in the climate system. The target for this dissemination has varied greatly from driving discussions with senior scientists to the informed public at large. A symposium on "Global Land-surface Evaporation and Climate" brought together leading researchers on this topic, it made use of multimedia to include overseas presentation and a recording of this was made. It is possible to hear the views of the participants, providing a lasting record of this event (http://www.eu-watch.org/news-and-events/symposium-on-evaporation-and-climate). An information portal was developed to describe to a wide audience the hydrological cycle, and how modellers interpret and represent the different factors involved in the water cycle. The details of this can be found at www.waterandclimatechange.eu. This site as well as the project website (www.eu-watch.eu) will continue after the project end date as will serve as an important point of call for those interested in the projects achievements as well as accessing the datasets generated under WATCH.

---

[1] Research Council of the United Kingdom
[2] Monsoon Asia Integrated Regional Study

9. The legacy of WATCH

WATCH leaves the clear legacy of an increased understanding of the water cycle in a time of global change. In addition, it has created an international group of experienced modellers working at the interface between hydrology and climate science. These scientists will go on to make valuable contributions to future global science.

Closer working between research communities
The culture of closer working that was nurtured during WATCH has led to a step-change in the level of mutual understanding between climate and water scientists. The dividends of this are clear, and they should provide the incentive – and give groups confidence – to develop the necessary future links with other groups such as oceanographic modellers.

New appreciation of the relationships between the drivers of past and future change in river flows and water resources
Climate change, demographic and land-use change, and changing patterns of consumption all drive changes in river flows and water resources. WATCH has provided a new appreciation of the relative importance of these individually, and also of how they interact.

New consolidated global and regional data sets to provide for a systematic analysis of the terrestrial water cycle
The new WATCH data sets for the 20th and 21st centuries have underpinned the research within the project and they are now readily available to a worldwide research community for use in future regional and global studies.

Improved and tested models of the terrestrial hydrological cycle and water resource assessment
A project the size of WATCH brings managerial challenges, but it also brings considerable opportunities, as Han Dolman explains. "With large projects you can take greater risks, and these are the areas with the most potential for high benefit breakthroughs. Smaller projects have much tighter deadlines and deliverables: They are safe science. WATCH allowed
an element of risk, and the benefits are there." WaterMIP is a prime example of this. It started out as a relatively small component of WATCH but was able to expand once the importance and potential benefits were recognised. To run 13 models side-by-side at a global scale and to compare and analyse the results has accelerated model development far beyond what was originally anticipated.

Quantification of the uncertainties in modelling of the global hydrological Cycle
The quantification of uncertainty will lead to new ways of assessing impact and adaptation studies, and should provide an agenda for integrated model development in coming years Ronald Hutjes said, "The different groups are working much better together and this is leading to better estimations of the future water resources – and even better appreciation of the uncertainty of the estimations."

New global and regional analyses of major floods and droughts of the 20th century, and an outlook for the 21st century
WATCH has demonstrated that extremes – both floods and droughts – can be analysed regionally and globally using 50km x 50km data. The availability of the WATCH data sets should give groups the confidence to undertake further studies at these scales, and to utilise the novel methods of presentation that have been pioneered in producing the flood and drought atlases.

A global analysis of water scarcity in the 20th and 21st centuries
The WATCH global analysis and the resulting data sets are the core of the original ambitions of WATCH: to go beyond climate and river flows, and to integrate these with current and future human demands and drivers. The outputs should be an invitation and incentive for further more ambitious studies in the future.

Improved understanding and quantification of the feedbacks between the land surface and the atmosphere in the Earth system
WATCH has modelled land surface / atmosphere feedbacks using a range of models. "WATCH has shown the benefits of using a multi-model approach, and it is of particular importance when modelling feedbacks," said Ronald Hutjes. "By using a range of models you are more likely to detect an effect that may not have been considered or foreseen. This is because the water cycle is complex, and man is adding to the complexity. Multi- models are an insurance policy."

This stage of WATCH is now complete. Many of its outputs are summarised in this document and can now be applied to the task of formulating evidence-based policy with a foundation of sound science.

Highlighting key publications generated under WATCH:

Berg, P., Haerter, J.O., Thejll, P., Piani, C., Hagemann, S. and Christensen, J.H., 2009. Seasonal characteristics of the relationship between daily precipitation intensity and surface temperature. J. Geophys. Res., 114, doi:10.1029/2009JD012008

Biemans, H., Haddeland, I., Kabat, P., Ludwig, F., Hutjes, R.W.A., Heinke, J., von Bloh, W., Gerten, D., 2011. Impact of reservoirs on river discharge and irrigation water supply during the 20th century. Water Resources Res. 47, W03509

Blyth, E.M., C.M.J. Jacobs. Developing a feedbacks toolkit for Regional water resource assessments. IAHS Publ 344, 27-31

Corzo Perez G.A., van Huijgevoort, M.H.J., Voss, F. & van Lanen, H.A.J. (2011a) On the spatio-temporal analysis of hydrological droughts from global hydrological models. Hydrol. Earth Syst. Sci. 15: 2963-2978, doi:10.5194/hess-15-2963-2011.

Döll,P., Fiedler, K., Zhang, J. (2009): Global-scale analysis of river flow alterations due to water withdrawals and reservoirs, Hydrol. Earth Syst. Sci. Diss., 6, 4773-4812.

Fader M., Rost S., Müller C, Bondeau A, and Gerten, D. (2010) Virtual water content of temperate cereals and maize: Present and potential future patterns Journal of Hydrology 384 218–231

Falloon, P., Betts, R., Wiltshire, A., Dankers, R., Mathison, C., McNeall, D., Bates, P., Trigg M., 2011. Validation of river flows in HadGEM1 and HadCM3 with the TRIP river flow model. J. Hydrometeo., doi: 10.1175/2011JHM1388.1.

Fleig, A.K., Tallaksen, L.M., Hisdal, H. & Hannah, D.M. (2011) Regional hydrological drought in north-western Europe: linking a new Regional Drought Area Index with weather types. Hydrological Processes 25, 1163-1179, doi: 10.1002/hyp.7644

Gerten, D., Heinke, J., Hoff, H., Biemans, H., Fader, M., and Waha, K., (2011) Global water availability and requirements for future food production, Journal of Hydrometeorology, 12, 885-899, doi: 10.1175/2011JHM1328.1

Haerter, J.O., and Berg, P., 2009. Unexpected rise in extreme precipitation caused by a shift in rain type? Nature Geosci., 2, 372, DOI 10.1038/ngeo523.

Haerter, J.O., S. Hagemann, C. Moseley and C. Piani (2011) Climate model bias correction and the role of timescales. Hydrol. Earth Syst. Sci. 15, doi:10.5194/hess-15-1-2011: 1065-1079

Haddeland, I., Clark, D.B., Franssen, W., Ludwig, F., Voß, F., Arnell, N.W., Bertrand, N., Best, M., Folwell, S., Gerten, D., Gomes, S., Gosling, S.N., Hagemann, S., Hanasaki, N., Harding, R.J., Heinke, J., Kabat, P., Koirala, S., Oki, T., Polcher, J., Stacke, T., Viterbo, P., Weedon, G.P. and Yeh, P. (2011). Multi-Model Estimate of the Global Terrestrial Water Balance: Setup and First Results. Journal of Hydrometeorology., 12, 869-884, doi: 10.1175/2011JHM1324.1.

Hagemann, S., C. Chen, J.O. Haerter, D. Gerten, J. Heinke, C. Piani (2011) Impact of a statistical bias correction on the projected hydrological changes obtained from three GCMs and two hydrology models. J. Hydrometeor., doi:10.1175/2011JHM1336.1.

Hanasaki N., Inuzuka T., Kanae S., and Oki T. (2010) An estimation of global virtual water flow and sources of water withdrawal 3 for major crops and livestock products using a global hydrological model Journal of Hydrology Volume 384, Issues 3-4

Hannaford, J., Lloyd-Hughes, B., Keef, C., Parry, S., Prudhomme, C. (2011). Examining the large-scale spatial coherence of European drought using regional indicators of rainfall and streamflow deficit. Hydrological Processes. 25 (7). 1146 – 1162. DOI: 10.1002/hyp.7725

Harding R, Best M, Blyth E, Hagemann S, Kabat P, Tallaksen LM, Warnaars T, Wiberg D, Weedon GP, van Lanen H, Ludwig F, Haddeland I, 2011. Preface to the "Water and Global Change (WATCH) special collection: Current knowledge of the terrestrial Global Water Cycle, Journal of Hydrometeorology (doi: 10.1175/JHM-D-11-024.1).

Harding, R. J. and Warnaars T. A. 2011 Water and Global Change: the WATCH project Outreach report, Centre for Ecology and Hydrology Wallingford 40pp

Hoff,H., Falkenmark, M., Gerten, D., Gordon, L., Karlberg, L., Rockström, J., (2010) Greening the global water system. Journal of Hydrology Volume 384, Issues 3-4, 177-186

J´odar, J., Carrera,J., and Cruz, A. (2010) Irrigation enhances precipitation at the mountains downwind Hydrol. Earth Syst. Sci., 14, 2003–2010

Jung, M., Reichstein, M., Ciais, P., Seneviratne, S.I., Sheffield, J., Goulden, M.L., Bonan, G., Cescatti, A., Chen, J., de Jeu, R., Dolman, A.J., Eugster, W., Gerten, D. et al. 2010: Recent decline in the global land evapotranspiration trend due to limited moisture supply. Nature 467, 951–954.

Koutroulis, A. G., Vrohidou, A. K., andTsanis I. K., (2011). Spatiotemporal Characteristics of Meteorological Drought for the Island of Crete, Journal of Hydrometeorology Vol. 12, Iss. 2, pp. 206–226.

Kundzewicz, Z.W., Hirabayashi, Y., Kanae, S. (2010) River Floods in the Changing Climate—Observations and Projections. Water Resour. Management, 24, 2633-2646, doi: 10.1007/s11269-009-9571-6

Lucas-Picher, P., J.H. Christensen, F. Saeed, P. Kumar, S. Asharaf, B. Ahrens, A. Wiltshire, D. Jacob and S. Hagemann (2011) Can regional climate models represent the Indian monsoon? J. Hydrometeor., 10.1175/2011JHM1327.1,

Miralles, D.G., De Jeu, R.A.M., Gash, J.H., Holmes, T.R.H., and Dolman, A.J.: Magnitude and variability of land evaporation and its components at the global scale, Hydrol. Earth Syst. Sci., 15, 967-981, doi:10.5194/hess-15-967-2011, 2011.

Pall, P., Tolu Aina, Dáithí A. Stone, Peter A. Stott, Toru Nozawa, Arno G. J. Hilberts, Dag Lohmann & Myles R. Allen (2011) Anthropogenic greenhouse gas contribution to flood risk in England and Wales in autumn 2000. Nature 470, 382–385

Piani, C., G.P. Weedon, M. Best, S. Gomes, P. Viterbo, S. Hagemann, and J.O. Haerter (2010) Statistical bias correction of global simulated daily precipitation and temperature for the application of hydrological models. J. Hydrol., 395, 199–215.

Prudhomme, C., Parry, S., Hannaford, J., Clark, D.B., Hagemann, S., Voss, F. (In press). How well do large-scale models reproduce regional hydrological extremes in Europe? In press: Journal of Hydrometeorology. DOI: 10.1175/2011JHM1387.1

Saeed, F., S. Hagemann, and D. Jacob (2009) Impact of irrigation on the South Asian summer monsoon. Geophys. Res. Lett., 36, L20711, doi:10.1029/2009GL040625.

Scipal, K., Holmes, T., de Jeu, R., Naeimi, V. and Wagner, W. (2008) A possible solution for the problem of estimating the error structure of global soil moisture data sets. Geophysical Research Letters, Vol. 35, L24403, doi:10.1029/2008GL035599

Stahl, K., Tallaksen, L.M., Gudmundsson, L. & Christensen, J.H. (2011) Streamflow data from small basins: a challenging test to high resolution regional climate modeling. Journal of Hydrometeorology. doi: 10.1175/2011JHM1356.1

Stahl, K., Hisdal, H., Hannaford, J., Tallaksen, L. M., van Lanen, H. A. J., Sauquet, E., Demuth, S., Fendekova, M., and Jódar, J. (2010) Streamflow trends in Europe: evidence from a dataset of near-natural catchments Hydrol. Earth Syst. Sci. Discuss., 7, 5769-5804

Tallaksen, L.M., Hisdal, H. & van Lanen, H.A.J. (2009) Space-time modeling of catchment scale drought characteristics. J. Hydrol., 375, 363-372 (doi:10.1016/j.jhydrol.2009.06.032)

Taylor CM. 2010. Feedbacks on convection from an African wetland. Geophys. Res. Lett. 37: L05406.

Tuinenburg, O. A., Hutjes, R. W. A., Jacobs, C. M. J. and Kabat, P. (2011) Diagnosis of Local Land–Atmosphere Feedbacks in India. J. Climate, 24, 251–266.

Weedon, G.P., Gomes, S., Viterbo, P., Shuttleworth, W.J., Blyth, E., Österle, H., Adam, J.C., Bellouin, O., and Best, M., (2011). Creation of the WATCH Forcing Data and its use to assess global and regional reference crop evaporation over land during the twentieth century. J. Hydrometeology 12, 823-848doi: 10.1175/2011JHM1369.1

Wong, W.K., Beldring, S., Engen-Skaugen, T., Haddeland, I. and Hisdal, H. (2011) Climate Change effects on spatiotemporal patterns of hydroclimatological summer droughts in Norway. J. Hydrometeorol. doi: 10.1175/2011JHM1357.1.

Wood, E. F., J. K. Roundy, T. J. Troy, R. van Beek, M. Bierkens, E. Blyth, A. de Roo, P. Doell, M. B. Ek, J. Famiglietti, D. Gochis, N. van de Giesen, P. Houser, P. R. Jaffe, S. Kollet, B. Lehner, D. P. Lettenmaier, C. Peters-Lidard, M. Sivapalan, J. Sheffield, A. Wade, and P. Whitehead. Hyperresolution global land surface modeling: Meeting a grand challenge for monitoring Earth's terrestrial water. Water Resources Research, doi:10.1029/2010WR010090